Wave propagation in fractal trees. Mathematical and Numerical Issues

Patrick Joly, Maryna Kachanovska, Adrien Semin

▶ **To cite this version:**

Patrick Joly, Maryna Kachanovska, Adrien Semin. Wave propagation in fractal trees. Mathematical and Numerical Issues. Networks and Heterogeneous Media, 2019, 14 (2), 10.3934/nhm.2019010 . hal-01801394v2

HAL Id: hal-01801394
https://hal.science/hal-01801394v2

Submitted on 2 Apr 2021

HAL is a multi-disciplinary open access archive for the deposit and dissemination of scientific research documents, whether they are published or not. The documents may come from teaching and research institutions in France or abroad, or from public or private research centers.

L'archive ouverte pluridisciplinaire **HAL**, est destinée au dépôt et à la diffusion de documents scientifiques de niveau recherche, publiés ou non, émanant des établissements d'enseignement et de recherche français ou étrangers, des laboratoires publics ou privés.

doi:10.3934/nhm.xx.xx.xx

Volume **X**, Number **0X**, XX **20xx** pp. **X–XX**

WAVE PROPAGATION IN FRACTAL TREES. MATHEMATICAL AND NUMERICAL ISSUES

PATRICK JOLY

POems (UMR 7231 CNRS-INRIA-ENSTA)
828 Boulevard des Maréchaux
Palaiseau, F-91120, France

MARYNA KACHANOVSKA

POems (UMR 7231 CNRS-INRIA-ENSTA)
828 Boulevard des Maréchaux
Palaiseau, F-91120, France

ADRIEN SEMIN

Technische Universität Darmstadt
Fachgebiet Mathematik, AG Numerik und Wissenschaftliches Rechnen
Dolivostraße 10
Darmstadt, D-64293, Germany

(Communicated by the associate editor name)

ABSTRACT. We propose and analyze a mathematical model for wave propagation in infinite trees with self-similar structure at infinity. This emphasis is put on the construction and approximation of transparent boundary conditions. The performance of the constructed boundary conditions is then illustrated by numerical experiments.

Received xxxx 20xx; revised xxxx 20xx.

Introduction. In the recent years, there has been a surge of interest in the investigation of problems defined by partial differential equations along the edges of a network (or graph), with particular transmission conditions at the nodes (or vertexes) of the graph (please see [12, 14] for the usual terminology in graph theory). To cite only a few representative examples, see [26] for the case of an elliptic operator in a ramified domain, [30, 31] for the Helmholtz equation in a network seen as a limit of a two-dimensional thin domain, or [1] for the resolution of the Hamilton-Jacobi equation. Respective problems are typically referred to as problems posed on quantum graphs, see [11].

The works that inspired the present article concern the modeling of the respiratory system [23]. To a first approximation, the human lung can be seen as a network of many small tubes (the bronchioli) inside which the air flows. In some models [23], the tubes are assumed to be thin enough so that the air pressure is constant in each cross-section: as a consequence, each tube can be represented by a (1D) edge of a graph. In addition, to take into account that the number of bronchioli is very large, the bronchioli network is modeled as an infinite tree with some fractal and self-similarity properties (as defined in the reference monograph [22]). Finally, one models the air flow by solving the Laplace equation in such a network

2010 *Mathematics Subject Classification.* Primary: 35J05, 37E25, 65D15; Secondary: 35J20.

Key words and phrases. Laplace equation, Helmholtz equation, fractal, graph domain, boundary operator, functional approximation.

(which includes implicitly nodal transmission conditions). The infinite nature of the tree is indeed the main source of difficulty from both mathematical and numerical points of view. In particular, to complete the model, one needs to impose some "boundary condition at infinity" whose precise meaning requires to work with the weak formulation of the problem and an adequate functional framework, as explained in more detail later in the paper.

Our motivation was to study the propagation of sound in such a structure. This is important in applications since sound propagation in the human lung can be used for the detection of some pathologies of the respiratory system [27, 32]. Therefore, we have to study the wave equation (in short $\partial_t^2 u + \mathcal{A}u = 0$, where $\mathcal{A}$ is a second order differential operator along the tree), instead of the Laplace equation. One of the particularities / difficulties of our model is that we need to consider a weighted wave equation, in order to account for the fact that the bronchioli have different thicknesses. This model can be justified by an asymptotic analysis with respect to the small transverse dimensions of the bronchiolar tubes (see [18, 21]). From the physical point of view, such a model is somewhat unrealistic in the sense that it assumes that the boundaries of the bronchioli are rigid, neglecting the interaction with the parenchyma, which is the "elasto-acoustic" domain inside which the bronchioli network is embedded (see for instance [13] for the modelling of sound propagation inside the parenchyma, or [28] for the coupling issue, in the context of the air flow modelling). Thus, from the point of view of this particular application, studying this model has to be seen as a first step forward a more realistic modelling. Moreover, as we shall see in this paper, this "simple" model already raises exciting and challenging questions, from both mathematical and numerical points of view.

In particular, as far as numerical computations are concerned, the main source of difficulty is the infinite number of edges in the tree. Thus, we need to address the problem of truncating the computational domain to a finite subtree, which raises the question of the identification of the boundary condition [15] to be put at the artificial extremities of the truncated tree. This is the main motivation of this work. As we are going to see, we are able to give an answer to this question under the assumption that, after a certain generation, the subtrees are self-similar. It is worthwhile mentioning that the same type of questions was considered in a series of papers by Y. Achdou, N. Tchou and their collaborators: in these works, they do not study fractal trees but (particular) domains with a fractal boundary. In many papers they treat the Laplace operator [5, 6, 7], but also the time harmonic wave (Helmholtz) equation [3, 2, 4], for the solution of which they propose a particular iterative algorithm.

As a matter of fact, applying the Fourier-Laplace transform equation to the wave equation leads to study a family of Helmholtz equations parametrized by the frequency. This is the point of view that we shall adhere to for the construction of transparent boundary conditions. This approach emphasizes the close link between the properties of the solution of the wave equation and the spectral theory of the underlying elliptic operator $\mathcal{A}$. Such a theory has been extensively studied in the literature when $\mathcal{A}$ is the Laplace operator (see e.g. [36], [23]). However, those results concern only a special case of non-weighted Laplacians, and thus cannot be directly applied to our weighted "operator" $\mathcal{A}$. On the other hand, an eigenvalue problem for the Laplacian with weights was considered in [24]; nonetheless, the problem setting is quite different from ours and does not seem easily adaptable to the problem we consider. For other related problems, in particular, properties of Sobolev and L^p spaces on trees please see [25, 35, 34]. Let us finally remark that some properties of

weighted spaces on infinite graphs were studied in [16], however, in the context of the discrete Laplacian and respective energy norms.

The paper is organized as follows. In section 1, we provide a geometrical and functional framework for studying wave propagation problems defined on infinite trees. In particular, we define weighted Sobolev spaces on such trees, which allows to formulate rigorously the Dirichlet and Neumann problem on a tree, and to obtain the corresponding well-posedness result for the time-domain wave equation. Next, we discuss the question of the construction of transparent boundary conditions for truncating the computational domain to a finite tree. Such construction is based on a use of the Dirichlet-to-Neumann (DtN) operator. Finally, we recall some classical results about the well-posedness of the Helmholtz equation for complex frequencies, as well as the representation of the solution to the Helmholtz equation in the case when the resolvent of the Laplace operator is compact.

In section 2, we define a notion of a self-similar $p-$adic weighted tree. In this short section we introduce specific notation, which we will use throughout the paper. Section 3 is dedicated to various properties of the Sobolev spaces defined on self-similar p-adic weighted trees. Sections 3.1, 3.2 are devoted to a particular class of trees, for which prove the existence and continuity of a trace operator at infinity (section 3.1) and characterize its image and kernel (section 3.2). This operator is important for understanding the distinction between the Dirichlet and Neumann problems for this class of trees. This question is treated in complete detail in section 3.3. For the convenience of the reader, the summary of the results of sections 3.1-3.3 is given in section 3.4. Finally, in section 3.5, we study the crucial question of compactness of the embedding of Sobolev spaces, which governs the nature of the spectrum of the Laplacian and implies the meromorphicity of its resolvent.

Section 4 is dedicated to the analysis of the properties of the solutions of a family of Helmholtz equations parametrized by frequency. In particular, in section 4.1 we introduce the notion of quasi-self-similarity for functions depending on frequency, and show that on self-similar trees the solutions of the Helmholtz equation are quasi-self-similar. In section 4.2 we consider a particular case of the Lapace equation, for which the solutions are self-similar and can be obtained in explicit form.

Section 5 is devoted to various characterizations of transparent boundary conditions (the DtN operator) for the Helmholtz equation on self-similar trees. First of all, based on the results of the previous sections, we show the meromorphicity of the symbol of the DtN operator in section 5.1. In section 5.2 we demonstrate that it satisfies a certain non-linear equation. We prove in particular the uniqueness of the solution to this equation under appropriate conditions. Next, section 5.3 is dedicated to certain positivity properties of the symbol of the DtN, related to the stability of the transparent boundary conditions in the time domain. In section 5.4, we provide an algorithm for the evaluation of the symbol of the DtN for complex frequencies. The numerical results obtained with the help of this algorithm are given in section 5.5.

In section 6 we propose an approximation of the DtN operators that stems from the truncation of the Taylor series for their symbol. We thus obtain first- and second-order transparent boundary conditions, for which we prove the stability. Their efficiency is validated with the help of the numerical experiments.

Finally, section 7 is dedicated to the open questions and possible extensions of this work.

1. **Description of the problem.**

1.1. **The wave equation in a graph.** In this work we will conciliate the view of the graph as an algebraic structure with its vision as a geometric object, see [11]. A graph $\mathbb{G}$ is defined by a set of vertices $\boldsymbol{\mathcal{V}} := \{M_v,\ v \in \mathcal{V}\}$, seen geometrically as a subset of $\mathbb{R}^d$, $d = 2, 3$, and a set of edges $\boldsymbol{\mathcal{E}} := \{\Sigma_e,\ e \in \mathcal{E}\} \subset \boldsymbol{\mathcal{V}} \times \boldsymbol{\mathcal{V}}$, with $\mathcal{V}$, $\mathcal{E}$ being countable sets. We consider an oriented graph, i.e. two vertices $(M_v, M_{v'})$ are connected by at most one edge Σ_e identified to the segment $[M_v,\ M_{v'}] \subset \mathbb{R}^d$. This implies $M_v \neq M_{v'}$. This edge is given an orientation via an abscissa $s_e \in [a_e,\ b_e]$. The *origin* M_v corresponds to $s_e = a_e \in \mathbb{R}$, the *end* point $M_{v'}$ corresponds to $s_e = b_e := a_e + |M_{v'} - M_v|$, and also

$$\Sigma_e = \{M_v + (b_e - a_e)^{-1}(M_{v'} - M_v)(s_e - a_e), \quad s_e \in [a_e,\ b_e]\}.$$

By definition, M_v is the origin, and $M_{v'}$ is the end. This point of view allows to identify the algebraic object $\mathbb{G}$ with the geometric structure

$$\mathbb{G} = \bigcup_{e \in \mathcal{E}} \Sigma_e.$$

For any $v \in \mathcal{V}$, we denote by $\mathcal{E}_v$ the subset of $\mathcal{E}$ corresponding to all edges adjacent to M_v:

$$\mathcal{E}_v = \{e \in \mathcal{E} \ / \ M_v \in \Sigma_e\}. \tag{1}$$

We assume in the following that $\mathcal{E}_v$ is a finite set for all v. We use the notation s for the collection of the s_i's, which can be seen as a generalized coordinate along $\mathbb{G}$.
Let us finally remark that the dimension d does not play any role in the analysis of the problem considered in this article, but, as we will see in section 1.2, it occurs when interpreting the model studied in this work as a limit model defined in an open set in $\mathbb{R}^d$.

Definition 1.1 (Weight)**.** *A weight is a function $\mu : \mathbb{G} \to \mathbb{R}^+_*$ such that, on each edge Σ_e, μ is constant and takes the value μ_e.*

Remark 1.2. *Choosing the weight function μ constant along each edge is not essential but simplifies the presentation.*

Remark 1.3. *We will denote a graph $\mathbb{G}$, to which the weight μ is assigned, by $(\mathbb{G}, \mu)$.*

Definition 1.4 (Wave equation)**.** *A solution of the weighted wave equation on $\mathbb{G}$, with weight μ, is a function $u(s,t) : \mathbb{G} \times \mathbb{R}^+ \to \mathbb{R}$ satisfying, with $u_e = u|_{\Sigma_e}$,*

$$\partial_t^2 u_e - \partial_s^2 u_e = 0, \quad \text{on } \Sigma_e \times \mathbb{R}^+, \quad \forall\, e \in \mathcal{E}, \tag{2}$$

and at each node M_v of $\mathbb{G}$, which is an intersection of at least two edges, i. e. $\#\,\mathcal{E}_v \geqslant 2$,

$$\begin{cases} u_e(M_v, t) = u_{e'}(M_v, t), \quad \forall\, (e, e') \in \mathcal{E}_v^2 & (i) \\ \displaystyle\sum_{e \in \mathcal{E}_v} \varepsilon_{v,e}\, \mu_e\, \partial_s u_e(M_v, t) = 0, & (ii) \end{cases} \tag{3}$$

where μ_e is given by definition 1.1, and $\varepsilon_{v,e}$ depends of the orientation of Σ_e:

$$\varepsilon_{v,e} = \begin{cases} 1, & \text{if } v \text{ is the origin of } e, \\ -1, & \text{if } v \text{ is the end of } e. \end{cases} \tag{4}$$

Note that (3)(i) is nothing but the continuity of u at M_v while (3)(ii) is a generalized Kirchhoff condition. Equations (2) and (3) can be collected in a single equation, using a (very intuitive) notion of distributional derivative along $\mathbb{G}$, as follows

$$\mu\, \partial_t^2 u - \partial_s(\mu\, \partial_s u) = 0, \quad \text{on } \mathbb{G} \times \mathbb{R}^+, \tag{5}$$

where $\mu : \mathbb{G} \to \mathbb{R}^+_*$ is a piecewise constant function that takes the value μ_e along Σ_e. This will be made more precise in the next section in the case where $\mathbb{G}$ is a tree.

1.2. **A physical justification of the model (3).** One of the particularities of the model (3), at least with respect to more standard cases, is the presence of the weight function μ. As a matter of fact, this weight function occurs when considering the wave propagation in a 'thick' graph $\mathbb{G}^\delta$, which we can define as follows based on a given *finite* graph $\mathbb{G}$:

$$\mathbb{G}^\delta = \bigcup_{e\in\mathcal{E}} \Sigma_e^\delta, \quad \Sigma_e^\delta = \bigcup_{x\in\Sigma_e} \{x + \mu_e^{\frac{1}{d-1}}\, B(0,\delta)\},$$

where $\mathcal{E}$ is a finite set, and $B(0,\delta)$ is the open ball of $\mathbb{R}^d$ of center 0 and radius δ. One sees here that the coefficients μ_i are characteristic of the geometry of the "thick graph" $\mathbb{G}^\delta$. Then u, which solves (2), can be seen as the limit of the solution u^δ of the $d-$dimensional acoustic wave equation (with velocity 1) in $\mathbb{G}^\delta$ satisfying Neumann conditions on $\partial\mathbb{G}^\delta$ (see [21, 30, 18] for various justifications):

$$\partial_t^2 u^\delta - \Delta u^\delta = 0 \text{ in } \mathbb{G}^\delta, \quad \partial_n u^\delta = 0 \text{ on } \partial\mathbb{G}^\delta.$$

In [18], it is explained how the conditions (3) can be improved to get a more accurate model with respect to δ.

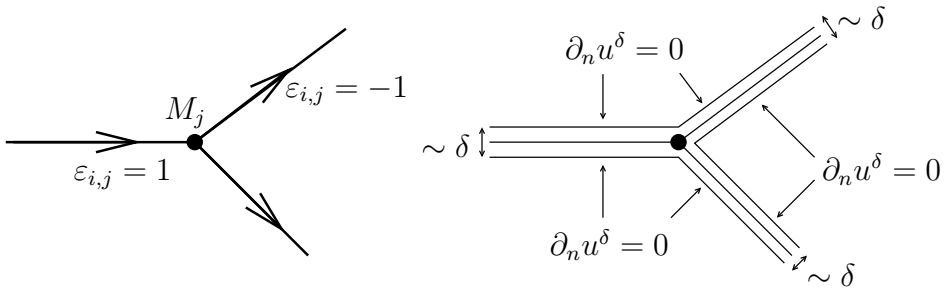

FIGURE 1. Left: the limit tree $\mathbb{G}$. Right: the thick tree $\mathbb{G}^\delta$.

1.3. **Infinite trees.** In the following, we consider a particular case where the graph $\mathbb{G}$ is an infinite rooted oriented tree, as illustrated by figure 2. The notation and terminology that we use below may deviate from a classical notation/terminology used in the graph theory, but are better adapted for our purposes.

First of all, let us provide an auxiliary definition.

Definition 1.5 (Child/parent of an edge and of a vertex)**.** *Given two oriented edges $\Sigma = [M_\star,\, M]$ and $\Sigma' = [M_\star{}',\, M']$, we will call Σ a parent of Σ' (or, equivalently, Σ' is a child of Σ) if $M \equiv M_\star{}'$. Accordingly, we shall say that the edge Σ is a parent of the vertex M, and Σ' is a child of the vertex M.*

Definition 1.6 (Rooted graph and a root)**.** *We shall say that a graph $\mathcal{T}$ is rooted if it has a unique edge that has no parents. This edge is called root and denoted Σ.*

Definition 1.7 (Tree)**.** *We will call a tree a rooted connected graph $\mathcal{T}$ that has no cycles (i.e. every two vertices are connected by a single path).*

The above definition is equivalent to saying that

- each edge (apart from the root) has only one parent;
- except from the origin of the root, each vertex has one parent.

Definition 1.8 (Generations of a tree)**.** *In a tree, we define a generation* $\mathcal{G}^n$, $n \in \mathbb{N}_0$, *as a union of edges of this tree as follows:*

- *the generation* $\mathcal{G}^0 = \{\Sigma\}$*;*
- *the generation* $\mathcal{G}^k$ *is a union of children of the edges belonging to* $\mathcal{G}^{k-1}$, $k \geqslant 1$.

Definition 1.9 (Infinite trees)**.** *If for all* $n \geqslant 0$, $\mathcal{G}^n \neq \emptyset$*, such a tree is called infinite.*

Evidently, an infinite tree, as a geometric object, satisfies

$$\mathcal{T} = \bigcup_{k \in \mathbb{N}_0} \mathcal{G}^k, \tag{6}$$

and in such trees each vertex M_v, $v \in \boldsymbol{\mathcal{V}}$ belongs to at most two successive generations. In what follows we will be using the notation $\mathcal{G}^n(\mathcal{T})$ instead of $\mathcal{G}^n$, to indicate that we are looking at the n-th generation of the graph $\mathcal{T}$. A typical example of infinite trees in $\mathbb{R}^2$ is provided in figure 2.

With the above definition, we can introduce the following notation:

- we will denote by $J(n)+1$ the number of the edges of the n-th generation $\mathcal{G}^n(\mathcal{T})$;
- $\mathcal{E}$ has a natural numbering with two indexes $e \equiv (n, j)$, with $n \in \mathbb{N}$ describing the numbering of the generation and $0 \leqslant j \leqslant J(n)$ with j corresponding to the edge numbering inside $\mathcal{G}^n(\mathcal{T})$:

$$\mathcal{G}^n(\mathcal{T}) = \bigcup_{j=0}^{J(n)} \Sigma_{n,j}. \quad \text{In particular, with this notation, } \Sigma_{0,0} = \Sigma. \tag{7}$$

- for each $n \in \mathbb{N}$, $0 \leqslant j \leqslant J(n)$, we shall write $\Sigma_{n,j} = [M^*_{n,j},\, M_{n,j}]$.

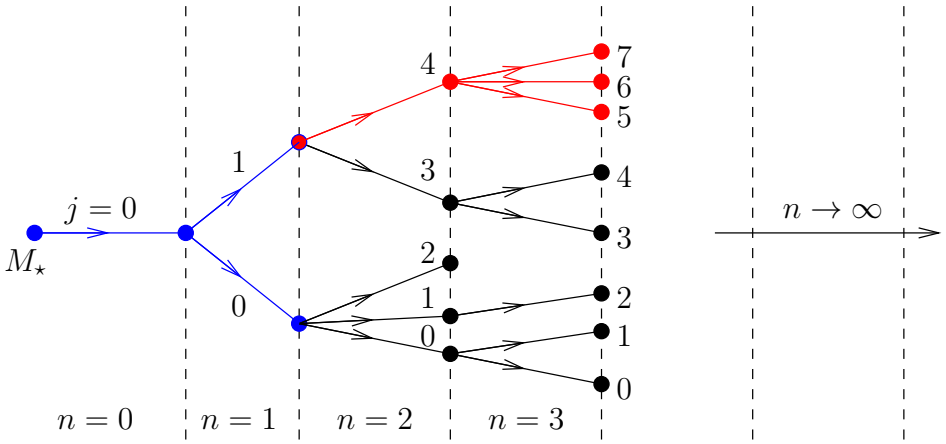

FIGURE 2. General tree. We numbered here the edges. We plotted in red the subtree $\mathcal{T}_{2,4}$ and in blue the truncated tree $\mathcal{T}^1$.

Let us define the set of children indices of a given vertex $M_{n,j}$:

$$\mathcal{C}_{n,j} := \{k \in [0, J(n)] / \ \Sigma_{n+1,k} \text{ is a child of } M_{n,j}\}. \tag{8}$$

According to (8) and to the orientation of the tree, the Kirchhoff condition (3)(ii) at $M_{n,j}$ can be rewritten, with $u_{n,j} = u|_{\Sigma_{n,j}}$, as

$$\mu_{n,j}\,\partial_s u_{n,j}(M_{n,j}) = \sum_{k\in\mathcal{C}_{n,j}} \mu_{n+1,k}\,\partial_s u_{n+1,k}(M_{n,j}), \tag{9}$$

where $\mu_{n,j}$ is the weight associated to the edge $\Sigma_{n,j}$.
For convenience, we denote the value of a continuous function u in a vertex $M_{n,j}$ by

$$\mathbf{u}_{n,j} = u(M_{n,j}). \tag{10}$$

Definition 1.10 (Truncated tree)**.** *We denote by $\mathcal{T}^n$ the truncated tree at generation n, i. e. the union of the m-th generations $\mathcal{G}^m(\mathcal{T})$, for $m \leqslant n$ (see figure 2 for $\mathcal{T}^1$).*

Definition 1.11 (Subtree)**.** *For any $(n,j) \in \mathcal{I}$, we denote by $\mathcal{T}_{n,j}$ a subtree with the root $\Sigma_{n,j}$, that constitutes the largest connected subgraph of $\mathcal{T}\setminus\mathcal{T}^{n-1}$ that contains $M_{n,j}$ (and none of the $M_{n,k}$, for $k \neq j$).*

For an illustration of the notion of the subtree see figure 2 for $\mathcal{T}_{2,4}$. It is not difficult to notice that $\mathcal{T}\setminus\mathcal{T}^{n-1}$ is the union of the subtrees $\mathcal{T}_{n,j}$ for $0 \leqslant j \leqslant J(n)$.

One of the goals of this work is to study the wave equation on such infinite trees. Of course, in this case the wave equation needs to be completed by a boundary condition at the root $M_\star$ of the tree, for instance the Dirichlet entrance condition ($f(t)$ represents the source term)

$$u(M_\star, t) = f(t), \tag{11}$$

by the boundary conditions on the leaves of the tree (which we will discuss in a moment), by initial conditions, for instance homogeneous initial conditions

$$u(\cdot,0) = \partial_t u(\cdot,0) = 0, \quad \text{in } \mathcal{T}, \tag{12}$$

but also, in general, by a "boundary condition at infinity", which is trickier to define and will be made precise in Section 1.5.

In the following we shall very soon restrict our discussion to **compact** trees.

Definition 1.12 (Compact tree)**.** *Let $\mathcal{T}$ be a tree. An path of $\mathcal{T}$ is by definition a connected (possibly infinite) union of edges of $\mathcal{T}$. By definition, the tree is compact if there exists a uniform bound for the lengths of all paths of $\mathcal{T}$. This implies in particular that $\mathcal{T}$ is included in a compact set of $\mathbb{R}^d$, for some $d \geqslant 1$.*

In what follows, we will study only the following subclass of infinite trees.

Assumption 1.13. *A tree $\mathcal{T}$ is compact and has no leaves.*

1.4. **Functional spaces on a weighted tree.** Let us first consider a very degenerate case of an infinite tree. Given $L > 0$, $\mu \equiv 1$, $\alpha \in (0,1)$, let us set $x_0 = 0$ and

$$x_{n+1} := L\,(1-\alpha)\sum_{\ell=0}^{n} \alpha^\ell = L\,(1-\alpha^{n+1}), \quad n \in \mathbb{N},$$

that form a strictly increasing sequence of real numbers $x_n \to L$, as $n \to \infty$ (see figure 3 for $\alpha = 0.5$). We can construct a corresponding "1D tree", defined as follows:

$$J(n) = 0, \quad M_n = x_{n+1}, \quad \Sigma_{n,0} = [x_n, x_{n+1}], \quad \forall\, n \geqslant 0.$$

In this case, each generation $\mathcal{G}^n(\mathcal{T})$ is reduced to the segment $[x_n, x_{n+1}]$, and we thus

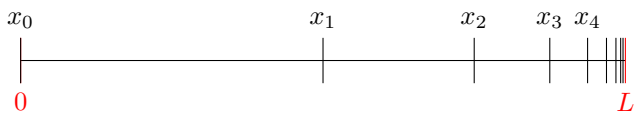

FIGURE 3. "1D tree" corresponding to the case $\alpha = 0.5$.

have

$$\mathcal{T} = \bigcup_{n=0}^{+\infty} [x_n, x_{n+1}] = [0, L), \tag{13}$$

It is then easy to check that the wave equation (2, 3) on such a tree is nothing but the 1D wave equation along $(0, L)$. Indeed, we need to equip it with proper boundary conditions, in the root vertex x_0, and at the 'infinite' boundary of the tree $x = L$. The natural space in which, for each $t \geqslant 0$, finite energy solutions $u(., t)$ of (5) live, is the Sobolev space $\mathrm{H}^1(0, L)$. Our goal in this paragraph is to define the equivalent of such a space in a weighted infinite tree, as it was done in similar situations in [23]. In the following, when not explicitly mentioned, the functions we consider can be real- or complex-valued, depending on the context.

Definition 1.14 (Functional spaces)**.** *Let $(\mathcal{T}, \mu)$ be a weighted tree.*

1. *Lebesgue space of square-integrable functions. We denote by $\mathrm{L}^2_\mu(\mathcal{T})$ the set of functions $u : \mathcal{T} \to \mathbb{C}$ having a finite $\mathrm{L}^2_\mu(\mathcal{T})$-norm, namely*

$$\|u\|^2_{\mathrm{L}^2_\mu(\mathcal{T})} = \int_{\mathcal{T}} \mu\, |u|^2 := \sum_{n\geqslant 0} \sum_{j=0}^{J(n)} \mu_{n,j}\, \|u\|^2_{\mathrm{L}^2(\Sigma_{n,j})} < +\infty \tag{14}$$

2. *Sobolev space. We denote by $\mathrm{H}^1_\mu(\mathcal{T})$ the space made of continuous $\mathrm{L}^2_\mu(\mathcal{T})$ functions $u : \mathcal{T} \to \mathbb{C}$ having a finite $\mathrm{H}^1_\mu(\mathcal{T})$-semi-norm, namely*

$$|u|^2_{\mathrm{H}^1_\mu(\mathcal{T})} = \int_{\mathcal{T}} \mu\, |\partial_s u|^2 := \sum_{n\geqslant 0} \sum_{j=0}^{J(n)} \mu_{n,j}\, \|\partial_s u\|^2_{\mathrm{L}^2(\Sigma_{n,j})} < +\infty, \tag{15}$$

and the $\mathrm{H}^1_\mu(\mathcal{T})$-norm of u is defined by

$$\|u\|^2_{\mathrm{H}^1_\mu(\mathcal{T})} := \|u\|^2_{\mathrm{L}^2_\mu(\mathcal{T})} + |u|^2_{\mathrm{H}^1_\mu(\mathcal{T})}\,. \tag{16}$$

All the above spaces are then obviously equipped with a Hilbert space structure and will provide an adequate framework for studying the wave equation on $\mathcal{T}$.

Notation. In what follows, for any $(u, v) \in \mathrm{L}^2_\mu(\mathcal{T})$ we shall denote

$$\int_{\mathcal{T}} \mu\, u\, v := \sum_{n\geqslant 0} \sum_{j=0}^{J(n)} \mu_{n,j} \int_{\Sigma_{n,j}} u_{n,j}\, \overline{v_{n,j}}\, ds, \quad u_{n,j} := u|_{\Sigma_{n,j}}, v_{n,j} := v|_{\Sigma_{n,j}}. \tag{17}$$

1.5. **Dirichlet and Neumann initial boundary value problems.** We are now in position to provide a rigorous definition of the problems that we are interested in. Let us first explain our approach for the case when $\mathcal{T}$ is the degenerate tree (13), *i. e.* $\mathcal{T} \equiv [0, L)$. In this tree $x = L$ would correspond to "the boundary at infinity" of the tree. As it is well-known,

there are two standard homogeneous boundary conditions at $x = L$ that can be associated with the 1D wave equation along $(0,\ L)$, namely

$$\partial_s u(L,t) = 0 \quad \text{(Neumann condition)}, \quad u(L,t) = 0 \quad \text{(Dirichlet condition)}.$$

These conditions are perfectly reflecting: in particular, they are energy preserving in the absence of the source term. We consider below the generalization of these boundary conditions for a general infinite tree $\mathcal{T}$. For this, we shall pass through the notion of weak solution of the wave equation that reduces the distinction between Dirichlet and Neumann conditions to the distinction between the functional spaces in which the solution is searched and the test functions live. Since the Dirichlet condition is systematically considered at the entrance of the tree, see (11), the denomination Dirichlet or Neumann only refers to the condition at infinity. We begin with the Neumann condition.

The Neumann initial boundary value problem $(\mathcal{P}_\mathfrak{n})$. Provided the Hilbert space

$$V_\mathfrak{n} = \{v \in \mathrm{H}^1_\mu(\mathcal{T}) \ / \ v(M_\star) = 0 \ \}, \tag{18}$$

which is a closed subspace of $\mathrm{H}^1_\mu(\mathcal{T})$, the Neumann problem $(\mathcal{P}_\mathfrak{n})$ reads

$$\left\{ \begin{array}{l} \text{Find } u \in C^2\big(0,T;\mathrm{L}^2_\mu(\mathcal{T})\big) \cap C^1\big(0,T;\mathrm{H}^1_\mu(\mathcal{T})\big) \quad \text{s. t. } \ u(M_\star,t) = f(t), \\ u(.,0) = \partial_t u(.,0) = 0 \ \text{ and} \\ \dfrac{d^2}{dt^2}\displaystyle\int_\mathcal{T} \mu\, u(\cdot,t)\, v + \int_\mathcal{T} \mu\, \partial_s\, u(\cdot,t) \partial_s v = 0, \ \forall\ v \in V_\mathfrak{n}. \end{array} \right. \tag{$\mathcal{P}_\mathfrak{n}$}$$

In the case of the degenerate tree (13), $V_\mathfrak{n} = \{u \in \mathrm{H}^1(0,L) \ / \ u(0) = 0\}$. For the Dirichlet condition, one should replace in the weak formulation $V_\mathfrak{n}$ by $V_\mathfrak{d} = \{u \in V_\mathfrak{n} \ / \ u(L) = 0\}$, which is also characterized as the closure in $V_\mathfrak{n}$ of compactly supported in $(0,L)$ functions of $V_\mathfrak{n}$. We shall adapt this approach to define the corresponding problems in the case of an infinite tree. We first define the subspace of $\mathrm{H}^1_\mu(\mathcal{T})$, which consists of functions that "vanish at infinity" in the following way.

Definition 1.15. *Let $(\mathcal{T},\mu)$ be a weighted tree.*

1. *$\mathrm{H}^1_{\mu,c}(\mathcal{T})$ is the subspace of $\mathrm{H}^1_\mu(\mathcal{T})$ of compactly supported functions, i. e.*

$$\mathrm{H}^1_{\mu,c}(\mathcal{T}) = \big\{ v \in \mathrm{H}^1_\mu(\mathcal{T}) \quad \textit{such that} \quad \exists\ N \in \mathbb{N} \ / \ v = 0 \textit{ in } \mathcal{T} \setminus \mathcal{T}^N \big\}. \tag{19}$$

2. *$\mathrm{H}^1_{\mu,0}(\mathcal{T})$ the closure of $\mathrm{H}^1_{\mu,c}(\mathcal{T})$ in $\mathrm{H}^1_\mu(\mathcal{T})$:*

$$\mathrm{H}^1_{\mu,0}(\mathcal{T}) = \overline{\mathrm{H}^1_{\mu,c}(\mathcal{T})}^{\mathrm{H}^1_\mu(\mathcal{T})}. \tag{20}$$

Remark 1.16. *As one can expect, in certain cases, the space $\mathrm{H}^1_{\mu,0}(\mathcal{T})$ can be related to the closed subspace of $\mathrm{H}^1_\mu(\mathcal{T})$, whose "trace at infinity" (defined in a certain way) vanishes. This will be made more precise in the case of a p-adic self-similar tree in section 3.2.*

The Dirichlet initial boundary value problem $(\mathcal{P}_\mathfrak{d})$. Provided the Hilbert space

$$V_\mathfrak{d} = \{v \in \mathrm{H}^1_{\mu,0}(\mathcal{T}) \ / v(M_\star) = 0 \ \}, \tag{21}$$

which is a closed subspace of $\mathrm{H}^1_{\mu,0}(\mathcal{T})$, the Dirichlet problem $(\mathcal{P}_\mathfrak{d})$ reads

$$\left\{\begin{array}{l} \text{Find } u \in C^2\big(0,T;\mathrm{L}^2_\mu(\mathcal{T})\big) \cap C^1\big(0,T;\mathrm{H}^1_{\mu,0}(\mathcal{T})\big) \quad \text{s. t. } \ u(M_\star,t) = f(t), \\ u(.,0) = \partial_t u(.,0) = 0 \ \ \text{and} \\ \dfrac{d^2}{dt^2}\displaystyle\int_{\mathcal{T}} \mu\, u(\cdot,t)\, v + \int_{\mathcal{T}} \mu\, \partial_s u(\cdot,t)\, \partial_s v = 0, \ \forall v \in V_\mathfrak{d}. \end{array}\right. \tag{$\mathcal{P}_\mathfrak{d}$}$$

Let us state, without proof, a classical result about problems $(\mathcal{P}_\mathfrak{n})$ and $(\mathcal{P}_\mathfrak{d})$.

Proposition 1.17. *Let $T \in \mathbb{R}^+_*$, and let $f \in C^2([0,T])$, with $f(0) = f'(0) = 0$. Then, the problem $(\mathcal{P}_\mathfrak{n})$ (resp. $(\mathcal{P}_\mathfrak{d})$) admits a unique solution.*

When one considers the problem of the numerical approximation of $(\mathcal{P}_\mathfrak{n})$ and $(\mathcal{P}_\mathfrak{d})$, one immediately faces the question of truncating the tree after a finite number of generations and constructing corresponding transparent or absorbing boundary conditions, which is the main objective of the present paper.

1.6. **About the construction of transparent boundary conditions.** Numerically, a natural objective would be to restrict the computation to the solution u of $(\mathcal{P}_\mathfrak{n})$ or $(\mathcal{P}_\mathfrak{d})$ to a truncated tree $\mathcal{T}^n$ by imposing some (transparent) Dirichlet-to-Neumann (DtN) condition at each end point $M_{n,j}$ of $\mathcal{T}^n$. This can be made by combining the Kirchhoff condition (9) with the use of DtN operators $\Lambda_{n+1,k}$ associated to each of the subtrees $\big\{\mathcal{T}_{n+1,k},\ k \in \mathcal{C}_{n,j}\big\}$. More precisely, $\varphi(t) \mapsto \Lambda_{n+1,k}\ \varphi(t)$ is the DtN operator

$$\Lambda_{n+1,k}\ \varphi(t) := -\partial_s \widetilde{u}^{\varphi}_{n+1,k}(M_{n,j},t), \tag{22}$$

where $\widetilde{u}^{\varphi}_{n+1,k}(\cdot,t) : \mathcal{T}_{n+1,k} \mapsto \mathbb{R}$ is defined on the subtree $\mathcal{T}_{n+1,k}$ as the unique solution of the Dirichlet (or Neumann) problem (in the sense of section 1.5) of the wave equation, posed in the subtree $\mathcal{T}_{n+1,k}$, with the Dirichlet condition at the root vertex of this tree $M_{n,j}$ $\widetilde{u}^{\varphi}_{n+1,k}(M_{n,j},t) = \varphi(t)$.

The transparent condition at the end point $M_{n,j}$ then relates $u_{n,j}(M_{n,j},.)$ to $\partial_s u_{n,j}(M_{n,j},.)$ according to

$$\mu_{n,j}\, \partial_s u_{n,j}(M_{n,j},\cdot) + \mathcal{B}_{n,j}\ u_{n,j}(M_{n,j},\cdot) = 0, \tag{23}$$

where

$$\mathcal{B}_{n,j}\ u_{n,j}(M_{n,j},\cdot) = \sum_{k \in \mathcal{C}_{n,j}} \mu_{n+1,k}\ \Lambda_{n+1,k}\ u_{n,j}(M_{n,j},\cdot). \tag{24}$$

Since the wave equation has constant coefficients in time, it is clear that $\Lambda_{n+1,k}$ is a time convolution operator. More precisely, using the Fourier-Laplace transform in time

$$\widehat{g}(\omega) = (\mathcal{F}g)(\omega) = \int_0^\infty g(t)\exp(\imath\omega t)\, dt, \quad \omega \in \mathbb{C}, \quad \mathcal{I}m\,\omega > 0, \tag{25}$$

we get a relation of the form

$$(\mathcal{F}\Lambda_{n+1,k}\varphi)(\omega) = \mathbf{\Lambda}_{n+1,k}(\omega)\ \mathcal{F}\varphi(\omega). \tag{26}$$

The symbol $\mathbf{\Lambda}_{n+1,k}(\omega)$ is given by

$$\mathbf{\Lambda}_{n+1,k}(\omega) := -\partial_s \widehat{u}_{n+1,k}(M_{n,j},\omega), \tag{27}$$

where $\widehat{u}_{n+1,k}(\cdot,\omega)$ is the solution of the (Dirichlet or Neumann, we omit for simplicity the condition at infinity) Helmholtz problem

$$\begin{cases} -\mu\,\omega^2\,\widehat{u}_{n+1,k}(\cdot,\omega) - \partial_s(\mu\,\partial_s\widehat{u}_{n+1,k})(\cdot,\omega) = 0, \quad s \in \mathcal{T}_{n+1,k},\ k \in \mathcal{C}_{n,j}, \\ \widehat{u}_{n+1,k}(M_{n,j},\omega) = 1. \end{cases} \tag{$\mathcal{P}_{\mathrm{H}}$}$$

At this point, we have not advanced much, since the computation of the symbol $\mathbf{\Lambda}_{n+1,k}$ requires solution of a subtree problem which is as difficult as the original problem! However, this problem can be simplified when the tree $\mathcal{T}$ admits, starting from the n-th generation, a certain structure. In particular, we shall investigate in this paper trees with such a structure, namely, **fractal** trees [22], for which, at least for n large enough, all subtrees $(\mathcal{T}_{n,j},\mu)$ are self-similar weighted trees, as defined in section 2.

We finish this section by some results on the Helmholtz equation in general trees, in particular, the well-posedness and the meromorphicity of the solution with respect to the frequency for some particular classes of trees.

1.7. **Helmholtz equation in general trees: basic results.** We consider the following problem on a weighted tree $(\mathcal{T},\,\mu)$. Given a complex frequency $\omega \in \mathbb{C}$, we look for the solution $u : \mathcal{T} \to \mathbb{C}$ to the Helmholtz equation with non-homogeneous Dirichlet data at the entrance of the tree

$$\begin{cases} -\mu\,\omega^2 u - \partial_s(\mu\,\partial_s u) = 0 \qquad \text{in } \mathcal{T}, \\ u(M_\star) = 1, \end{cases} \tag{28}$$

completed, like the wave equation in section 1.5, by a homogeneous (Dirichlet or Neumann) condition at infinity. More rigorously, using the functional framework of section 1.4 and the Hilbert spaces $V_{\mathfrak{n}}$ and $V_{\mathfrak{d}}$ introduced in section 1.5 by (18) and (21), we can define the Dirichlet and Neumann (at infinity) problems as follows

$$\begin{cases} \text{Find } u \in \mathrm{H}^1_{\mu}(\mathcal{T}) \,/\, u(M_\star) = 1, \text{such that} \\ \displaystyle\int_{\mathcal{T}} \mu\,\partial_s u\,\partial_s v - \omega^2 \int_{\mathcal{T}} \mu\,u\,v = 0, \quad \forall v \in V_{\mathfrak{n}}, \end{cases} \tag{$\mathcal{P}_{\mathfrak{n},\omega}$}$$

$$\begin{cases} \text{Find } u \in \mathrm{H}^1_{\mu,0}(\mathcal{T}) \,/\, u(M_\star) = 1, \text{such that} \\ \displaystyle\int_{\mathcal{T}} \mu\,\partial_s u\,\partial_s v - \omega^2 \int_{\mathcal{T}} \mu\,u\,v = 0, \quad \forall v \in V_{\mathfrak{d}}. \end{cases} \tag{$\mathcal{P}_{\mathfrak{d},\omega}$}$$

1.7.1. *Existence and uniqueness results.* For these two problems, we can immediately state the well-posedness result for non-real frequencies.

Proposition 1.18. *For each $\omega \notin \mathbb{R}$, ($\mathcal{P}_{\mathfrak{n},\omega}$) (resp. ($\mathcal{P}_{\mathfrak{d},\omega}$)) admits a unique solution*

$$u_{\mathfrak{n}}(\cdot,\omega) \qquad (\textit{resp. } u_{\mathfrak{d}}(\cdot,\omega)). \tag{29}$$

Proof. It is a simple application of the Lax-Milgram theorem left to the reader. □

Since μ is real-valued,

$$\text{for } \mathfrak{a} = \mathfrak{n},\mathfrak{d}, \quad \forall\,\omega \notin \mathbb{R}, \quad u_{\mathfrak{a}}(\cdot,-\omega) = u_{\mathfrak{a}}(\cdot,\omega), \quad u_{\mathfrak{a}}(\cdot,\overline{\omega}) = \overline{u_{\mathfrak{a}}(\cdot,\omega)}. \tag{30}$$

A complementary point of view consists in introducing the two unbounded positive self-adjoint operators in $\mathcal{H} := \mathrm{L}^2_{\mu}(\mathcal{T})$, namely $\mathcal{A}_{\mathfrak{d}}$ and $\mathcal{A}_{\mathfrak{n}}$, associated to ($\mathcal{P}_{\mathfrak{d},\omega}$) and ($\mathcal{P}_{\mathfrak{n},\omega}$). Namely, given a sesquilinear form

$$a(u,v) := \int_{\mathcal{T}} \mu\,\partial_s u\,\partial_s v,$$

we define these operators as follows:

$$\begin{cases} D(\mathcal{A}_{\mathfrak{d}}) = \big\{ u \in V_{\mathfrak{d}} \ / \ \exists\, C > 0 \text{ such that } |a(u,v)| \leqslant C\, \|v\|_{\mathrm{L}^2_\mu(\mathcal{T})}, \forall\, v \in V_{\mathfrak{d}} \big\}, \\ \forall\, u \in D(\mathcal{A}_{\mathfrak{d}}), \quad (\mathcal{A}_{\mathfrak{d}} u, v)_{\mathrm{L}^2_\mu(\mathcal{T})} = a(u,v), \quad \forall\, v \in V_{\mathfrak{d}}; \end{cases} \tag{31}$$

$$\begin{cases} D(\mathcal{A}_{\mathfrak{n}}) = \big\{ u \in V_{\mathfrak{n}} \ / \ \exists\, C > 0 \text{ such that } |a(u,v)| \leqslant C\, \|v\|_{\mathrm{L}^2_\mu(\mathcal{T})}, \forall\, v \in V_{\mathfrak{n}} \big\}, \\ \forall\, u \in D(\mathcal{A}_{\mathfrak{n}}), \quad (\mathcal{A}_{\mathfrak{n}} u, v)_{\mathrm{L}^2_\mu(\mathcal{T})} = a(u,v), \quad \forall\, v \in V_{\mathfrak{n}}. \end{cases} \tag{32}$$

It is easy to check that, defining

$$\widetilde{\mathrm{H}}^2_\mu(\mathcal{T}) = \Big\{ v \in \mathrm{H}^1_\mu(\mathcal{T}) :\ v_{n,j} \in \mathrm{H}^2(\Sigma_{n,j}),\ 0 \leqslant j \leqslant p^n - 1,\ n \geqslant 0, \text{ and satisfies (33)} \Big\},$$

$$\sum_{n=0}^{\infty} \sum_{j=0}^{p^n-1} \int_{\Sigma_{n,j}} \mu |\partial_s^2 v_{n,j}|^2 < \infty. \tag{33}$$

the domains of the operators $\mathcal{A}_{\mathfrak{d}}$, $\mathcal{A}_{\mathfrak{n}}$ are given by

$$\begin{cases} D(\mathcal{A}_{\mathfrak{d}}) = \big\{ u \in V_{\mathfrak{d}} \ / u \in \widetilde{\mathrm{H}}^2_\mu(\mathcal{T}), \text{ and (9) holds} \big\}, \\ D(\mathcal{A}_{\mathfrak{n}}) = \big\{ u \in V_{\mathfrak{n}} \ / u \in \widetilde{\mathrm{H}}^2_\mu(\mathcal{T}), \text{ and (9) holds} \big\}, \end{cases} \tag{34}$$

and thus $D(\mathcal{A}_{\mathfrak{d}}) \subseteq D(\mathcal{A}_{\mathfrak{n}})$. These operators are positive definite since

$$\forall\, u \in V_{\mathfrak{n}}, \quad a(u,u) = \int_{\mathcal{T}} \mu\, |\partial_s u|^2 \quad \text{and} \quad a(u,u) = 0 \Rightarrow u = 0 \quad (u(M_\star) = 0). \tag{35}$$

The solutions to the problems ($\mathcal{P}_{\mathfrak{n},\omega}$) and ($\mathcal{P}_{\mathfrak{d},\omega}$) can be expressed via the resolvents of the operators defined above as follows. Let u_r be a function supported in $\Sigma_{0,0}$, $u_r(M_\star) = 1$ and $u_r \in \mathrm{H}^2(\Sigma_{0,0})$. With

$$f_r(\omega) := \mu^{-1} \left[\partial_s \big(\mu\, \partial_s u_r \big) + \omega^2\, \mu\, u_r \right] \in \mathrm{L}^2_\mu(\mathcal{T}), \tag{36}$$

the functions $u_{\mathfrak{n}}(\cdot,\omega)$ and $u_{\mathfrak{d}}(\cdot,\omega)$ are given by

$$u_{\mathfrak{n}}(\cdot,\omega) = u_r + \big(\mathcal{A}_{\mathfrak{n}} - \omega^2 \big)^{-1}\, f_r(\omega), \quad u_{\mathfrak{d}}(\cdot,\omega) = u_r + \big(\mathcal{A}_{\mathfrak{d}} - \omega^2 \big)^{-1}\, f_r(\omega). \tag{37}$$

From standard properties of the resolvent of self-adjoint operators [19, 29], we deduce the

Proposition 1.19. *The functions $\omega \mapsto u_{\mathfrak{d}}(\cdot,\omega)$ and $\omega \mapsto u_{\mathfrak{n}}(\cdot,\omega)$ are analytic functions in $\mathbb{C} \setminus \mathbb{R}$ with values in $D(\mathcal{A}_{\mathfrak{d}})$ and $D(\mathcal{A}_{\mathfrak{n}})$ (equipped with their graph norm) respectively.*

1.7.2. *The compact case : meromorphicity with respect to the frequency.* Let us consider the case when one of the two following assumptions holds true:

$$(Compactness) \quad \begin{cases} (\mathfrak{d}) & \text{The injection } V_{\mathfrak{d}} \subset \mathrm{L}^2_\mu(\mathcal{T}) \text{ is compact.} \\ (\mathfrak{n}) & \text{The injection } V_{\mathfrak{n}} \subset \mathrm{L}^2_\mu(\mathcal{T}) \text{ is compact.} \end{cases} \tag{38}$$

Of course, (38)-$\mathfrak{n}$ is stronger than (38)-$\mathfrak{d}$. Both assumptions rely on properties of the tree and the weight function μ. For instance, in the case where $\mu = 1$, it is shown in [36] that the compactness of the tree (cf. definition 1.12) is a sufficient condition for (38)-$\mathfrak{n}$ and (38)-$\mathfrak{d}$ to hold. We shall investigate this question in more detail in the case of fractal trees in section 3.5.

The properties (38)-$\mathfrak{n}$, (38)-$\mathfrak{d}$ play an important role in this article. If (38)-$\mathfrak{n}$ (resp. (38)-$\mathfrak{d}$) holds, the operator $\mathcal{A}_\mathfrak{n}$ (resp. $\mathcal{A}_\mathfrak{d}$) has a compact resolvent, and thus its spectrum is a pure point spectrum with strictly positive eigenvalues (here repeated with their multiplicities):

$$\begin{cases} \text{(38)-}\mathfrak{n} \;\Rightarrow\; \sigma(\mathcal{A}_\mathfrak{n}) = \{(\omega_\mathfrak{n}^n)^2, n \geqslant 1\}, \quad \omega_\mathfrak{n}^{n+1} \geqslant \omega_\mathfrak{n}^n > 0, \quad \lim_{n\to+\infty} \omega_\mathfrak{n}^n = +\infty, \\ \text{(38)-}\mathfrak{d} \;\Rightarrow\; \sigma(\mathcal{A}_\mathfrak{d}) = \{(\omega_\mathfrak{d}^n)^2, n \geqslant 1\}, \quad \omega_\mathfrak{d}^{n+1} \geqslant \omega_\mathfrak{d}^n > 0, \quad \lim_{n\to+\infty} \omega_\mathfrak{d}^n = +\infty. \end{cases} \tag{39}$$

Remark 1.20. *Let us remark that $\omega = 0$ is not an eigenvalue of $\mathcal{A}_\mathfrak{n}$ and $\mathcal{A}_\mathfrak{d}$. This can be shown by contradiction. If $\omega = 0$ were an eigenvalue and u an associated eigenfunction, then this would imply, in particular, that $a(u,u) = 0$, and hence $\partial_s u = 0$. Since $u(M_\star) = 0$, necessarily, $u = 0$.*

The corresponding eigenfunctions, which form a Hilbert basis in $\mathrm{L}^2_\mu(\mathcal{T})$, are

$$\begin{cases} \{\varphi_\mathfrak{n}^n, n \geqslant 1\}, \quad \varphi_\mathfrak{n}^n \in D(\mathcal{A}_\mathfrak{n}), \quad \mathcal{A}_\mathfrak{n}\,\varphi_\mathfrak{n}^n = (\omega_\mathfrak{n}^n)^2\,\varphi_\mathfrak{n}^n, \\ \{\varphi_\mathfrak{d}^n, n \geqslant 1\}, \quad \varphi_\mathfrak{d}^n \in D(\mathcal{A}_\mathfrak{d}), \quad \mathcal{A}_\mathfrak{d}\,\varphi_\mathfrak{d}^n = (\omega_\mathfrak{d}^n)^2\,\varphi_\mathfrak{d}^n. \end{cases} \tag{40}$$

In particular, under the assumption (38)-$\mathfrak{n}$ (correspondingly, (38)-$\mathfrak{d}$), the zero-frequency Neumann (Dirichlet) problem is well-posed. This result is classical (hence we provide no proof here) and relies on the Lax-Milgram theorem combined with the Poincaré inequality for $V_\mathfrak{d}$ ($V_\mathfrak{n}$), the latter valid because of the compactness assumption and the fact that $\omega = 0$ is not an eigenvalue of $\mathcal{A}_\mathfrak{d}$ ($\mathcal{A}_\mathfrak{n}$), see remark 1.20 (see e.g. [37, Theorem 2.6]).

Lemma 1.21 (Poincaré inequality)**.** *If (38)-$\mathfrak{n}$ (resp. (38)-$\mathfrak{d}$) holds, then*

$$\|u\|_{\mathrm{L}^2_\mu(\mathcal{T})} \leqslant C\|\partial_s u\|_{\mathrm{L}^2_\mu(\mathcal{T})}, \qquad \text{for all } u \in V_\mathfrak{n} \text{ (resp. } u \in V_\mathfrak{d}). \tag{41}$$

The well-posedness result then reads.

Lemma 1.22. *If (38)-$\mathfrak{n}$ (resp. (38)-$\mathfrak{d}$) holds, the problem ($\mathcal{P}_{\mathfrak{n},\omega}$) (resp. ($\mathcal{P}_{\mathfrak{d},\omega}$)) for $\omega = 0$ admits a unique solution denoted by $u_\mathfrak{n}(.,0)$ (resp. $u_\mathfrak{d}(.,0)$).*

We will use the above lemma and (37) to express the solution to the (Dirichlet or Neumann) Helmholtz problems in the basis of the corresponding eigenfunctions.

Proposition 1.23. *If (38)-$\mathfrak{n}$ holds, the function $u_\mathfrak{n}(\cdot,\omega) : \mathbb{C} \ni \omega \to \mathrm{H}^1_\mu(\mathcal{T})$ is an even meromorphic function in $\mathbb{C}$ with poles $\{\pm\omega_\mathfrak{n}^n, n \geqslant 1\}$. It is given by*

$$u_\mathfrak{n}(\cdot,\omega) = u_\mathfrak{n}(.,0) + \sum_{n=0}^{+\infty} \frac{\omega^2 c_\mathfrak{n}^n}{(\omega_\mathfrak{n}^n)^2 - \omega^2}\,\varphi_\mathfrak{n}^n, \qquad c_\mathfrak{n}^n = \partial_s\varphi_\mathfrak{n}^n(M_\star)\,(\omega_\mathfrak{n}^n)^{-2}\,. \tag{42}$$

Similarly, if (38)-$\mathfrak{d}$ holds, $u_\mathfrak{d}(\cdot,\omega) : \mathbb{C} \ni \omega \to \mathrm{H}^1_{\mu,0}(\mathcal{T})$ is an even meromorphic function in $\mathbb{C}$ with poles $\{\pm\omega_\mathfrak{d}^n, n \geqslant 1\}$. It is given by

$$u_\mathfrak{d}(\cdot,\omega) = u_\mathfrak{d}(.,0) + \sum_{n=0}^{+\infty} \frac{\omega^2 c_\mathfrak{d}^n}{(\omega_\mathfrak{d}^n)^2 - \omega^2}\,\varphi_\mathfrak{d}^n, \qquad c_\mathfrak{d}^n = \partial_s\varphi_\mathfrak{d}^n(M_\star)\,(\omega_\mathfrak{d}^n)^{-2}\,. \tag{43}$$

Proof. We will show the proof for $u_\mathfrak{n}(\cdot,\omega)$, with the proof for $u_\mathfrak{d}(\cdot,\omega)$ being verbatim the same. First, let us consider the function

$$u = u_\mathfrak{n}(\cdot,\omega) - u_\mathfrak{n}(\cdot,0), \qquad u \in V_\mathfrak{n}.$$

Defining

$$f_\mathfrak{n} := \mu^{-1}\left(\partial_s(\mu\partial_s u_\mathfrak{n}(.,0)) + \omega^2\mu u_\mathfrak{n}(.,0)\right) = \omega^2 u_\mathfrak{n}(.,0) \in \mathrm{L}^2_\mu(\mathcal{T}),$$

we deduce that

$$u = \left(\mathcal{A}_{\mathfrak{n}} - \omega^2\right)^{-1} f_{\mathfrak{n}}, \text{ hence } u_{\mathfrak{n}}(\cdot,\omega) = u_{\mathfrak{n}}(\cdot,0) + \omega^2 \left(\mathcal{A}_{\mathfrak{n}} - \omega^2\right)^{-1} u_{\mathfrak{n}}(.,0). \tag{44}$$

Next, we expand $u_{\mathfrak{n}}(.,0)$ into a series of the eigenfunctions of $\mathcal{A}_{\mathfrak{n}}$. For this we remark that

$$(u_{\mathfrak{n}}(.,0), \varphi^n_{\mathfrak{n}})_{\mathrm{L}^2_\mu(\mathcal{T})} = -\left(\omega^n_{\mathfrak{n}}\right)^{-2} (u_{\mathfrak{n}}(.,0), \mu^{-1}\partial_s(\mu\partial_s\varphi^n_{\mathfrak{n}}))_{\mathrm{L}^2_\mu(\mathcal{T})},$$

where we use that $\varphi^n_{\mathfrak{n}}$ is an eigenfunction of $\mathcal{A}_{\mathfrak{n}}$. Thus, integrating the above by parts and using the fact that $u_{\mathfrak{n}}(.,0)$ satisfies ($\mathcal{P}_{\mathfrak{n},\omega}$) with $\omega = 0$, we obtain

$$(u_{\mathfrak{n}}(.,0), \varphi^n_{\mathfrak{n}})_{\mathrm{L}^2_\mu(\mathcal{T})} = \left(\omega^n_{\mathfrak{n}}\right)^{-2} \partial_s\varphi^n_{\mathfrak{n}}(M_\star) u_{\mathfrak{n}}(M_\star,0) = \left(\omega^n_{\mathfrak{n}}\right)^{-2} \partial_s\varphi^n_{\mathfrak{n}}(M_\star).$$

Thus, the desired result follows by inserting the expansion of $u_{\mathfrak{n}}(.,0)$ into (44). □

Remark 1.24. *The series (42) (resp. (43)) converges uniformly in ω on any compact subset of $\mathbb{C} \setminus \{\pm\omega^n_{\mathfrak{n}}, n \geqslant 1\}$ (resp. $\mathbb{C} \setminus \{\pm\omega^n_{\mathfrak{d}}, n \geqslant 1\}$), in $D(\mathcal{A}_{\mathfrak{n}})$-norm (resp. $D(\mathcal{A}_{\mathfrak{d}})$-norm).*

2. Self-similar trees.

In this section, we introduce a notion of a self-similar weighted p-adic tree. We start with the definition of a non-weighted p-adic tree.

Definition 2.1 (p-adic tree)**.** *A tree $\mathcal{T}$ is p-adic if every edge of $\mathcal{T}$ has precisely p children.*

Remark 2.2. *Any p-adic tree is infinite. The number of edges in the n-th generation of a p-adic tree is p^n, i.e. $J(n) = p^n - 1$.*

Later on, we will need to provide a numbering for edges and vertices of a p-adic tree. For this we will use the p-adic representation of integers. Let $\mathcal{I}_p := \{0, 1, \dots, p-1\}$. Given $(i_1, i_2, \dots, i_n) \in \mathcal{I}_p^n$, one denotes by $(i_1 i_2 \cdots i_n)_p$ an integer (see [20, pp. 22–25])

$$(i_1 i_2 \cdots i_n)_p := \sum_{j=1}^{n} i_j\, p^{n-j}. \tag{45}$$

The map $\Phi : (i_1, i_2, \dots, i_n) \to (i_1 i_2 \cdots i_n)_p$ defines (for all n) a bijection from $\mathcal{I}_p^n$ into $\{0, 1, \dots, p^n - 1\}$. The role of this notation and its meaning will become clear later. Now we have the ingredients necessary to define a self-similar p-adic tree.

Definition 2.3 (Self-similar p-adic tree)**.** *Let a root segment be $\Sigma_{0,0} = [M_\star, M_{0,0}]$ (where without loss of generality we assume that $M_\star$ is the origin). Let $\{\sigma_i, 0 \leqslant i \leqslant p-1\}$ in $\mathbb{R}^d$ be affine direct similitudes, defined as*

$$\sigma_i = \tau_i \circ h_i \circ \Theta_i, \qquad 0 \leqslant i \leqslant p-1,$$

where

- *$\tau_i \equiv \tau$ is the translation (common to all similitudes) by a vector $\overrightarrow{M_\star M_{0,0}}$;*
- *h_i is a homothety with the center in the origin of the ratio α_i (also called a ratio of the similitude): $h_i(x) = \alpha_i x$, $x \in \mathbb{R}^d$;*
- *Θ_i is a rotation (all the rotations Θ_i are assumed to be distinct).*

Let additionally these similitudes satisfy the following assumption: for all $\ell, k \in \mathbb{N}$, $i_1, \dots, i_\ell$, $j_1, \dots, j_k \in \{0, \dots, p-1\}$,

$$\begin{aligned} &\sigma_{i_1}\sigma_{i_2}\dots\sigma_{i_\ell}(M_{0,0}) = \sigma_{j_1}\sigma_{j_2}\dots\sigma_{j_k}(M_{0,0}) \text{ if and only if} \\ &k = \ell \text{ and } (i_1, \dots, i_\ell) = (j_1, \dots, j_k). \end{aligned} \tag{46}$$

Then a tree $\mathcal{T}$, defined as in (6), whose generations are given by

$$\mathcal{G}^0 = \{\Sigma_{0,0}\}, \qquad \mathcal{G}^k = \bigcup_{i=0}^{p-1} \sigma_i(\mathcal{G}^{k-1}), \qquad k \geqslant 1, \tag{47}$$

is called a self-similar p-adic tree.

The assumption (46) ensures that the object constructed in the definition 2.3 defines a p-adic tree (in particular, the absence of cycles in such a graph, and the fact that it is a connected object), see lemma 2.4.

By construction, for a self-similar tree as in definition 2.3, any *edge* of $\mathcal{G}^n$ is the result of the product of n similitudes $\{\sigma_{i_k}, 1 \leqslant k \leqslant n\}$ applied to the root edge $\Sigma_{0,0}$. In what follows, we chose to number the edges $\{\Sigma_{n,j}, 0 \leqslant j \leqslant p^n - 1\}$ in the following order (see also figure 4):

$$\Sigma_{n,j} = \sigma_{n,j}(\Sigma_{0,0}), \qquad j = 0, \dots, p^n - 1, \tag{48}$$

where

$$\sigma_{n,j} := \sigma_{j_1}\, \sigma_{j_2} \cdots \sigma_{j_n} \quad \text{for} \quad j = (j_1 j_2 \cdots j_n)_p. \tag{49}$$

Obviously $\sigma_{n,j}$ is a similitude. Moreover,

$$\sigma_{n,j} = \tau_{n,j} \circ h_{n,j} \circ \Theta_{n,j} \tag{50}$$

where $\tau_{n,j}$ is a translation by vector $[M_\star, M_{n,j}]$, $\Theta_{n,j}$ is the rotation $\Theta_{n,j} = \Theta_{j_1}\Theta_{j_2} \dots \Theta_{j_n}$ and $h_{n,j}$ is the homothety $h_{n,j} = h_{j_1} h_{j_2} \cdots h_{j_n}$. The ratio $\alpha_{n,j}$ of $\sigma_{n,j}$, which is also the ratio between the lengths of $\Sigma_{n,j}$ and $\Sigma_{0,0}$, is thus

$$\alpha_{n,j} = \alpha_{j_1}\, \alpha_{j_2} \cdots \alpha_{j_n}, \quad \text{for} \quad j = (j_1 j_2 \cdots j_n)_p. \tag{51}$$

By construction, $\Sigma_{n,j} = [M^\star_{n,j}, M_{n,j}]$ oriented from $M^\star_{n,j} = \sigma_{j_1}\, \sigma_{j_2} \cdots \sigma_{j_n}(M_\star)$ towards $M_{n,j} = \sigma_{j_1}\, \sigma_{j_2} \cdots \sigma_{j_n}(M_{0,0})$.

The fact that definition 2.3 does construct a connected p-adic tree is a consequence of the following lemma.

Lemma 2.4. *Let $\mathcal{G}^n$, $n \geqslant 0$, be defined in (47). Then $\mathcal{T} = \bigcup_{n\in\mathbb{N}} \mathcal{G}^n$ is a p-adic tree.*

Moreover, p edges of the generation $\mathcal{G}^{n+1}$ that are connected to $\Sigma_{n,j}$, namely

$$\{\Sigma_{n+1,pj+i}, 0 \leqslant i \leqslant p-1\}$$

are numbered in a consecutive way, from pj to $pj + p - 1$.

Proof. This proof is left to the reader. In particular, one can use the assumption (46) to show that the constructed graph has no loops. In order to show that it is connected, one can employ the numbering (48). □

For the clarity of some proofs, we will need following notation:

- we shall distinguish an integer j in its p-adic representation $j = (j_1 j_2 \cdots j_n)_p$, and the corresponding sequence of integers $j_1 j_2 \cdots j_n$ which we will denote by the bold letter $\boldsymbol{j} = j_1 j_2 \cdots j_n$.

- $\Sigma_{\boldsymbol{j}} = \Sigma_{j_1 j_2 \cdots j_n} := \Sigma_{n,j}$, $u_{\boldsymbol{j}} = u_{j_1 \cdots j_n} := u_{n,j}$ and, similarly, the nodal values, cf. (10), $\mathbf{u}_{\boldsymbol{j}} = \mathbf{u}_{j_1 \cdots j_n} := \mathbf{u}_{n,j}$.

- with $k_1, k_2, \dots, k_m \in \{0, 1, \dots, p-1\}$, defining $\ell = (j_1 j_2 \cdots j_n k_1 k_2 \cdots k_m)_p$,

$$\Sigma_{\boldsymbol{j}k_1 \cdots k_m} = \Sigma_{n+m,\ell}, \qquad u_{\boldsymbol{j}k_1 \cdots k_m} = u_{n+m,\ell}, \qquad \mathbf{u}_{\boldsymbol{j}k_1 \cdots k_m} = \mathbf{u}_{n+m,\ell}.$$

From the definition 1.11 of a subtree, it is clear that, a subtree $\mathcal{T}_{1,i}$ of $\mathcal{T}$ being defined by definition 2.3, can be identified with

$$\mathcal{T}_{1,i} = \sigma_i(\mathcal{T}), \quad \forall\, 0 \leqslant i \leqslant p-1,$$

and that, as a consequence,

$$\mathcal{T} = \Sigma_{0,0} \cup \bigcup_{i=0}^{p-1} \sigma_i(\mathcal{T}). \tag{52}$$

In fact, the above property can be seen as an alternative to definition 2.3.

Definition 2.5 (Reference self-similar p-adic tree)**.** *Given a self-similar tree $\mathcal{T}$, constructed with the help of similitude transformations $\{\sigma_i,\ i = 0,\dots,p-1\}$ as in definition 2.3, we will call a reference tree a self-similar tree $\mathcal{T}_r$, whose root $\Sigma_{0,0}$ is the segment $[\mathbf{0},\mathbf{1}]$ with $\mathbf{1} := (0,\cdots,0,1) \in \mathbb{R}^d$, and which is constructed as in definition 2.3 based on the similitude transformations $\{\sigma_i,\ i = 0,\dots,p-1\}$.*

For the reference tree, the length of $\Sigma_{n,j}$ is $\alpha_{n,j}$. Moreover, any tree obeying definition 2.3 is obviously obtained from the reference tree $\mathcal{T}_r$ by applying a scaling of ratio ℓ (the length of the root edge). This means that the most important geometric properties of any self-similar tree are encoded in the $p-$uplet

$$\boldsymbol{\alpha} := (\alpha_0, \alpha_2, \dots, \alpha_{p-1}) \in \left(\mathbb{R}_*^+\right)^p. \tag{53}$$

When convenient, we shall denote $\mathcal{T} \equiv \mathcal{T}_{\boldsymbol{\alpha}}$ to indicate that we consider a self-similar p-adic tree whose geometry is associated to the p-uplet $\boldsymbol{\alpha}$.

Compact self-similar trees. The reader will easily remark that

$$\mathcal{T} \equiv \mathcal{T}_{\boldsymbol{\alpha}} \text{ is compact (cf. definition 1.12) if and only if } \quad |\boldsymbol{\alpha}|_\infty := \max_{0\leqslant i\leqslant p-1} \alpha_i < 1. \tag{54}$$

Definition 2.6 (Self-similar weighted p-adic tree)**.** *Let $\mathcal{T}$ be a self-similar p-adic tree, and let μ be a weight function on $\mathcal{T}$. Then $(\mathcal{T},\mu)$ is a self-similar weighted p-adic tree if there exist p positive numbers $\{\mu_i\}_{0\leqslant i<p}$ such that (with an obvious abuse of notation defining $\sigma_i(s)$ as the abscissa of $\sigma_i(\Sigma)$ if s is the abscissa of Σ)*

$$\mu_{0,0} = 1 \ \text{ and } \ \mu(\sigma_i(s)) = \mu_i\, \mu(s), \quad s \in \mathcal{T}, \quad 0 \leqslant i < p. \tag{55}$$

In particular, we have

$$\mu(s) = \mu_{n,j} := \mu_{j_1}\mu_{j_2}\cdots\mu_{j_n} \ \text{ along } \ \Sigma_{n,j} \ \text{ if } \ j = (j_1 j_2 \cdots j_n)_p. \tag{56}$$

A weighted self-similar tree is thus characterized by two $p-$uplets $(\boldsymbol{\alpha},\boldsymbol{\mu}) \in (\mathbb{R}_*^+)^p \times (\mathbb{R}_*^+)^p$, where $\boldsymbol{\mu} = (\mu_0,\dots,\mu_{p-1})$. When necessary, we will denote the corresponding tree $\mathcal{T}_{\boldsymbol{\alpha},\boldsymbol{\mu}}$. We shall often use in the sequel the following computational trick.

Proposition 2.7. *Let $(\boldsymbol{\alpha},\boldsymbol{\mu}) \in (\mathbb{R}_*^+)^p \times (\mathbb{R}_*^+)^p$. For any $\zeta \in \mathbb{R}$,*

$$\sum_{j=0}^{p^n-1} \mu_{n,j}\, \alpha_{n,j}^{\zeta} = \left(\sum_{i=0}^{p-1} \mu_i\, \alpha_i^{\zeta}\right)^n. \tag{57}$$

Proof. Taking all possible j in $\{0,\dots,p^n-1\}$ is equivalent to taking all possible n-uples $(j_1,j_2,\dots,j_n) \in \{0,\dots,p-1\}^n$. Then, using (51) and (56), we have

$$\sum_{j=0}^{p^n-1} \mu_{n,j}\alpha_{n,j}^{\zeta} = \sum_{j_1=0}^{p-1}\sum_{j_2=0}^{p-1}\cdots\sum_{j_n=0}^{p-1} (\mu_{j_1}\alpha_{j_1}^{\zeta})\,(\mu_{j_2}\alpha_{j_2}^{\zeta})\cdots(\mu_{j_n}\alpha_{j_n}^{\zeta}). \tag{58}$$

The formula (57) follows then from the discrete version of Fubini's theorem. □

Example : Regular and geometric trees. By definition, a self-similar p-adic tree is called *equilibrated* or *regular* (according for instance to the terminology of Solomyak in [36]) if there exists $\alpha \in (0,1)$ such that

$$\alpha_i = \alpha, \quad \forall\, 0 \leqslant i \leqslant p-1.$$

We illustrate in figure 4 all the notions and notations introduced above in the case of a symmetric regular dyadic tree, for which

$$d = 2, \quad p = 2, \quad \alpha_1 = \alpha_2 = 1/2$$

and where Θ_1 and Θ_2 are the plane rotations of respective angles $\pi/4$ and $-\pi/4$.

A tree is called d-geometric when it is seen as the limit of a thick tree $\mathcal{T}^\delta$ in $\mathbb{R}^d$ (constructed

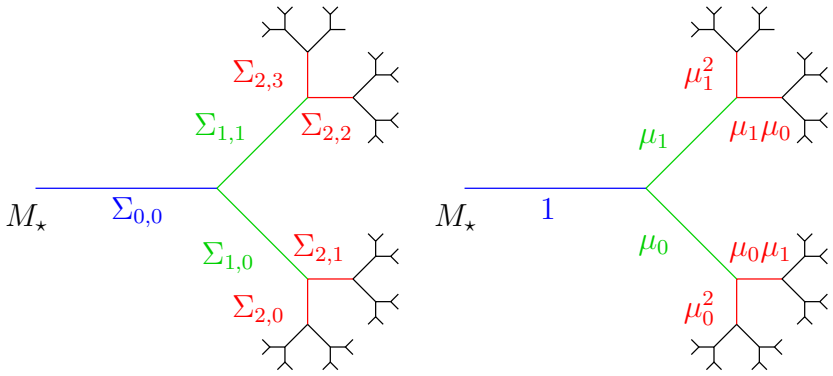

FIGURE 4. Example of p-adic tree for p=2. Left: iterative construction. Right: weight repartition.

as $\mathbb{G}^\delta$ in Section 1.2), in which the ratio between the transverse and longitudinal dimensions of the edges are preserved along all generations. This corresponds to the relation $\mu_i = \alpha_i^{d-1}, \forall\, 0 \leqslant i \leqslant p-1$. A good illustration of a symmetric 3-geometric dyadic tree is the human lung, as modelled e.g. in [23].

3. **Sobolev spaces on compact self-similar trees.** As discussed before, the principal goal of this work is to provide a theoretical and numerical basis for approximating the DtN operator, cf. section 1.6. For this we need to understand the following:

- whether the solutions to the problems ($\mathcal{P}_\mathfrak{n}$) and ($\mathcal{P}_\mathfrak{d}$) differ;
- whether (38)-$\mathfrak{d}$ or (38)-$\mathfrak{n}$ holds.

The goal of this section is to answer these questions in the case of self-similar trees. In all the derivations of this section, we will use the following simplifying assumption.

Assumption 3.1. *A tree $(\mathcal{T}, \mu)$ is a self-similar weighted reference **compact** tree, which we denote for brevity by $\mathcal{T}$.*

All the results of this section are valid for compact self-similar trees, and some of them hold for arbitrary, not necessarily compact, self-similar trees. This will be stated explicitly.

3.1. **Trace operator.** In this section, we will introduce a notion of the trace at infinity for functions in the Sobolev space $\mathrm{H}^1_\mu(\mathcal{T})$. On one hand, this allows to characterize the solution of the Dirichlet problem, defined in a variational way in ($\mathcal{P}_\mathfrak{d}$), by the Dirichlet condition at infinity. On the other hand, studying the trace will help us to answer other questions, e.g. whether the solutions of ($\mathcal{P}_\mathfrak{d}$) and ($\mathcal{P}_\mathfrak{n}$) differ.

Let us first define the "boundary at infinity" Γ_∞ of the tree $\mathcal{T}$ as a segment $[0,1]$, i.e.

$$\Gamma_\infty := [0,1]. \tag{59}$$

Next, we wish to define the trace at infinity of a function $u \in \mathrm{H}^1_\mu(\mathcal{T})$ as the limit of the trace of the same function at the boundary of the truncated tree $\mathcal{T}^n$. It is constructed from the finite set of the values at each end point $M_{n,j}, 0 \leqslant j \leqslant p^n - 1$, as a piecewise constant function on a very particular partition (mesh) of Γ_∞, namely:

$$\Gamma_n = \bigcup_{j=0}^{p^n-1} [a_{n,j}, a_{n,j+1}] \quad (\equiv \Gamma_\infty), \quad a_{n,0} = 0, \quad a_{n,p^n} = 1. \tag{60}$$

To define intermediate values $a_{n,j}$, let us introduce the following quantity (which, as we will see later, plays an important role in the analysis):

$$\left\langle \frac{\boldsymbol{\mu}}{\boldsymbol{\alpha}} \right\rangle := \sum_{i=0}^{p-1} \frac{\mu_i}{\alpha_i}. \tag{61}$$

Then (the reason for the choice of this particular partition will be explained later),

$$a_{n,0} = 0, \qquad a_{n,j+1} = a_{n,j} + \frac{\mu_{n,j}}{\alpha_{n,j}} \left\langle \frac{\boldsymbol{\mu}}{\boldsymbol{\alpha}} \right\rangle^{-n}, \qquad j = 0, \dots, p^n - 1. \tag{62}$$

First of all, notice that using (57) with $\zeta = -1$, we recover $a_{n,p^n-1} = 1$. Also, when μ_j/α_j is independent of j, (62) defines a uniform mesh of a stepsize p^{-n}. We choose the partition like in (62), because, first of all, this choice ensures that the mesh $\{a_{n+1,j}, 0 \leqslant j \leqslant p^{n+1} - 1\}$ at the stage $n+1$ can be seen as a sub-mesh of the mesh $\{a_{n,j}, 0 \leqslant j \leqslant p^n - 1\}$ at the stage n. In this case a segment of the coarser mesh is divided into p segments whose respective lengths are proportional to the ratio μ_i/α_i. This particular choice of the ratio is motivated by the proof of the trace theorem 3.2. Moreover, it appears to be consistent with the existing works, cf. [23]. To see how we obtain the finer mesh from the coarser one, let us introduce

$$\gamma_i := \frac{\mu_i}{\alpha_i} \left\langle \frac{\boldsymbol{\mu}}{\boldsymbol{\alpha}} \right\rangle^{-1}, \quad 0 \leqslant i \leqslant p-1, \quad \text{so that} \sum_{i=0}^{p-1} \gamma_i = 1. \tag{63}$$

Then the passage from step n to $n+1$ is defined by the following (see also figure 5):

$$\begin{cases} [a_{n,j}, a_{n,j+1}] = \bigcup_{i=0}^{p-1} [\, a_{n+1,pj+i}, a_{n+1,pj+i+1} \,], \\ a_{n+1,pj} = a_{n,j}, \quad a_{n+1,pj+i+1} - a_{n+1,pj+i} = \gamma_i \, (a_{n,j+1} - a_{n,j}), \end{cases} \tag{64}$$

which leads, after some calculations, to (62).

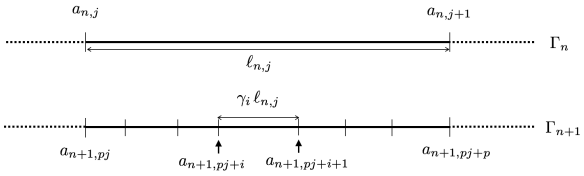

FIGURE 5. Inductive construction of the mesh Γ_n

Next, for any $n \geqslant 0$, we define the trace map at a generation n, i. e. the end of the truncated tree $\mathcal{T}^n$. More precisely, we define $\tau_n u \in \mathbb{P}_0(\Gamma_n) \subset L^\infty(\Gamma_\infty)$ (here $\mathbb{P}_0(\Gamma_n)$ is the space of functions that are piecewise constant with respect to the mesh Γ_n), as follows:

$$\tau_n(x) := \mathbf{u}_{n,j} \equiv u(M_{n,j}), \quad \text{for } x \in [a_{n,j}, a_{n,j+1}], \quad 0 \leqslant j \leqslant p^n - 1\,. \tag{65}$$

Theorem 3.2. *Assume that*

$$\left\langle \frac{\boldsymbol{\mu}}{\boldsymbol{\alpha}} \right\rangle > 1. \tag{66}$$

Then, for any u in $\mathrm{H}^1_\mu(\mathcal{T})$, the following limit

$$\tau_\infty u := \lim_{n\to+\infty} \tau_n u \quad \textit{exists in } L^2(\Gamma_\infty), \tag{67}$$

and the application τ_∞ defines a continuous trace operator from $\mathrm{H}^1_\mu(\mathcal{T})$ into $L^2(\Gamma_\infty)$:

$$\forall\, u \in \mathrm{H}^1_\mu(\mathcal{T}), \quad \|\tau_\infty u\|_{L^2(\Gamma_\infty)} \leqslant C_\infty\, \|u\|_{\mathrm{H}^1_\mu(\mathcal{T})}. \tag{68}$$

Moreover,

$$\mathrm{H}^1_{\mu,0}(\mathcal{T}) \subseteq \textit{Ker}\ \tau_\infty = \{u \in \mathrm{H}^1_\mu(\mathcal{T}) \,/\, \tau_\infty u = 0\}. \tag{69}$$

Proof. Let $u \in \mathrm{H}^1_\mu(\mathcal{T})$. To prove (67), we will show that $\tau_{n+1}u - \tau_n u$, where τ_n is defined by (65), is a convergent series in $L^2(\Gamma_\infty)$.

The difference $\tau_{n+1}u - \tau_n u$ is constant along each segment

$$[\,a_{n+1,pj+\ell}, a_{n+1,pj+\ell+1}],\ 0 \leqslant j \leqslant p^n - 1,\ 0 \leqslant \ell \leqslant p-1,$$

where it takes the value $\mathbf{u}_{n+1,pj+\ell} - \mathbf{u}_{n,j}$. As a consequence, using (62) (and (64)),

$$\|\tau_{n+1}u - \tau_n u\|^2_{L^2(\Gamma_\infty)} = \left\langle \frac{\boldsymbol{\mu}}{\boldsymbol{\alpha}} \right\rangle^{-n-1} \sum_{j=0}^{p^n-1} \sum_{\ell=0}^{p-1} \frac{\mu_{n,j}}{\alpha_{n,j}} \frac{\mu_\ell}{\alpha_\ell}\, |\mathbf{u}_{n+1,pj+\ell} - \mathbf{u}_{n,j}|^2. \tag{70}$$

Recall that $M_{n,j}$ is connected to each of the p points $M_{n+1,pj+\ell}, 0 \leqslant \ell \leqslant p-1$, via the corresponding edge $\Sigma_{n+1,pj+\ell}$, cf. lemma 2.4. Hence,

$$\mathbf{u}_{n+1,pj+\ell} - \mathbf{u}_{n,j} = \int_{\Sigma_{n+1,pj+\ell}} \partial_s u. \tag{71}$$

Using the Cauchy-Schwarz inequality, we have

$$|\mathbf{u}_{n+1,pj+\ell} - \mathbf{u}_{n,j}|^2 \leqslant \left(\int_{\Sigma_{n+1,pj+\ell}} \mu^{-1} \right) \left(\int_{\Sigma_{n+1,pj+\ell}} \mu\, |\partial_s u|^2 \right), \tag{72}$$

that is to say

$$\left| \begin{array}{rcl} |\mathbf{u}_{n+1,pj+\ell} - \mathbf{u}_{n,j}|^2 & \leqslant & \dfrac{\alpha_{n+1,pj+\ell}}{\mu_{n+1,pj+\ell}} \displaystyle\int_{\Sigma_{n+1,pj+\ell}} \mu\, |\partial_s u|^2 \\ & = & \dfrac{\alpha_\ell}{\mu_\ell} \dfrac{\alpha_{n,j}}{\mu_{n,j}} \displaystyle\int_{\Sigma_{n+1,pj+\ell}} \mu\, |\partial_s u|^2. \end{array} \right.$$

After multiplication by $(\mu_{n,j}/\alpha_{n,j})\cdot(\mu_\ell/\alpha_\ell)$ (cf. the right hand side of (70)) and summation over $\ell\in\{0,\dots,p-1\}$ and $j\in\{0,\dots,p^n-1\}$, we get (this is where the coefficients α_ℓ, μ_ℓ, $\alpha_{n,\ell}$, $\mu_{n,\ell}$ disappear at the right hand side, justifying the choice of the mesh Γ_n):

$$\left|\begin{array}{l}\displaystyle\sum_{j=0}^{p^n-1}\sum_{\ell=0}^{p-1}\frac{\mu_{n,j}}{\alpha_{n,j}}\,\frac{\mu_\ell}{\alpha_\ell}\,|\mathbf{u}_{n+1,pj+\ell}-\mathbf{u}_{n,j}|^2\\ \qquad\leqslant\displaystyle\sum_{j=0}^{p^n-1}\sum_{\ell=0}^{p-1}\int_{\Sigma_{n+1,pj+\ell}}\mu\,|\partial_s u|^2=\int_{\mathcal{G}^{n+1}}\mu\,|\partial_s u|^2.\end{array}\right.$$

Thus, we deduce from (70) that

$$\|\tau_{n+1}u-\tau_n u\|^2_{L^2(\Gamma_\infty)}\leqslant\left\langle\frac{\boldsymbol{\mu}}{\boldsymbol{\alpha}}\right\rangle^{-n-1}\int_{\mathcal{G}^{n+1}}\mu\,|\partial_s u|^2\leqslant\left\langle\frac{\boldsymbol{\mu}}{\boldsymbol{\alpha}}\right\rangle^{-n-1}\int_{\mathcal{T}}\mu\,|\partial_s u|^2.$$

This proves, since $\left\langle\dfrac{\boldsymbol{\mu}}{\boldsymbol{\alpha}}\right\rangle>1$, that the series $\|\tau_{n+1}u-\tau_n u\|_{L^2(\Gamma_\infty)}$ converges. Finally,

$$\left|\begin{array}{rcl}\|\tau_\infty u\|_{L^2(\Gamma_\infty)}&\leqslant&\|\tau_0 u\|_{L^2(\Gamma_\infty)}+\displaystyle\sum_{n=0}^{+\infty}\left\langle\frac{\boldsymbol{\mu}}{\boldsymbol{\alpha}}\right\rangle^{-\frac{n+1}{2}}\|\partial_s u\|_{\mathrm{L}^2_\mu(\mathcal{T})}\\ &=&\|\tau_0 u\|_{L^2(\Gamma_\infty)}+\left\langle\dfrac{\boldsymbol{\mu}}{\boldsymbol{\alpha}}\right\rangle^{-\frac12}\left(\left\langle\dfrac{\boldsymbol{\mu}}{\boldsymbol{\alpha}}\right\rangle^{\frac12}-1\right)^{-1}\|\partial_s u\|_{\mathrm{L}^2_\mu(\mathcal{T})}.\end{array}\right.$$

To estimate $\|\tau_0 u\|_{L^2(\Gamma_\infty)}$, we apply the usual trace theorem in $H^1(\Sigma_{0,0})\equiv H^1(0,1)$:

$$\|\tau_0 u\|_{L^2(\Gamma_\infty)}=|u(M_\star)|\leqslant C_0\,\|u\|_{H^1(\Sigma_{0,0})}\leqslant C_0\,\|u\|_{\mathrm{H}^1_\mu(\mathcal{T})}.$$

For the embedding (69), note that if u is compactly supported in the sense of (19), for n large enough $\tau_n u=0$ which implies $\tau_\infty u=0$, in other words $\mathrm{H}^1_{\mu,\mathrm{c}}(\mathcal{T})\subseteq\mathrm{Ker}\,\tau_\infty$. Taking the closures in $\mathrm{H}^1_\mu(\mathcal{T})$, since $\mathrm{Ker}\,\tau_\infty$ is closed, we get (69) (see definition 1.15). □

Remark 3.3. *It is not difficult to see that (66) is a necessary condition for the existence of the trace, at least for compact regular trees with regular weights, i.e. when*

$$\alpha_i=\alpha,\quad \mu_i=\mu,\quad \forall\,0\leqslant i\leqslant p-1,\ \textit{in which case}\ \left\langle\frac{\boldsymbol{\mu}}{\boldsymbol{\alpha}}\right\rangle\equiv\frac{p\mu}{\alpha}.$$

Let the length of the root edge be $1-\alpha$. For any complex-valued function defined on such a tree, its restriction to the generation n can be identified to a collection of functions

$$\big\{u_{n,j}(x):I_n\longrightarrow\mathbb{C},\quad 0\leqslant j\leqslant p^n-1\big\}\ \textit{with}\ I_n=[x_n,x_{n+1}]\ \textit{and}\ x_n=1-\alpha^n.$$

A function u will be called symmetric if

$$u_{n,j}(x)=u_n(x),\quad \textit{for all}\ \ 0\leqslant j\leqslant p^n-1.$$

Any symmetric function can be identified to a 1D function defined on an interval:

$$\hat u(x):I\longrightarrow\mathbb{C}\ \textit{with}\ I=\bigcup_{j=0}^{p^n-1}I_n\equiv[0,1],\ \textit{s.t.}\ \hat u|_{I_n}=u_n,\quad\forall\,n\in\mathbb{N}.$$

Let us introduce the space

$$\mathrm{H}^1_{\mu,s}(\mathcal{T})=\{u\in\mathrm{H}^1_\mu(\mathcal{T})\ /\ u\ \textit{is symmetric}\}.$$

According to the identification process $u\equiv\hat u$, one easily checks that for $u\in\mathrm{H}^1_{\mu,s}(\mathcal{T})$, $\hat u$ is continuous in I, with H^1-regularity in each I_n and that

$$\|u\|^2_{\mathrm{H}^1_{\mu,s}(\mathcal{T})}=\int_0^1\left(|\hat u'(x)|^2+|\hat u(x)|^2\right)w_d(x)\,dx,\tag{73}$$

where the piecewise constant weight function w_d is defined by

$$w_d(x) = w_n := (p\mu)^n \ \text{ for } x \in I_n = [x_n, x_{n+1}].$$

Noticing that $w_n = (p\mu)^{\frac{\log(1-x_n)}{\log\alpha}}$, it is straightforward to check that the norm (73) is equivalent to the norm defined by

$$\|\hat{u}\|^2_{1,w} = \int_0^1 \left(|\hat{u}'(x)|^2 + |\hat{u}(x)|^2\right) w(x)\, dx, \quad w(x) = (1-x)^\beta, \quad \beta = \frac{\log(p\mu)}{\log\alpha}. \tag{74}$$

Since $\alpha < 1$, the condition (66) is not satisfied if and only if $\beta \geqslant 1$. On the other hand, the trace $\tau_n u$ for $u \in \mathrm{H}^1_{\mu,s}(\mathcal{T})$ is a constant function (on Γ_∞) equal to $\hat{u}(x_n)$. Thus to prove that the trace operator τ_∞ is not defined for some $u \in \mathrm{H}^1_{\mu,s}(\mathcal{T}) \subset \mathrm{H}^1_\mu(\mathcal{T})$, it suffices to find a function $\hat{u} : [0,1] \to \mathbb{C}$, such that $\|\hat{u}\|^2_{1,w}$ is finite and $|\hat{u}(x)| \to +\infty$ when x tends to 1.

When $\beta > 1$, one of such functions is $\hat{u}(x) = \log(1-x)$. In particular,

$$\int_0^1 \hat{u}'(x)^2\, w(x)\, dx = \int_0^1 (1-x)^{\beta-2}\, dx < +\infty \quad \text{since } \beta > 1.$$

For the limit case $\beta = 1$, the reader will easily check that

$$\hat{u}(x) = \begin{cases} \log|\log(1-x)| & x > 1/2, \\ \log\log 2, & x \leqslant 1/2, \end{cases}$$

has a finite norm $\|\hat{u}\|_{1,w}$, and yet $\|\tau_\infty u\|_{L^2(\Gamma_\infty)} = \infty$.

In what follows, we will use the notation $\|\tau_n u\| := \|\tau_n u\|_{\mathrm{L}^2(\Gamma_\infty)}$. Moreover, we will need the explicit expression for $\|\tau_n u\|^2$:

$$\|\tau_n u\|^2 = \left\langle \frac{\boldsymbol{\mu}}{\boldsymbol{\alpha}} \right\rangle^{-n} \sum_{j=0}^{p^n-1} \frac{\mu_{n,j}}{\alpha_{n,j}} |\mathbf{u}_{n,j}|^2. \tag{75}$$

Remark 3.4. *Theorem 3.2 holds both for compact and non-compact trees.*

3.2. **Kernel and image of the trace operator.** We are now going to prove that, just like for the usual Sobolev spaces on the interval, the inclusion (69) is in fact an equality. This provides a useful characterization of $\mathrm{H}^1_{\mu,0}(\mathcal{T})$, as well as justifies the way to look at the solution $u_\mathfrak{d}$ of the Dirichlet problem for the wave equation as a limit when n goes to infinity of the solution $u^n_\mathfrak{d}$ to the wave equation in the truncated tree $\mathcal{T}^n$ with homogeneous Dirichlet conditions at each end point $M_{n,j}$ of $\mathcal{T}^n$.

Theorem 3.5. *Assume that (66) holds, so that the trace operator τ_∞ is well-defined, then*

$$\mathrm{H}^1_{\mu,0}(\mathcal{T}) = \mathit{Ker}\ \tau_\infty. \tag{76}$$

The proof of this theorem is quite long. It will use the following lemma that provides a sufficient condition for a function in $\mathrm{H}^1_\mu(\mathcal{T})$ to belong to $\mathrm{H}^1_{\mu,0}(\mathcal{T})$. Let us emphasize the fact that this result is valid independently of whether the trace operator τ_∞ is well-defined or not, i.e. it does not require (66).

Lemma 3.6. *Let $u \in \mathrm{H}^1_\mu(\mathcal{T})$. If*

$$n^{-1}\left\langle \frac{\boldsymbol{\mu}}{\boldsymbol{\alpha}} \right\rangle^n \|\tau_n u\|^2 \to 0, \qquad n \to +\infty, \tag{77}$$

then $u \in \mathrm{H}^1_{\mu,0}(\mathcal{T})$.

Proof. The proof relies on an approximation process adapted from [33]. Let $u \in \mathrm{H}^1_\mu(\mathcal{T})$, for which (77) holds true. Next, let a piecewise-linear function φ_n be defined as follows:

$$\begin{cases} \varphi_n|_{\mathcal{T}^n} \equiv 1, \qquad \varphi_n|_{\mathcal{T}\setminus\mathcal{T}^{2n}} \equiv 0, \\ \varphi_n(M_{n+\ell,j}) = 1 - \frac{\ell}{n}, \qquad j = 0, \dots, p^{n+\ell} - 1, \qquad 0 \leqslant \ell \leqslant n. \end{cases}$$

Notice that the support of φ_n' lies in $\mathcal{T}^{2n} \setminus \mathcal{T}^n$. Also, for any $\ell \leqslant n$

$$\varphi_n'|_{\Sigma_{n+\ell,j}} = (n\,\alpha_{n+\ell,j})^{-1}, \quad j = 0, \dots, p^{n+\ell} - 1. \tag{78}$$

Our goal is to prove that $u_n = \varphi_n u \in \mathrm{H}^1_{\mu,\mathrm{c}}(\mathcal{T})$ converges to u in $\mathrm{H}^1_\mu(\mathcal{T})$. For this it suffices to show that, as $n \to \infty$, the sequences

$$u_n \to u \ \text{ and } \ u_n' = \varphi_n' u + \varphi_n u' \to u' \qquad \text{in } \mathrm{L}^2_\mu(\mathcal{T}). \tag{79}$$

By Lebesgue's dominated convergence theorem,

$$u_n \to u, \quad \varphi_n u' \to u', \ n \to +\infty, \qquad \text{in } \mathrm{L}^2_\mu(\mathcal{T}). \tag{80}$$

Therefore, it remains to show that $\|\varphi_n' u\|_{L^2_\mu(\mathcal{T})} \to 0$. Using $\operatorname{supp} \varphi_n \subset \mathcal{T}^{2n} \setminus \mathcal{T}^n$ and (78),

$$\|\varphi_n' u\|^2_{L^2_\mu(\mathcal{T})} = \sum_{m=n+1}^{2n} \sum_{j=0}^{p^m-1} \int\limits_{\Sigma_{m,j}} \mu\,(\varphi_n')^2\,|u|^2 = \sum_{m=n+1}^{2n} \sum_{j=0}^{p^m-1} (n\,\alpha_{m,j})^{-2} \int\limits_{\Sigma_{m,j}} \mu\,|u|^2. \tag{81}$$

Since we want to bound the above using the traces $\tau_m u$, we will bound $\|u\|^2_{\mathrm{L}^2_\mu(\Sigma_{m,j})}$ by a quantity involving the value of u in the vertex $M_{m,j}$ (and, eventually, its derivative $\partial_s u$).

For this we will use the following 1D Poincaré inequality

$$\forall\, v \in \mathrm{H}^1(0,L) \ \text{ with } \ v(L) = 0, \quad \int\limits_0^L |v|^2 ds \leqslant \frac{4}{\pi^2}\, L^2 \int\limits_0^L |v'|^2\, ds. \tag{82}$$

Let us introduce a piecewise-constant interpolant Πu defined by

$$\Pi u|_{\Sigma_{n,j}} = \tilde{\mathbf{u}}_{n,j} := \text{ the constant function } \mathbf{u}_{n,j}, \quad 0 \leqslant j \leqslant p^n - 1, \quad n \geqslant 0. \tag{83}$$

Then, thanks the the Poincaré inequality, applied to the function $u - \Pi u$,

$$\|u - \Pi u\|^2_{\mathrm{L}^2_\mu(\Sigma_{m,j})} \leqslant \frac{4}{\pi^2}\, \alpha^2_{m,j} \|\partial_s u\|^2_{\mathrm{L}^2_\mu(\Sigma_{m,j})}. \tag{84}$$

With the above and

$$\|u\|^2_{\mathrm{L}^2_\mu(\Sigma_{m,j})} \leqslant 2\,\|\Pi u\|^2_{\mathrm{L}^2_\mu(\Sigma_{m,j})} + 2\,\|u - \Pi u\|^2_{\mathrm{L}^2_\mu(\Sigma_{m,j})},$$

we deduce the following upper bound on $\|u\|^2_{\mathrm{L}^2_\mu(\Sigma_{m,j})}$:

$$\|u\|^2_{\mathrm{L}^2_\mu(\Sigma_{m,j})} \leqslant \frac{8}{\pi^2}\, \alpha^2_{m,j}\, \|\partial_s u\|^2_{\mathrm{L}^2_\mu(\Sigma_{m,j})} + 2\,\mu_{m,j}\alpha_{m,j}\, |\mathbf{u}_{m,j}|^2. \tag{85}$$

Plugging in the above bound into (81), we end up with the following expression:

$$\|\varphi_n' u\|^2_{L^2_\mu(\mathcal{T})} \leqslant \frac{8}{n^2\pi^2} \sum_{m=n+1}^{2n} \sum_{j=0}^{p^m-1} \|\partial_s u\|^2_{\mathrm{L}^2_\mu(\Sigma_{m,j})} + \frac{2}{n^2} \sum_{m=n+1}^{2n} \sum_{j=0}^{p^m-1} \frac{\mu_{m,j}}{\alpha_{m,j}} |\mathbf{u}_{m,j}|^2$$

$$= \frac{8}{n^2\pi^2} \|\partial_s u\|^2_{\mathrm{L}^2_\mu(\mathcal{T}^{2n}\setminus\mathcal{T}^n)} + \frac{2}{n^2} \sum_{m=n+1}^{2n} \left\langle \frac{\boldsymbol{\mu}}{\boldsymbol{\alpha}} \right\rangle^m \|\tau_m u\|^2, \qquad \text{cf. (75)}.$$

Obviously, the first term in the above tends to 0 as $n \to +\infty$. So does the second term, thanks to the condition (77). Indeed, (77) can be rewritten as

$$\left\langle \frac{\boldsymbol{\mu}}{\boldsymbol{\alpha}} \right\rangle^m \|\tau_m u\|^2 = m\,\varepsilon_m, \quad \varepsilon_m \to 0 \quad (m \to +\infty).$$

Then the second term in the above bound can be estimated as follows:

$$\frac{2}{n^2} \sum_{m=n+1}^{2n} \left\langle \frac{\boldsymbol{\mu}}{\boldsymbol{\alpha}} \right\rangle^m \|\tau_m u\|^2 = \frac{2}{n^2} \sum_{m=n+1}^{2n} m\,\varepsilon_m \leqslant 4 \max_{m=n,\dots,2n} \varepsilon_m \to 0, \quad (n \to +\infty).$$

Thus, $\varphi_n' u \to 0$ in $\mathrm{L}^2_\mu(\mathcal{T})$, and with (79, 80), $\varphi_n u \to u$ in $\mathrm{H}^1_\mu(\mathcal{T})$. □

To prove theorem 3.5, it remains to show that (77) holds for any $u \in \operatorname{Ker} \tau_\infty$. This proof relies on two technical lemmas that aim at connecting the norm of the traces at generations n and $n+N$, namely $\tau_n u$ and $\tau_{n+N} u$. Our first result connects each nodal value $\mathbf{u}_{n,j}$ with the values of u at all the end points of $\mathcal{G}^{n+N}$ that are connected to $M_{n,j}$, namely:

$$\big\{\mathbf{u}_{\boldsymbol{j}\ell_1\dots\ell_N},\, 0 \leqslant \ell_k \leqslant p-1,\, 1 \leqslant k \leqslant N\big\}. \tag{86}$$

Lemma 3.7. *Let $u \in \mathrm{H}^1_\mu(\mathcal{T})$. Let additionally $\{q_\ell,\, 0 \leqslant \ell \leqslant p-1\}$ satisfy*

$$q_\ell \geqslant 0, \quad 0 \leqslant \ell \leqslant p-1, \qquad \sum_{\ell=0}^{p-1} q_\ell = 1.$$

Then the nodal value $\mathbf{u}_{n,j} = \mathbf{u}_{\boldsymbol{j}}$ is related to the nodal values (86) via

$$\mathbf{u}_{n,j} = P^N_{n,j} - \sum_{k=1}^{N} D^k_{n,j}, \tag{87}$$

$$P^N_{n,j} = \sum_{\ell_1=0}^{p-1} \cdots \sum_{\ell_N=0}^{p-1} q_{\ell_1} \cdots q_{\ell_N}\, \mathbf{u}_{\boldsymbol{j}\ell_1\cdots\ell_N}, \tag{88}$$

$$D^k_{n,j} = \sum_{\ell_1=0}^{p-1} \cdots \sum_{\ell_k=0}^{p-1} q_{\ell_1} \cdots q_{\ell_k} \int_{\Sigma_{\boldsymbol{j}\ell_1\cdots\ell_k}} \partial_s u. \tag{89}$$

In the above $P^N_{n,j}$ is a convex combination of point values at the end points of $\mathcal{G}^{n+N}$ that are connected to $M_{n,j}$, cf. (86), while each $D^k_{n,j}$ is a convex combination of integrals of $\partial_s u$ along the edges of the generation $\mathcal{G}^{n+k}$ that are connected to $M_{n,j}$.

Proof. The proof is done by induction. It consists essentially in playing with the basic identity (71) and in exploiting, in order to get an optimal result, all the paths that connect $M_{n,j}$ to the possible end points of the generation $\mathcal{G}^{n+N}$.
Let us first consider the case $N = 1$. According to (71),

$$\forall\, 0 \leqslant \ell_1 \leqslant p, \quad \mathbf{u}_{\boldsymbol{j}} = \mathbf{u}_{\boldsymbol{j}\ell_1} - \int_{\Sigma_{\boldsymbol{j}\ell_1}} \partial_s u.$$

To exploit all the possible paths between $M_{\boldsymbol{j}}$ and the $M_{\boldsymbol{j}\ell_1}$'s we make a convex linear combination of these equalities, using the coefficients q_{ℓ_1}, to obtain the identity

$$\mathbf{u}_{\boldsymbol{j}} = \sum_{\ell_1=0}^{p-1} q_{\ell_1} \mathbf{u}_{\boldsymbol{j}\ell_1} - \sum_{\ell_1=0}^{p-1} q_{\ell_1} \int_{\Sigma_{\boldsymbol{j}\ell_1}} \partial_s u \tag{90}$$

which is (87) for $N = 1$. Let us now assume that (87) holds and let us prove it for $N + 1$. We use an analogue of (90) for $\mathbf{u}_{\boldsymbol{j}\ell_1\cdots\ell_N}$ instead of $\mathbf{u}_{\boldsymbol{j}}$:

$$\mathbf{u}_{\boldsymbol{j}\ell_1\cdots\ell_N} = \sum_{\ell_{N+1}=0}^{p-1} q_{\ell_{N+1}} \mathbf{u}_{\boldsymbol{j}\ell_1\cdots\ell_N\ell_{N+1}} - \sum_{\ell_{N+1}=0}^{p-1} q_{\ell_{N+1}} \int_{\Sigma_{\boldsymbol{j}\ell_1\cdots\ell_N\ell_{N+1}}} \partial_s u,$$

which we substitute into (87), using (88) and (89),

$$\mathbf{u}_{\boldsymbol{j}} = P_{n,j}^{N+1} - \sum_{\ell_1=0}^{p-1} \cdots \sum_{\ell_N=0}^{p-1} \sum_{\ell_{N+1}=0}^{p-1} q_{\ell_1} \cdots q_{\ell_N} q_{\ell_{N+1}} \int_{\Sigma_{\boldsymbol{j}\ell_1\cdots\ell_N\ell_{N+1}}} \partial_s u - \sum_{k=1}^{N} D_{n,j}^k,$$

which is the desired result since the central term above is nothing but $D_{n,j}^{N+1}$. □

Remark 3.8. *For the functions of the class $\mathrm{H}^1_{\mu,s}(\mathcal{T})$, when the tree and its weight is regular, cf. remark 3.3 for the definition and the notation, the above result is simply the fundamental theorem of calculus.*

In order to prove theorem 3.5, we first need to relate the traces $\tau_n u$ and $\tau_{n+N} u$ in the norm. For this we will apply lemma 3.7 with $q_\ell = \gamma_\ell$, where $\{\gamma_\ell,\ 0 \leqslant \ell \leqslant p-1\}$ are defined in (63). Let us introduce a related quantity:

$$C_{\boldsymbol{\alpha}\boldsymbol{\mu}}^N = \sum_{k=1}^{N} \left\langle \frac{\boldsymbol{\mu}}{\boldsymbol{\alpha}} \right\rangle^{-k}. \tag{91}$$

Lemma 3.9. *For all $u \in \mathrm{H}^1_\mu(\mathcal{T})$, all $n,\ N \geqslant 1$,*

$$\left\langle \frac{\boldsymbol{\mu}}{\boldsymbol{\alpha}} \right\rangle^{n} \|\tau_n u\|^2 \leqslant 2C_{\boldsymbol{\alpha}\boldsymbol{\mu}}^N \|\partial_s u\|^2_{\mathrm{L}^2_\mu(\mathcal{T}\setminus\mathcal{T}^n)} + 2\left\langle \frac{\boldsymbol{\mu}}{\boldsymbol{\alpha}} \right\rangle^{n} \|\tau_{n+N} u\|^2. \tag{92}$$

Proof. By definition of $\tau_n u$, we have, cf. (75),

$$\left\langle \frac{\boldsymbol{\mu}}{\boldsymbol{\alpha}} \right\rangle^{n} \|\tau_n u\|^2 = \sum_{j=0}^{p^n-1} \frac{\mu_{n,j}}{\alpha_{n,j}} \left|\mathbf{u}_{n,j}\right|^2. \tag{93}$$

Thus, using (87) with $q_\ell = \gamma_\ell$, where $\{\gamma_\ell,\ 0 \leqslant \ell \leqslant p-1\}$ are as in (63),

$$\left\langle \frac{\boldsymbol{\mu}}{\boldsymbol{\alpha}} \right\rangle^{n} \|\tau_n u\|^2 \leqslant 2 \sum_{j=0}^{p^n-1} \frac{\mu_{n,j}}{\alpha_{n,j}} \left|P_{n,j}^N\right|^2 + 2 \sum_{j=0}^{p^n-1} \frac{\mu_{n,j}}{\alpha_{n,j}} \left| \sum_{k=1}^{N} D_{n,j}^k \right|^2. \tag{94}$$

By convexity of $x \to x^2$, we deduce from (88) that

$$\left|\begin{array}{rcl} |P_{n,j}^N|^2 & \leqslant & \displaystyle\sum_{\ell_1=0}^{p-1} \cdots \sum_{\ell_N=0}^{p-1} \gamma_{\ell_1} \cdots \gamma_{\ell_N} \left|\mathbf{u}_{\boldsymbol{j}\ell_1\cdots\ell_N}\right|^2 \\ & = & \displaystyle\left\langle \frac{\boldsymbol{\mu}}{\boldsymbol{\alpha}} \right\rangle^{-N} \sum_{\ell_1=0}^{p-1} \cdots \sum_{\ell_N=0}^{p-1} \frac{\mu_{\ell_1}}{\alpha_{\ell_1}} \cdots \frac{\mu_{\ell_N}}{\alpha_{\ell_N}} \left|\mathbf{u}_{\boldsymbol{j}\ell_1\cdots\ell_N}\right|^2. \end{array}\right. \tag{95}$$

After multiplication by $\mu_{n,j}/\alpha_{n,j}$ and summation over $0 \leqslant j \leqslant p^n - 1$, we get

$$\sum_{j=0}^{p^n-1} \frac{\mu_{n,j}}{\alpha_{n,j}} \left|P_{n,j}^N\right|^2 \leqslant \left\langle \frac{\boldsymbol{\mu}}{\boldsymbol{\alpha}} \right\rangle^{-N} \sum_{j=0}^{p^n-1} \sum_{\ell_1=0}^{p-1} \cdots \sum_{\ell_N=0}^{p-1} \frac{\mu_{n,j}}{\alpha_{n,j}} \frac{\mu_{\ell_1}}{\alpha_{\ell_1}} \cdots \frac{\mu_{\ell_N}}{\alpha_{\ell_N}} \left|\mathbf{u}_{\boldsymbol{j}\ell_1\cdots\ell_N}\right|^2,$$

or, alternatively, thanks to (93) for $n+N$ instead of n,

$$\sum_{j=1}^{p^n-1} \frac{\mu_{n,j}}{\alpha_{n,j}} \left|P_{n,j}^N\right|^2 \leqslant \left\langle \frac{\boldsymbol{\mu}}{\boldsymbol{\alpha}} \right\rangle^{n} \|\tau_{n+N} u\|^2. \tag{96}$$

In the same way, by convexity again, we deduce from (89) that

$$|D_{n,j}^k|^2 \leqslant \left\langle \frac{\boldsymbol{\mu}}{\boldsymbol{\alpha}} \right\rangle^{-k} \sum_{\ell_1=0}^{p-1} \cdots \sum_{\ell_k=0}^{p-1} \frac{\mu_{\ell_1}}{\alpha_{\ell_1}} \cdots \frac{\mu_{\ell_k}}{\alpha_{\ell_k}} \left| \int_{\Sigma_{\boldsymbol{j}\ell_1\cdots\ell_k}} \partial_s u \right|^2. \tag{97}$$

Using the Cauchy-Schwarz inequality (like in (72))

$$|D_{n,j}^k|^2 \leqslant \left\langle \frac{\boldsymbol{\mu}}{\boldsymbol{\alpha}} \right\rangle^{-k} \left(\frac{\mu_{n,j}}{\alpha_{n,j}}\right)^{-1} \sum_{\ell_1=0}^{p-1} \cdots \sum_{\ell_k=0}^{p-1} \int_{\Sigma_{\boldsymbol{j}\ell_1\cdots\ell_k}} \mu \left|\partial_s u\right|^2. \tag{98}$$

Next, using the discrete Cauchy-Schwarz inequality and the definition of $C_{\boldsymbol{\alpha\mu}}^N$, we obtain

$$\left| \sum_{k=1}^{N} D_{n,j}^k \right|^2 = \left| \sum_{k=1}^{N} \left\langle \frac{\boldsymbol{\mu}}{\boldsymbol{\alpha}} \right\rangle^{-\frac{k}{2}} \left\langle \frac{\boldsymbol{\mu}}{\boldsymbol{\alpha}} \right\rangle^{\frac{k}{2}} D_{n,j}^k \right|^2 \leqslant C_{\boldsymbol{\alpha\mu}}^N \sum_{k=1}^{N} \left\langle \frac{\boldsymbol{\mu}}{\boldsymbol{\alpha}} \right\rangle^{k} |D_{n,j}^k|^2. \tag{99}$$

Multiplying the above by $\frac{\mu_{n,j}}{\alpha_{n,j}}$ and using (98) results in the following inequality:

$$\frac{\mu_{n,j}}{\alpha_{n,j}} \left| \sum_{k=1}^{N} D_{n,j}^k \right|^2 \leqslant C_{\boldsymbol{\alpha\mu}}^N \sum_{k=1}^{N} \sum_{\ell_1=0}^{p-1} \cdots \sum_{\ell_k=0}^{p-1} \int_{\Sigma_{\boldsymbol{j}\ell_1\cdots\ell_k}} \mu \left|\partial_s u\right|^2. \tag{100}$$

Since the sets $\left\{\Sigma_{\boldsymbol{j}\ell_1\cdots\ell_k}, 0 \leqslant \ell_1, \ldots, \ell_k \leqslant p-1\right\}$ form, when $0 \leqslant j \leqslant p^n - 1$, a partition of the generation $\mathcal{G}^{n+k}$,

$$\sum_{j=0}^{p^n-1} \sum_{\ell_1=0}^{p-1} \cdots \sum_{\ell_k=0}^{p-1} \int_{\Sigma_{\boldsymbol{j}\ell_1\cdots\ell_k}} \mu \left|\partial_s u\right|^2 = \int_{\mathcal{G}^{n+k}} \mu \left|\partial_s u\right|^2. \tag{101}$$

Thus, after summation of (100) over $0 \leqslant j \leqslant p^n - 1$, we get

$$\sum_{j=0}^{p^n-1} \frac{\mu_{n,j}}{\alpha_{n,j}} \left| \sum_{k=1}^{N} D_{n,j}^k \right|^2 \leqslant C_{\boldsymbol{\alpha\mu}}^N \sum_{k=1}^{N} \int_{\mathcal{G}^{n+k}} \mu \left|\partial_s u\right|^2 = C_{\boldsymbol{\alpha\mu}}^N \int_{\mathcal{T}^{n+N}\setminus\mathcal{T}^n} \mu \left|\partial_s u\right|^2. \tag{102}$$

Finally, the inequality (92) is obtained by gathering (94), (96) and (102). □

Now we have all the ingredients necessary to prove theorem 3.5.

Proof of theorem 3.5. By theorem 3.2, see (69), it suffices to prove that $\operatorname{Ker} \tau_\infty \subseteq \mathrm{H}^1_{\mu,0}(\mathcal{T})$. In particular, we will show that following holds true:

$$\forall\, u \in \operatorname{Ker} \tau_\infty, \quad \left\langle \frac{\boldsymbol{\mu}}{\boldsymbol{\alpha}} \right\rangle^{n} \|\tau_n u\|^2 \to 0, \qquad n \to \infty. \tag{103}$$

By lemma 3.6 this will imply that $\operatorname{Ker} \tau_\infty \subseteq \mathrm{H}^1_{\mu,0}(\mathcal{T})$.

First, since (66) holds, we can define

$$C_{\boldsymbol{\alpha\mu}} := \sum_{k=1}^{+\infty} \left\langle \frac{\boldsymbol{\mu}}{\boldsymbol{\alpha}} \right\rangle^{-k} = \left(\left\langle \frac{\boldsymbol{\mu}}{\boldsymbol{\alpha}} \right\rangle - 1 \right)^{-1}. \tag{104}$$

From lemma 3.9 it follows that for all $u \in \mathrm{H}^1_\mu(\mathcal{T})$, $n,\ N \geqslant 1$,

$$\left\langle \frac{\boldsymbol{\mu}}{\boldsymbol{\alpha}} \right\rangle^n \|\tau_n u\|^2 \leqslant 2C_{\boldsymbol{\alpha\mu}} \, \|\partial_s u\|^2_{\mathrm{L}^2_\mu(\mathcal{T}\setminus\mathcal{T}^n)} + 2 \left\langle \frac{\boldsymbol{\mu}}{\boldsymbol{\alpha}} \right\rangle^n \|\tau_{n+N} u\|^2.$$

Let us assume $u \in \mathrm{Ker}\ \tau_\infty$. Then, taking $N \to +\infty$ in the above, we obtain

$$\left\langle \frac{\boldsymbol{\mu}}{\boldsymbol{\alpha}} \right\rangle^n \|\tau_n u\|^2 \leqslant 2C_{\boldsymbol{\alpha\mu}} \|\partial_s u\|^2_{\mathrm{L}^2_\mu(\mathcal{T}\setminus\mathcal{T}^n)}. \tag{105}$$

Since $u \in \mathrm{H}^1_\mu(\mathcal{T})$, the right-hand side of the above tends to zero as $n \to \infty$, from where (103) follows, and hence $u \in \mathrm{H}^1_{\mu,0}(\mathcal{T})$. □

It is natural to ask how big the image $\mathrm{Im}\ \tau_\infty$ of the map τ_∞ is. The answer to this question involves another fundamental quantity, namely

$$\langle \boldsymbol{\mu\alpha} \rangle := \sum_{i=0}^{p-1} \mu_i \, \alpha_i, \quad \left(\langle \boldsymbol{\mu\alpha} \rangle < \left\langle \frac{\boldsymbol{\mu}}{\boldsymbol{\alpha}} \right\rangle \text{ since } |\boldsymbol{\alpha}|_\infty < 1 \right). \tag{106}$$

Theorem 3.10. *Assume that*

$$\langle \boldsymbol{\mu\alpha} \rangle < 1 < \left\langle \frac{\boldsymbol{\mu}}{\boldsymbol{\alpha}} \right\rangle. \tag{107}$$

Then, for any $n \geqslant 1$, $\mathbb{P}_0(\Gamma_n) \subset$ Im τ_∞. In particular, Im τ_∞ is dense in $L^2(\Gamma_\infty)$.

Proof. Let $\mathbb{1}_\mathcal{T}$ be a function that equals identically to 1 on $\mathcal{T}$. It is easy to verify that

$$\langle \boldsymbol{\mu\alpha} \rangle < 1 \quad \Longleftrightarrow \quad \mathbb{1}_\mathcal{T} \in \mathrm{L}^2_\mu(\mathcal{T}). \tag{108}$$

Let $\varphi \in \mathbb{P}_0(\Gamma_n)$ and $\boldsymbol{\varphi}_{n,j}$ be the value of φ in the interval $[a_{n,j}, a_{n,j+1}]$. Let us construct $u \in \mathrm{H}^1_\mu(\mathcal{T})$ as follows

$$\begin{cases} u \equiv 0, & \text{in the truncated tree } \mathcal{T}^{n-1}, \\ u = \boldsymbol{\varphi}_{n,j}\ \mathbb{1}_\mathcal{T}, & \text{in each subtree } \mathcal{T}_{n,j}, 0 \leqslant j \leqslant p^n - 1, \\ u \text{ is affine}, & \text{along each edge of the generation } \mathcal{G}^n. \end{cases}$$

Remark that $u \in \mathrm{L}^2_\mu(\mathcal{T})$ is a consequence of (108). By construction, $\tau_\infty u = \varphi$. Thus, $\mathbb{P}_0(\Gamma_n) \subset \mathrm{Im}\ \tau_\infty$. The density of $\mathrm{Im}\,\tau_\infty$ follows from the approximation property of spaces $\mathbb{P}_0(\Gamma_n)$. □

Remark 3.11. *Theorem 3.5, lemmas 3.6, 3.7, 3.9 and theorem 3.10 hold both for compact and non-compact trees.*

Remark 3.12. *The following result proves that τ_∞ in not surjective: the traces posses some (weak) Sobolev regularity. In* [33, Section 5.4]*, it was proven that*

$$\tau_\infty \in \mathcal{L}\big(\mathrm{H}^1_\mu(\mathcal{T}), \mathrm{H}^\nu(\Gamma_\infty)\big) \quad \textit{for any } \nu < \nu^*,$$

where the critical Sobolev regularity exponent ν^* is defined as follows :

$$\nu^* = \min\left(\frac{1}{2}, \min_{0 \leqslant i \leqslant p-1} \left(\frac{1}{2} - \frac{\log \frac{\mu_i}{\alpha_i}}{2 \log \gamma_i} \right) \right).$$

When $\langle \boldsymbol{\mu\alpha} \rangle \geqslant 1$, the situation is totally different: the image of τ_∞ is reduced to 0, or, equivalently, $\mathrm{H}^1_{\mu,0}(\mathcal{T}) = \mathrm{Ker}\,\tau_\infty = \mathrm{H}^1_\mu(\mathcal{T})$. This will be proven in section 3.3.

Theorem 3.13. *Assume that* $\langle \boldsymbol{\mu\alpha} \rangle \geqslant 1$. *Then*

$$\forall\, u \in \mathrm{H}^1_\mu(\mathcal{T}), \quad \tau_\infty u = 0 \quad \textit{(i.e. Im } \tau_\infty = \{0\} \textit{ or Ker } \tau_\infty = \mathrm{H}^1_\mu(\mathcal{T}).\textit{)} \tag{109}$$

Proof. By theorem 3.18, see section 3.3, $\mathrm{H}^1_{\mu,0}(\mathcal{T}) = \mathrm{H}^1_\mu(\mathcal{T})$; the result follows from

$$\mathrm{H}^1_{\mu,0}(\mathcal{T}) = \mathrm{Ker}\,\tau_\infty.$$

□

3.3. **On the distinction between $\mathbf{H}^1_\mu(\mathcal{T})$ and $\mathbf{H}^1_{\mu,0}(\mathcal{T})$.** In this section we present the conditions on $\boldsymbol{\alpha}$, $\boldsymbol{\mu}$ that ensure that the spaces $\mathrm{H}^1_{\mu,0}(\mathcal{T})$ and $\mathrm{H}^1_\mu(\mathcal{T})$ coincide, or, in other words, when compactly supported functions (in the sense of (19)) are dense in $\mathrm{H}^1_\mu(\mathcal{T})$. Our first result in this direction is the following.

Theorem 3.14. *If the condition* (107) *holds, then* $\mathrm{H}^1_{\mu,0}(\mathcal{T}) \subsetneq \mathrm{H}^1_\mu(\mathcal{T})$.

Proof. The result is an immediate consequence of the trace theorem 3.10, since the equality $\mathrm{H}^1_{\mu,0}(\mathcal{T}) = \mathrm{H}^1_\mu(\mathcal{T})$, according to theorem 3.5, implies in particular that $\mathrm{Im}\,\tau_\infty = \{0\}$. □

As we are going to see, when $\langle \boldsymbol{\mu\alpha} \rangle \geqslant 1$ or $\left\langle \dfrac{\boldsymbol{\mu}}{\boldsymbol{\alpha}} \right\rangle \leqslant 1$, then $\mathrm{H}^1_{\mu,0}(\mathcal{T}) \equiv \mathrm{H}^1_\mu(\mathcal{T})$.

We shall state this result as two theorems, whose proofs are quite different:

- theorem 3.15 for $\left\langle \dfrac{\boldsymbol{\mu}}{\boldsymbol{\alpha}} \right\rangle \leqslant 1$ (and, consequently, $\langle \boldsymbol{\mu\alpha} \rangle < 1$).
- theorem 3.18 for $\langle \boldsymbol{\mu\alpha} \rangle \geqslant 1$ (and, consequently, $\left\langle \dfrac{\boldsymbol{\mu}}{\boldsymbol{\alpha}} \right\rangle > 1$).

Theorem 3.15. *If* $\left\langle \dfrac{\boldsymbol{\mu}}{\boldsymbol{\alpha}} \right\rangle \leqslant 1$, *then* $\mathrm{H}^1_{\mu,0}(\mathcal{T}) = \mathrm{H}^1_\mu(\mathcal{T})$.

To prove this result, we shall use the following technical lemma.

Lemma 3.16. *Let* (x_n), (ε_n), $n \in \mathbb{N}$, *be two sequences of non-negative real numbers. Let one of the following hold true:*

(i) $x_{n+1} \leqslant \gamma\, x_n + \varepsilon_n$, *where* $0 < \gamma < 1$ *and* $\varepsilon_n \to 0$ *as* $n \to \infty$*;*

(ii) $x_{n+1} \leqslant \gamma_n\, x_n + \varepsilon_n$, *where* $\gamma_n = 1 - \frac{a}{n+1}$, $0 < a < 1$, *and* $\sum_{k=0}^{\infty} \varepsilon_k < +\infty$.

Then the sequence x_n *converges to* 0 *when* $n \to +\infty$.

Proof. See appendix A. □

Proof of theorem 3.15. By lemma 3.6, it suffices to prove that (77) holds for any $u \in \mathrm{H}^1_\mu(\mathcal{T})$. To do so, we compare the norms of two successive partial traces of u, cf. (75),

$$\begin{cases} \|\tau_n u\|^2 = \left\langle \dfrac{\boldsymbol{\mu}}{\boldsymbol{\alpha}} \right\rangle^{-n} \displaystyle\sum_{j=0}^{p^n-1} \frac{\mu_{n,j}}{\alpha_{n,j}}\, |\mathbf{u}_{\boldsymbol{j}}|^2, \\ \|\tau_{n+1} u\|^2 = \left\langle \dfrac{\boldsymbol{\mu}}{\boldsymbol{\alpha}} \right\rangle^{-n-1} \displaystyle\sum_{j=0}^{p^n-1} \sum_{\ell=0}^{p-1} \frac{\mu_{n,j}}{\alpha_{n,j}} \frac{\mu_\ell}{\alpha_\ell}\, |\mathbf{u}_{\boldsymbol{j}\ell}|^2. \end{cases} \tag{110}$$

Because

$$\mathbf{u}_{\boldsymbol{j}\ell} = \mathbf{u}_{\boldsymbol{j}} + \int_{\Sigma_{\boldsymbol{j}\ell}} \partial_s u,$$

we deduce, using the Young's inequality (with a parameter $\eta_n > 0$, which we will choose later) and the Cauchy-Schwarz inequality for the integral, cf. (72),

$$|\mathbf{u}_{\boldsymbol{j}\ell}|^2 \leqslant (1+\eta_n)\,|\mathbf{u}_{\boldsymbol{j}}|^2 + (1+\eta_n^{-1})\,\frac{\alpha_{n,j}}{\mu_{n,j}}\,\frac{\alpha_\ell}{\mu_\ell}\int\limits_{\Sigma_{\boldsymbol{j}\ell}} \mu\,|\partial_s u|^2.$$

Multiplying the above by $\dfrac{\mu_{n,j}}{\alpha_{n,j}}\,\dfrac{\mu_\ell}{\alpha_\ell}$ and summing over $0 \leqslant j \leqslant p^n - 1$ and $0 \leqslant \ell \leqslant p-1$ we obtain, with (110),

$$t_{n+1} \leqslant (1+\eta_n)\left\langle \frac{\boldsymbol{\mu}}{\boldsymbol{\alpha}} \right\rangle t_n + (1+\eta_n^{-1})\,\|\partial_s u\|^2_{\mathcal{G}^{n+1}}, \quad \text{where} \quad t_n := \left\langle \frac{\boldsymbol{\mu}}{\boldsymbol{\alpha}} \right\rangle^n \|\tau_n u\|^2. \tag{111}$$

In the above the term $\|\partial_s u\|^2_{\mathcal{G}^{n+1}}$ was obtained like in (101). Let us then consider separately, for the sake of clarity, the following two cases.

Case 1 : $\left\langle \dfrac{\boldsymbol{\mu}}{\boldsymbol{\alpha}} \right\rangle < 1$. We choose $\eta_n = \eta$, independent of n, so that

$$\gamma := (1+\eta)\left\langle \frac{\boldsymbol{\mu}}{\boldsymbol{\alpha}} \right\rangle < 1.$$

Then, by Lemma 3.16, case (i), we prove that $t_n \to 0$ as $n \to +\infty$ which implies in particular (77).

Case 2 : the limit case $\left\langle \dfrac{\boldsymbol{\mu}}{\boldsymbol{\alpha}} \right\rangle = 1$. Since $\left\langle \dfrac{\boldsymbol{\mu}}{\boldsymbol{\alpha}} \right\rangle = 1$, the previous approach will not work. To explain the choice of η_n, let us define $\widehat{t}_n := n^{-1}\,t_n$, so that (111) becomes

$$\widehat{t}_{n+1} \leqslant \big(1+\eta_n\big)\,\frac{n}{n+1}\,\widehat{t}_n + (1+\eta_n^{-1})\,(n+1)^{-1}\|\partial_s u\|^2_{\mathcal{G}^{n+1}}, \tag{112}$$

We choose η_n so that

$$\big(1+\eta_n\big)\,\frac{n}{n+1} = 1 - \frac{1}{2(n+1)} \quad \Longrightarrow \quad \eta_n = \frac{1}{2n} > 0.$$

Then, as $\varepsilon_n = (1+2n)\,(n+1)^{-1}\|\partial_s u\|^2_{\mathcal{G}^{n+1}} \leqslant 2\|\partial_s u\|^2_{\mathcal{G}^{n+1}}$ is summable, by Lemma 3.16, case (ii) (with $a = 1/2$), we prove that that $\widehat{t}_n \to 0$, i. e. (77). □

Remark 3.17. *We have shown that when* $\left\langle \dfrac{\boldsymbol{\mu}}{\boldsymbol{\alpha}} \right\rangle < 1$, $\left\langle \dfrac{\boldsymbol{\mu}}{\boldsymbol{\alpha}} \right\rangle^n \|\tau_n u\|^2 \to 0$ *as* $n \to \infty$.

This does not hold when $\left\langle \dfrac{\boldsymbol{\mu}}{\boldsymbol{\alpha}} \right\rangle = 1$, *with a counterexample provided by the identity function. Notice that*

$$\mathbb{1}_{\mathcal{T}} \in \mathrm{H}^1_\mu(\mathcal{T}),\ \textit{cf. (108)}, \quad \textit{and} \quad \left\langle \frac{\boldsymbol{\mu}}{\boldsymbol{\alpha}} \right\rangle^n \|\tau_n \mathbb{1}_{\mathcal{T}}\|^2 = \|\tau_n \mathbb{1}_{\mathcal{T}}\|^2 = 1.$$

Nonetheless, in this case $\mathbb{1}_{\mathcal{T}} \in \mathrm{H}^1_{\mu,0}(\mathcal{T}) = \mathrm{H}^1_\mu(\mathcal{T})$.

Finally, we consider the case $\langle \boldsymbol{\mu}\boldsymbol{\alpha} \rangle \geqslant 1$, and, in particular, (66) holds.

Theorem 3.18. *If* $\langle \boldsymbol{\mu}\boldsymbol{\alpha} \rangle \geqslant 1$, *then* $\mathrm{H}^1_{\mu,0}(\mathcal{T}) = \mathrm{H}^1_\mu(\mathcal{T})$.

The proof of this result is, in its structure, quite similar to the proof of $\mathrm{H}^1_{\mu,0}(\mathcal{T}) = \mathrm{Ker}\,\tau_\infty$, i.e. theorem 3.5, where we use extensively lemma 3.7 and convexity or the Cauchy-Schwarz inequality based arguments. However, we need to proceed differently, because, unlike in theorem 3.5, we do not assume any longer that $\|\tau_{n+N}u\|$ converges to 0. This prevents us from exploiting the inequality (92). The key trick will be to obtain an inequality similar to (92) where the quantity $\|\tau_{n+N}u\|$ is replaced by a similar quantity, related to $\tau_{n+N}u$, which tends to 0 when $N \to \infty$ and resembles (in a certain sense which will

be clear later) $\|u\|^2_{L^2(\mathcal{G}^{n+N})}$. Instead of working directly with the the squared L^2-norm, we shall use the fact that, when $n \to +\infty$, because the size of the edges of $\mathcal{T} \setminus \mathcal{T}^n$ decreases drastically, u in $\mathrm{H}^1_\mu(\mathcal{T} \setminus \mathcal{T}^n)$ can be accurately approximated by a piecewise-constant function, defined in (83), see the proof of lemma 3.6. This assertion is quantified by the following technical lemma.

Lemma 3.19. *For all $n \geqslant 1$, $u \in \mathrm{H}^1_\mu(\mathcal{T})$,*

$$\begin{cases} \dfrac{1}{2}\,\|\Pi u\|^2_{\mathrm{L}^2_\mu(\mathcal{T}\setminus\mathcal{T}^n)} - \dfrac{4}{\pi^2}\,|\boldsymbol{\alpha}|^{2n+2}_\infty\,\|\partial_s u\|^2_{\mathrm{L}^2_\mu(\mathcal{T}\setminus\mathcal{T}^n)} \leqslant \|u\|^2_{\mathrm{L}^2_\mu(\mathcal{T}\setminus\mathcal{T}^n)}, & (i) \\[2ex] \|u\|^2_{\mathrm{L}^2_\mu(\mathcal{T}\setminus\mathcal{T}^n)} \leqslant 2\,\|\Pi u\|^2_{\mathrm{L}^2_\mu(\mathcal{T}\setminus\mathcal{T}^n)} + \dfrac{8}{\pi^2}\,|\boldsymbol{\alpha}|^{2n+2}_\infty\,\|\partial_s u\|^2_{\mathrm{L}^2_\mu(\mathcal{T}\setminus\mathcal{T}^n)}. & (ii) \end{cases} \tag{113}$$

In particular, for all $u \in \mathrm{H}^1_\mu(\mathcal{T})$, $\displaystyle\lim_{n\to+\infty} \|\Pi u\|^2_{\mathrm{L}^2_\mu(\mathcal{T}\setminus\mathcal{T}^n)} = 0.$

Proof. The bounds (113) follow from

$$\begin{aligned} \|u\|^2_{\mathrm{L}^2_\mu(\mathcal{T}\setminus\mathcal{T}^n)} &\leqslant 2\,\|\Pi u\|^2_{\mathrm{L}^2_\mu(\mathcal{T}\setminus\mathcal{T}^n)} + 2\,\|u - \Pi u\|^2_{\mathrm{L}^2_\mu(\mathcal{T}\setminus\mathcal{T}^n)}, \\ \|\Pi u\|^2_{\mathrm{L}^2_\mu(\mathcal{T}\setminus\mathcal{T}^n)} &\leqslant 2\,\|u\|^2_{\mathrm{L}^2_\mu(\mathcal{T}\setminus\mathcal{T}^n)} + 2\,\|u - \Pi u\|^2_{\mathrm{L}^2_\mu(\mathcal{T}\setminus\mathcal{T}^n)}, \end{aligned} \tag{114}$$

and the bound (84) for $\|u - \Pi u\|^2_{\mathrm{L}^2_\mu(\mathcal{T}\setminus\mathcal{T}^n)}$, rewritten in the form

$$\|u - \Pi u\|^2_{\mathrm{L}^2_\mu(\Sigma_{n,j})} \leqslant \frac{4}{\pi^2}|\boldsymbol{\alpha}|^{2n}_\infty \|\partial_s u\|^2_{\mathrm{L}^2_\mu(\Sigma_{n,j})}.$$

The fact that $\displaystyle\lim_{n\to+\infty} \|\Pi u\|^2_{\mathrm{L}^2_\mu(\mathcal{T}\setminus\mathcal{T}^n)} = 0$ follows from the bound (114) and $|\boldsymbol{\alpha}|_\infty < 1$. □

The interest of working with Πu is that, inside $\mathcal{G}^n$, Πu is defined by the same nodal values as $\tau_n u$. As a consequence, it is easy to relate $\tau_n u$ to Πu in $\mathcal{G}^n$. This allows us to formulate an analogue of lemma 3.9, more precisely of the inequality (92). Let us first introduce

$$\widehat{C}^N_{\boldsymbol{\alpha}\boldsymbol{\mu}} = \sum_{\ell=1}^{N} \langle \boldsymbol{\mu}\boldsymbol{\alpha}\rangle^{-\ell} |\boldsymbol{\alpha}|^{2\ell}_\infty. \tag{115}$$

Lemma 3.20. *For any $u \in \mathrm{H}^1_\mu(\mathcal{T})$, $n,\ N \geqslant 1$,*

$$\left\langle \frac{\boldsymbol{\mu}}{\boldsymbol{\alpha}} \right\rangle^n \|\tau_n u\|^2 \leqslant 2\,\widehat{C}^N_{\boldsymbol{\alpha}\boldsymbol{\mu}}\,\|\partial_s u\|^2_{\mathrm{L}^2_\mu(\mathcal{T}\setminus\mathcal{T}^n)} + 2\,\langle \boldsymbol{\mu}\boldsymbol{\alpha}\rangle^{-N} |\boldsymbol{\alpha}^{-1}|^{2n}_\infty\,\|\Pi u\|^2_{\mathrm{L}^2_\mu(\mathcal{G}^{n+N})}. \tag{116}$$

Proof. Let us first remark that

$$\|\Pi u\|^2_{\mathrm{L}^2_\mu(\mathcal{G}^n)} = \sum_{j=0}^{p^n-1} \mu_{n,j}\alpha_{n,j}\,|\boldsymbol{u_j}|^2 \tag{117}$$

resembles $\left\langle \dfrac{\boldsymbol{\mu}}{\boldsymbol{\alpha}} \right\rangle^n \|\tau_n u\|^2$, cf. (75), with $\mu_{n,j}\alpha^{-1}_{n,j}$ replaced by $\mu_{n,j}\alpha_{n,j}$.
Thus, we will use the same idea as in the proof of lemma 3.9; we start with the inequality (94), however, we define $P^N_{n,j}$ and $D^k_{n,j}$ differently than in lemma 3.9. More precisely, we use lemma 3.7 with $q_\ell = \mu_\ell\alpha_\ell\langle\boldsymbol{\mu}\boldsymbol{\alpha}\rangle^{-1}$, $\ell = 0, \dots, p-1$.
As a consequence, proceeding as in the proof of lemma 3.9, we see that (94) is still valid but with different $P^N_{n,j}$ and $D^k_{n,j}$. In particular, the estimate (95) has to be replaced by

$$|P^N_{n,j}|^2 \quad\leqslant\quad \langle\boldsymbol{\mu}\boldsymbol{\alpha}\rangle^{-N} \sum_{\ell_1=0}^{p-1} \cdots \sum_{\ell_N=0}^{p-1} \mu_{\ell_1}\alpha_{\ell_1} \cdots \mu_{\ell_N}\alpha_{\ell_N}\,|\mathbf{u}_{\boldsymbol{j}\ell_1\dots\ell_N}|^2. \tag{118}$$

After multiplication by $\mu_{n,j}/\alpha_{n,j}$ and summation over $0 \leqslant j \leqslant p^n - 1$, we obtain

$$\sum_{j=0}^{p^n-1} \frac{\mu_{n,j}}{\alpha_{n,j}} \left|P_{n,j}^N\right|^2 \leqslant \left\langle \boldsymbol{\mu\alpha} \right\rangle^{-N} \sum_{j=0}^{p^n-1} \frac{\mu_{n,j}}{\alpha_{n,j}} \sum_{\ell_1=0}^{p-1} \cdots \sum_{\ell_N=0}^{p-1} \mu_{\ell_1}\alpha_{\ell_1} \cdots \mu_{\ell_N}\alpha_{\ell_N} \left|\mathbf{u}_{\boldsymbol{j}\ell_1\cdots\ell_N}\right|^2.$$

Since $\dfrac{\mu_{n,j}}{\alpha_{n,j}} = \mu_{n,j}\alpha_{n,j} \cdot \alpha_{n,j}^{-2} \leqslant \mu_{n,j}\alpha_{n,j} \left|\boldsymbol{\alpha}^{-1}\right|_\infty^{2n}$,

$$\begin{aligned}\sum_{j=0}^{p^n-1} \frac{\mu_{n,j}}{\alpha_{n,j}} \left|P_{n,j}^N\right|^2 &\leqslant \left\langle \boldsymbol{\mu\alpha} \right\rangle^{-N} \left|\boldsymbol{\alpha}^{-1}\right|_\infty^{2n} \sum_{k=0}^{p^{n+N}-1} \mu_{n+N,k}\,\alpha_{n+N,k} \left|\mathbf{u}_{n+N}, k\right|^2 \\ &= \left\langle \boldsymbol{\mu\alpha} \right\rangle^{-N} \left|\boldsymbol{\alpha}^{-1}\right|_\infty^{2n} \left\|\Pi u\right\|_{\mathrm{L}^2_\mu(\mathcal{G}^{n+N})}^2, \end{aligned} \tag{119}$$

where the last equality follows from (117).
To obtain an upper bound for $|D_{n,j}^k|^2$, cf. (97), we use the convexity argument:

$$|D_{n,j}^k|^2 \leqslant \left\langle \boldsymbol{\mu\alpha} \right\rangle^{-k} \sum_{\ell_1=0}^{p-1} \cdots \sum_{\ell_k=0}^{p-1} \mu_{\ell_1}\alpha_{\ell_1} \cdots \mu_{\ell_k}\alpha_{\ell_k} \left| \int_{\Sigma_{\boldsymbol{j}\ell_1\cdots\ell_k}} \partial_s u \right|^2.$$

Using the Cauchy-Schwarz inequality, like in (72),

$$\begin{aligned}|D_{n,j}^k|^2 &\leqslant \left\langle \boldsymbol{\mu\alpha} \right\rangle^{-k} \frac{\alpha_{n,j}}{\mu_{n,j}} \sum_{\ell_1=0}^{p-1} \cdots \sum_{\ell_k=0}^{p-1} \alpha_{\ell_1}^2 \cdots \alpha_{\ell_k}^2 \int_{\Sigma_{\boldsymbol{j}\ell_1\cdots\ell_k}} \mu \left|\partial_s u\right|^2 \\ &\leqslant \left\langle \boldsymbol{\mu\alpha} \right\rangle^{-k} \left|\boldsymbol{\alpha}\right|_\infty^{2k} \frac{\alpha_{n,j}}{\mu_{n,j}} \sum_{\ell_1=0}^{p-1} \cdots \sum_{\ell_k=0}^{p-1} \int_{\Sigma_{\boldsymbol{j}\ell_1\cdots\ell_k}} \mu \left|\partial_s u\right|^2 \end{aligned} \tag{120}$$

Using the discrete Cauchy-Schwartz inequality, introducing $\nu := \left\langle \boldsymbol{\mu\alpha} \right\rangle^{-\frac{1}{2}} |\boldsymbol{\alpha}|_\infty$, we obtain

$$\begin{aligned}\sum_{j=0}^{p^n-1} \frac{\mu_{n,j}}{\alpha_{n,j}} \left| \sum_{k=1}^{N} D_{n,j}^k \right|^2 &= \sum_{j=0}^{p^n-1} \frac{\mu_{n,j}}{\alpha_{n,j}} \left| \sum_{k=1}^{N} \left(\nu^k \cdot \nu^{-k} D_{n,j}^k\right) \right|^2 \\ &\leqslant \widehat{C}_{\boldsymbol{\alpha\mu}}^N \sum_{k=1}^{N} \sum_{j=0}^{p^n-1} \sum_{\ell_1=0}^{p-1} \cdots \sum_{\ell_k=0}^{p-1} \int_{\Sigma_{j\ell_1\cdots\ell_k}} \mu \left|\partial_s u\right|^2, \end{aligned}$$

where we used the bound (120) and the definition (115) of $\widehat{C}_{\boldsymbol{\alpha\mu}}^N$. With (101),

$$\sum_{j=0}^{p^n-1} \frac{\mu_{n,j}}{\alpha_{n,j}} \left| \sum_{k=1}^{N} D_{n,j}^k \right|^2 \leqslant \widehat{C}_{\boldsymbol{\alpha\mu}}^N \sum_{k=1}^{N} \int_{\mathcal{G}^{n+k}} \mu \left|\partial_s u\right|^2 = \widehat{C}_{\boldsymbol{\alpha\mu}}^N \|\partial_s u\|_{\mathrm{L}^2_\mu(\mathcal{T}^{n+N}\setminus\mathcal{T}^n)}^2. \tag{121}$$

The desired result is obtained by substituting (119) and (121) into (94). □

Now we have all the components necessary to prove theorem 3.18.

Proof of theorem 3.18. We will use the characterization of the space $\mathrm{H}^1_{\mu,0}(\mathcal{T})$ of lemma 3.6, namely, we will show that (77) holds for all $u \in \mathrm{H}^1_\mu(\mathcal{T})$. For this we employ (116).
Since the tree is compact, i.e. $|\boldsymbol{\alpha}_\infty| < 1$ and $\left\langle \boldsymbol{\mu\alpha} \right\rangle \geqslant 1$, the value $\widehat{C}_{\boldsymbol{\alpha\mu}}^N$ is bounded uniformly in N by

$$\widehat{C}_{\boldsymbol{\alpha\mu}} := \left\langle \boldsymbol{\mu\alpha} \right\rangle^{-1} |\boldsymbol{\alpha}|_\infty^2 \left(1 - \left\langle \boldsymbol{\mu\alpha} \right\rangle^{-1} |\boldsymbol{\alpha}|_\infty^2\right)^{-1}.$$

This allows us to take a limit $N \to +\infty$ in (116). Together with lemma 3.19 (namely, using the fact that $\lim_{N\to\infty} \|\Pi u\|^2_{\mathrm{L}^2_\mu(\mathcal{G}^{n+N})} = 0$), we obtain the following inequality, valid for all $u \in \mathrm{H}^1_\mu(\mathcal{T})$,

$$\left\langle \frac{\boldsymbol{\mu}}{\boldsymbol{\alpha}} \right\rangle^n \|\tau_n u\|^2 \leqslant 2\, \widehat{C}_{\boldsymbol{\alpha}\boldsymbol{\mu}}\, \|\partial_s u\|^2_{\mathrm{L}^2_\mu(\mathcal{T}\setminus\mathcal{T}^n)}.$$

This shows that $\left\langle \frac{\boldsymbol{\mu}}{\boldsymbol{\alpha}} \right\rangle^n \|\tau_n u\|^2 \to 0$ as $n \to \infty$, and, by lemma 3.6, $u \in \mathrm{H}^1_{\mu,0}(\mathcal{T})$. □

Remark 3.21. *Theorem 3.15 holds both for compact and non-compact trees. The proof of Theorem 3.18, however, uses the compactness of the tree.*

3.4. **Summary and different regions of parameters.** In this section we will summarize the results of the previous sections about the trace operator and relationship between the spaces $\mathrm{H}^1_{\mu,0}(\mathcal{T})$ and $\mathrm{H}^1_\mu(\mathcal{T})$. Such a brief outline is provided in figure 6.

	$\langle \boldsymbol{\mu}\boldsymbol{\alpha} \rangle < 1$	$\langle \boldsymbol{\mu}\boldsymbol{\alpha} \rangle \geq 1$
$\left\langle \frac{\boldsymbol{\mu}}{\boldsymbol{\alpha}} \right\rangle > 1$	$\boldsymbol{\tau}_\infty$ exists Ker $\boldsymbol{\tau}_\infty = \mathrm{H}^1_{\mu,0}(\mathcal{T})$ $\mathrm{H}^1_{\mu,0}(\mathcal{T}) \subsetneq \mathrm{H}^1_\mu(\mathcal{T})$ Im $\boldsymbol{\tau}_\infty$ is dense	$\boldsymbol{\tau}_\infty$ exists Ker $\boldsymbol{\tau}_\infty = \mathrm{H}^1_{\mu,0}(\mathcal{T})$ $\mathrm{H}^1_{\mu,0}(\mathcal{T}) = \mathrm{H}^1_\mu(\mathcal{T})$ Im $\boldsymbol{\tau}_\infty = \{0\}$
$\left\langle \frac{\boldsymbol{\mu}}{\boldsymbol{\alpha}} \right\rangle \leq 1$	$\boldsymbol{\tau}_\infty$ does not exist $\mathrm{H}^1_{\mu,0}(\mathcal{T}) = \mathrm{H}^1_\mu(\mathcal{T})$	

FIGURE 6. A summary of the results of sections 3.1-3.3.

This difference between different values of $\boldsymbol{\mu}$, $\boldsymbol{\alpha}$ will be expressed as well in the construction of transparent boundary conditions. Let us thus introduce the following space of parameters:

$$\mathbb{P} := \{(\boldsymbol{\mu},\, \boldsymbol{\alpha}) \in \left(\mathbb{R}^*_+\right)^p \times \left(\mathbb{R}^*_+\right)^p :\ |\boldsymbol{\alpha}|_\infty < 1\}.$$

According to figure 6, we can partition it into the three regions:

$$\begin{aligned}
\mathbb{P}_N &:= \{(\boldsymbol{\mu},\, \boldsymbol{\alpha}) \in \mathbb{P} :\ \left\langle \frac{\boldsymbol{\mu}}{\boldsymbol{\alpha}} \right\rangle \leqslant 1\},\\
\mathbb{P}_{ND} &:= \{(\boldsymbol{\mu},\, \boldsymbol{\alpha}) \in \mathbb{P} :\ \left\langle \frac{\boldsymbol{\mu}}{\boldsymbol{\alpha}} \right\rangle > 1,\, \left\langle \boldsymbol{\mu}\boldsymbol{\alpha} \right\rangle < 1\},\\
\mathbb{P}_D &:= \{(\boldsymbol{\mu},\, \boldsymbol{\alpha}) \in \mathbb{P} :\ \left\langle \boldsymbol{\mu}\boldsymbol{\alpha} \right\rangle \geqslant 1\}.
\end{aligned} \tag{122}$$

Note that (this will be used later)

$$\left\langle \frac{\boldsymbol{\mu}}{\boldsymbol{\alpha}} \right\rangle > 1 \iff (\boldsymbol{\mu},\, \boldsymbol{\alpha}) \in \mathbb{P}_{ND} \cup \mathbb{P}_D, \quad \left\langle \boldsymbol{\mu}\boldsymbol{\alpha} \right\rangle < 1 \iff (\boldsymbol{\mu},\, \boldsymbol{\alpha}) \in \mathbb{P}_{ND} \cup \mathbb{P}_N. \tag{123}$$

The choice of the notation with indices N, ND and D will become clear later, when constructing transparent boundary conditions(cf. corollary 5.6 and remark 5.7).

3.5. Compact Embedding of $\mathrm{H}^1_\mu(\mathcal{T})$ into $\mathrm{L}^2_\mu(\mathcal{T})$.

It appears that independently of $\boldsymbol{\mu}$, the embedding $\mathrm{H}^1_\mu(\mathcal{T}) \hookrightarrow \mathrm{L}^2_\mu(\mathcal{T})$ is compact. The proof of this result is lengthy, and, moreover, uses somewhat different approaches depending whether the case $\left\langle \boldsymbol{\mu}\boldsymbol{\alpha} \right\rangle \geqslant 1$ or $\left\langle \boldsymbol{\mu}\boldsymbol{\alpha} \right\rangle < 1$ is considered. Nonetheless, both approaches are based on the following characterization of the compactness, which follows from the works of F. Ali Mehmeti et S. Nicaise [8] and Y. Achdou et N. Tchou [6].

Lemma 3.22. *Let $V = \mathrm{H}^1_{\mu,0}(\mathcal{T})$ or $\mathrm{H}^1_\mu(\mathcal{T})$. The injection of V in $\mathrm{L}^2_\mu(\mathcal{T})$ is compact if and only there exists a sequence $(\gamma_n)_{n\in\mathbb{N}}$, s.t. $\lim_{n\to\infty} \gamma_n = 0$ and*

$$\forall\, u \in V, \quad \|u\|_{\mathrm{L}^2_\mu(\mathcal{T}\setminus\mathcal{T}^n)} \leqslant \gamma_n \, \|u\|_{\mathrm{H}^1_\mu(\mathcal{T})}\,. \tag{124}$$

Proof. See appendix B. □

Depending on the approach taken to prove the inequality (124), we split the compactness result into two theorems:

- the compactness of the embedding $\mathrm{H}^1_\mu(\mathcal{T}) \hookrightarrow \mathrm{L}^2_\mu(\mathcal{T})$ when $\left\langle \boldsymbol{\mu}\boldsymbol{\alpha} \right\rangle \geqslant 1$ (i.e. in $\mathbb{P}_D$) is the statement of theorem 3.23.
- the compactness of the embedding $\mathrm{H}^1_\mu(\mathcal{T}) \hookrightarrow \mathrm{L}^2_\mu(\mathcal{T})$ when $\left\langle \boldsymbol{\mu}\boldsymbol{\alpha} \right\rangle < 1$ (i.e. in $\mathbb{P}_N \cup \mathbb{P}_{ND}$) is the principal result of theorem 3.24.

We start with the case $\left\langle \boldsymbol{\mu}\boldsymbol{\alpha} \right\rangle \geqslant 1$, as it uses inequalities used in the proof of lemma 3.9.

Theorem 3.23. *If $\left\langle \boldsymbol{\mu}\boldsymbol{\alpha} \right\rangle \geqslant 1$, the embedding $\mathrm{H}^1_\mu(\mathcal{T}) \hookrightarrow \mathrm{L}^2_\mu(\mathcal{T})$ is compact.*

Proof. We use the criterion of lemma 3.22. Because of theorem 3.18, it suffices to demonstrate that (124) holds for any function from $\mathrm{H}^1_{\mu,0}(\mathcal{T})$. By lemma 3.19, in particular (113)-(ii), we can just show that (124) holds with $\|u\|_{\mathrm{L}^2_\mu(\mathcal{T}\setminus\mathcal{T}^n)}$ replaced by $\|\Pi u\|_{\mathrm{L}^2_\mu(\mathcal{T}\setminus\mathcal{T}^n)}$.

Let us first assume that $u \in \mathrm{H}^1_{\mu,\mathrm{c}}(\mathcal{T})$, i. e. $u|_{\mathcal{T}\setminus\mathcal{T}^N} = 0$ for some N. Thus, for all $n < N$,

$$\|\Pi u\|^2_{\mathrm{L}^2_\mu(\mathcal{T}\setminus\mathcal{T}^n)} = \sum_{m=n+1}^{N} \|\Pi u\|^2_{\mathrm{L}^2_\mu(\mathcal{G}^m)} = \sum_{m=n+1}^{N} \sum_{j=0}^{p^m-1} \alpha_{m,j}\mu_{m,j}|\mathbf{u}_{m,j}|^2. \tag{125}$$

First, we apply lemma 3.7 with $q_\ell = \gamma_\ell$, cf. (63), which gives, since $P^N_{n,j} \equiv 0$,

$$|\mathbf{u}_{m,j}|^2 = \left| \sum_{k=1}^{N-m} D^k_{m,j} \right|^2. \tag{126}$$

Together with (100), the above results in

$$\sum_{j=0}^{p^m-1} \alpha_{m,j}\mu_{m,j}|\mathbf{u}_{m,j}|^2 \leqslant C_{\boldsymbol{\alpha\mu}}^{N-m} \sum_{k=1}^{N-m} \sum_{j=0}^{p^m-1} \alpha_{m,j}^2 \sum_{\ell_1=0}^{p-1} \cdots \sum_{\ell_k=0}^{p-1} \|\partial_s u\|^2_{\mathrm{L}^2_\mu(\Sigma_{j\ell_1\cdots\ell_k})}.$$

With the bound $C_{\boldsymbol{\alpha\mu}}^k < C_{\boldsymbol{\alpha\mu}}$, $k \in \mathbb{N}$, see (104) (valid because $\left\langle \dfrac{\boldsymbol{\mu}}{\boldsymbol{\alpha}} \right\rangle > \langle \boldsymbol{\mu\alpha} \rangle \geqslant 1$), and the observation (101), the above inequality yields:

$$\sum_{j=0}^{p^m-1} \alpha_{m,j}\mu_{m,j}|\mathbf{u}_{m,j}|^2 \leqslant C_{\boldsymbol{\alpha\mu}}|\boldsymbol{\alpha}|_\infty^{2m} \|\partial_s u\|^2_{\mathrm{L}^2_\mu(\mathcal{T}^N\setminus\mathcal{T}^m)} = C_{\boldsymbol{\alpha\mu}}|\boldsymbol{\alpha}|_\infty^{2m} \|\partial_s u\|^2_{\mathrm{L}^2_\mu(\mathcal{T}\setminus\mathcal{T}^m)}.$$

Thus, for any $u \in \mathrm{H}^1_{\mu,\mathrm{c}}(\mathcal{T})$, any $n \geqslant 1$, the above and (125) imply

$$\|\Pi u\|^2_{\mathrm{L}^2_\mu(\mathcal{T}\setminus\mathcal{T}^n)} \leqslant C_{\boldsymbol{\alpha\mu}} \frac{|\boldsymbol{\alpha}|_\infty^{2n+2}}{1-|\boldsymbol{\alpha}|_\infty^2} \|\partial_s u\|^2_{\mathrm{L}^2_\mu(\mathcal{T}\setminus\mathcal{T}^n)}. \tag{127}$$

With (113)-(ii) and the density argument, a similar inequality holds for $\|u\|^2_{\mathrm{L}^2_\mu(\mathcal{T}\setminus\mathcal{T}^n)}$ whenever $u \in \mathrm{H}^1_{\mu,0}(\mathcal{T}) = \mathrm{H}^1_\mu(\mathcal{T})$. We conclude with lemma 3.22. □

The case $\langle \boldsymbol{\mu\alpha} \rangle < 1$ is slightly different, since we will show an inequality of the form

$$\|\Pi u\|^2_{\mathrm{L}^2_\mu(\mathcal{T}\setminus\mathcal{T}^n)} \leqslant \gamma_n \, \|\partial_s u\|^2_{\mathrm{L}^2_\mu(\mathcal{T}^n)}, \quad \text{with } \lim_{n\to+\infty} \gamma_n = 0. \tag{128}$$

Compared with (127), $\|\partial_s u\|^2_{\mathrm{L}^2_\mu(\mathcal{T}^n)}$ is replaced by $\|\partial_s u\|^2_{\mathrm{L}^2_\mu(\mathcal{T}\setminus\mathcal{T}^n)}$.

The reason is that when $\langle \boldsymbol{\mu\alpha} \rangle < 1$, $\mathrm{H}^1_{\mu,\mathrm{c}}(\mathcal{T})$ is not necessarily dense in $\mathrm{H}^1_\mu(\mathcal{T})$, cf. theorem 3.14, and thus the identity (126) is no longer valid.

Theorem 3.24. *If $\langle \boldsymbol{\mu\alpha} \rangle < 1$, the embedding $\mathrm{H}^1_\mu(\mathcal{T}) \hookrightarrow \mathrm{L}^2_\mu(\mathcal{T})$ is compact.*

Proof. Like in the proof of theorem 3.23, it suffices to show that for all $u \in \mathrm{H}^1_\mu(\mathcal{T})$,

$$\text{(124) holds with } \|u\|_{\mathrm{L}^2_\mu(\mathcal{T}\setminus\mathcal{T}^n)} \text{ replaced by } \|\Pi u\|_{\mathrm{L}^2_\mu(\mathcal{T}\setminus\mathcal{T}^n)}.$$

Without loss of generality, we may assume that $u(M_{0,0}) = 0$. As discussed, we will show that $\|\Pi u\|_{\mathrm{L}^2_\mu(\mathcal{G}^n)}$ is controlled by $\|\partial_s u\|_{\mathrm{L}^2_\mu(\mathcal{T}^n)}$. For this, let us express $\mathbf{u}_{n,j}$ as an integral of $\partial_s u$ over the path that joins $M_{0,0}$ and $M_{n,j}$:

$$\mathbf{u}_{n,j} = \mathbf{u}_{j_1\cdots j_n} = \sum_{\ell=1}^n \int_{\Sigma_{j_1\cdots j_\ell}} \partial_s u.$$

Using discrete and continuous (cf. (72)) Cauchy-Schwarz inequalities, we have

$$|\mathbf{u}_{j_1\cdots j_n}|^2 \leqslant n \sum_{\ell=1}^n \left| \int_{\Sigma_{j_1\cdots j_\ell}} \partial_s u \right|^2 = n \sum_{\ell=1}^n \frac{\alpha_{j_1}\cdots\alpha_{j_\ell}}{\mu_{j_1}\cdots\mu_{j_\ell}} \|\partial_s u\|^2_{\mathrm{L}^2_\mu(\Sigma_{j_1\cdots j_\ell})}.$$

After the multiplication by $\alpha_{n,j}\mu_{n,j} \equiv \alpha_{j_1\cdots j_n}\mu_{j_1\cdots j_n}$, the above yields:

$$\begin{aligned}
\alpha_{n,j}\mu_{n,j}|\mathbf{u}_{j_1\cdots j_n}|^2 &\leqslant n \sum_{\ell=1}^n \alpha_{j_1}^2\cdots\alpha_{j_\ell}^2\alpha_{j_{\ell+1}}\mu_{j_{\ell+1}}\cdots\alpha_{j_n}\mu_{j_n} \|\partial_s u\|^2_{\mathrm{L}^2_\mu(\Sigma_{j_1\cdots j_\ell})} \\
&\leqslant n \sum_{\ell=1}^n |\boldsymbol{\alpha}|_\infty^{2\ell} \alpha_{j_{\ell+1}}\mu_{j_{\ell+1}}\cdots\alpha_{j_n}\mu_{j_n} \|\partial_s u\|^2_{\mathrm{L}^2_\mu(\Sigma_{j_1\cdots j_\ell})}.
\end{aligned}$$

According to (117), by summation of the above over $0 \leqslant j \leqslant p^n - 1$, i. e. over $0 \leqslant j_1 \leqslant p-1, \cdots, 0 \leqslant j_n \leqslant p-1$, we get

$$\|\Pi u\|^2_{\mathrm{L}^2_\mu(\mathcal{G}^n)} \leqslant n \sum_{\ell=1}^{n} \sum_{j_1=0}^{p-1} \cdots \sum_{j_n=0}^{p-1} |\boldsymbol{\alpha}|_\infty^{2\ell}\, \alpha_{j_{\ell+1}} \mu_{j_{\ell+1}} \cdots \alpha_{j_n} \mu_{j_n}\, \|\partial_s u\|^2_{\mathrm{L}^2_\mu(\Sigma_{j_1 \cdots j_\ell})}.$$

Setting $A_{n,\ell} := \displaystyle\sum_{j_{\ell+1}=0}^{p-1} \cdots \sum_{j_n=0}^{p-1} \alpha_{j_{\ell+1}} \mu_{j_{\ell+1}} \cdots \alpha_{j_n} \mu_{j_n} \equiv \big\langle \boldsymbol{\mu\alpha} \big\rangle^{n-\ell}$ and writing

$$\sum_{j_1=0}^{p-1} \cdots \sum_{j_n=0}^{p-1} = \sum_{j_1=0}^{p-1} \cdots \sum_{j_\ell=0}^{p-1} \Big(\sum_{j_{\ell+1}=0}^{p-1} \cdots \sum_{j_n=0}^{p-1} \Big),$$

we get

$$\left| \begin{array}{rcl} \|\Pi u\|^2_{\mathrm{L}^2_\mu(\mathcal{G}^n)} & \leqslant & n \displaystyle\sum_{\ell=1}^{n} A_{n,\ell}\, |\boldsymbol{\alpha}|_\infty^{2\ell} \sum_{j_1=0}^{p-1} \cdots \sum_{j_\ell=0}^{p-1} \|\partial_s u\|^2_{\mathrm{L}^2_\mu(\Sigma_{j_1 \cdots j_\ell})} \\ & = & n \displaystyle\sum_{\ell=1}^{n} |\boldsymbol{\alpha}|_\infty^{2\ell} \big\langle \boldsymbol{\mu\alpha} \big\rangle^{n-\ell} \|\partial_s u\|^2_{\mathrm{L}^2_\mu(\mathcal{G}^\ell)} \\ & \leqslant & n \Big(\displaystyle\sum_{\ell=1}^{n} |\boldsymbol{\alpha}|_\infty^{2\ell} \big\langle \boldsymbol{\mu\alpha} \big\rangle^{n-\ell} \Big)\, \|\partial_s u\|^2_{\mathrm{L}^2_\mu(\mathcal{T}^n)}. \end{array} \right.$$

A direct computation yields

$$\begin{cases} \text{if } \big\langle \boldsymbol{\mu\alpha} \big\rangle = |\boldsymbol{\alpha}|_\infty^2, & \displaystyle\sum_{\ell=1}^{n} |\boldsymbol{\alpha}|_\infty^{2\ell} \big\langle \boldsymbol{\mu\alpha} \big\rangle^{n-\ell} = n \big\langle \boldsymbol{\mu\alpha} \big\rangle^{n}, \\ \text{if } \big\langle \boldsymbol{\mu\alpha} \big\rangle \neq |\boldsymbol{\alpha}|_\infty^2, & \displaystyle\sum_{\ell=1}^{n} |\boldsymbol{\alpha}|_\infty^{2\ell} \big\langle \boldsymbol{\mu\alpha} \big\rangle^{n-\ell} = |\boldsymbol{\alpha}|_\infty^2 \frac{\big\langle \boldsymbol{\mu\alpha} \big\rangle^{n} - |\boldsymbol{\alpha}|_\infty^{2n}}{\big\langle \boldsymbol{\mu\alpha} \big\rangle - |\boldsymbol{\alpha}|_\infty^2}. \end{cases}$$

Combining the above two expressions, we thus obtained (128) with

$$\gamma_n = C \sum_{k=n}^{\infty} k^2 \max\Big(\big\langle \boldsymbol{\mu\alpha} \big\rangle, |\boldsymbol{\alpha}|_\infty^2 \Big)^k \quad (\to 0 \ \text{ when } n \to +\infty),$$

where $C = C(\boldsymbol{\alpha}, \boldsymbol{\mu}) > 0$ is a constant depending only on $\big\langle \boldsymbol{\mu\alpha} \big\rangle$ and $|\boldsymbol{\alpha}|_\infty$. Using (113)-(ii), we deduce that (124) holds for all $u \in \mathrm{H}^1_\mu(\mathcal{T})$ and conclude with lemma 3.22. □

Remark 3.25. *The statement of lemma 3.22 is valid both for compact and non-compact trees. The results of theorems 3.24, 3.23 do not hold for non-compact trees. It appears that the necessary* [33, Theorem 6.1.7] *(and, as we have shown, sufficient) condition for the compactness of the embedding* $\mathrm{H}^1_\mu(\mathcal{T}) \hookrightarrow \mathrm{L}^2_\mu(\mathcal{T})$ *is* $|\boldsymbol{\alpha}|_\infty < 1$.

4. Helmholtz equation on compact self-similar trees.

As we will see later, in order to construct transparent boundary conditions, it will be necessary to understand the structure of the solutions to the Neumann ($\mathcal{P}_{\mathfrak{n},\omega}$) and the Dirichlet ($\mathcal{P}_{\mathfrak{d},\omega}$) problems for the Helmholtz equation. We address in this section the following questions:

- self-similarity (in a certain sense) of the solutions to ($\mathcal{P}_{\mathfrak{d},\omega}$) and ($\mathcal{P}_{\mathfrak{n},\omega}$);
- the continuity of the solutions to ($\mathcal{P}_{\mathfrak{d},\omega}$) and ($\mathcal{P}_{\mathfrak{n},\omega}$) in $\omega = 0$;
- the difference between the solutions to ($\mathcal{P}_{\mathfrak{d},\omega}$) and ($\mathcal{P}_{\mathfrak{n},\omega}$).

4.1. **Helmholtz equation on compact self-similar trees.** Let us introduce a notion of a quasi-self-similar function, which will play an important role in understanding of the structure of the solutions to the Helmholtz equation on self-similar trees.

Definition 4.1 (Quasi-self-similarity)**.** *A function $u : \mathcal{T} \times (\mathbb{C} \setminus \mathbb{R}) \to \mathbb{C}$ is called quasi-self-similar if there exists a complex-valued function $r : \mathbb{C} \setminus \mathbb{R} \to \mathbb{C}$ (quasi-self-similarity ratio) such that, for any $0 \leqslant i \leqslant p-1$ and for any $\omega \in \mathbb{C} \setminus \mathbb{R}$,*

$$u\big(\sigma_i(s), \omega\big) = r(\omega)\, u(s, \alpha_i \omega), \qquad s \in \mathcal{T}. \tag{129}$$

The above notion reduces to a classical notion of self-similarity in $\omega = 0$, namely

$$u\big(\sigma_i(s), 0\big) = r(0)\, u(s, 0), \qquad s \in \mathcal{T}. \tag{130}$$

For any quasi-self-similar function u, any $j = (j_1 \cdots j_n)_p$,

$$u(\sigma_{n,j}(s), \omega) = r(\omega) \left[\prod_{k=1}^{n-1} r(\alpha_{j_1} \cdots \alpha_{j_k} \omega) \right] u(s, \alpha_{n,j} \omega), \tag{131}$$

where $\sigma_{n,j}$, $\alpha_{n,j}$ are defined as in (49) and (51). It appears that solutions to the Dirichlet (Neumann) problems for the Helmholtz equation are quasi-self-similar.

Theorem 4.2. *The function $u_{\mathfrak{d}}(s, \omega)$ (resp. $u_{\mathfrak{n}}(s, \omega)$), which solves ($\mathcal{P}_{\mathfrak{d},\omega}$) (resp. ($\mathcal{P}_{\mathfrak{n},\omega}$)), is quasi-self-similar.*

Proof. We provide the proof for $u = u_{\mathfrak{d}}(s, \omega)$, the one for $u_{\mathfrak{n}}(x, \omega)$ being verbatim the same. Let

$$r(\omega) := u(M_{0,0}, \omega), \qquad \omega \in \mathbb{C} \setminus \mathbb{R}. \tag{132}$$

Our goal is to show that u is quasi-self-similar of ratio $r(\omega)$.

It is not difficult to notice that $r(\omega) \neq 0$ in $\mathbb{C} \setminus \mathbb{R}$. Otherwise, by uniqueness of the solution of the Dirichlet Helmholtz problem in each subtree $\mathcal{T}_{1,i}$, $u(\cdot, \omega)$ would have vanished identically in each $\mathcal{T}_{1,i}$, or, in other words $u(\cdot, \omega)$ would have been supported in $\Sigma_{0,0}$. Using the Kirchhoff condition at the node $M_{0,0}$, we would have $\partial_s u(M_{0,0}, \omega) = 0$. And, since u is solution of the Helmholtz equation along $\Sigma_{0,0}$ and satisfies $u(M_{0,0}, \omega) \equiv r(\omega) = 0$, this would imply that $u|_{\Sigma_{0,0}} = 0$ (hence a contradiction to the boundary condition $u(M_\star, \omega) = 1$).

Let us define the following quantity:

$$u_i(s, \omega) := r(\omega)^{-1}\, u\big(\sigma_i(s), \omega\big). \tag{133}$$

Notice that $u_i(M_\star, \omega) = 1$. Also,

$$\partial_s u_i(s, \omega) = r(\omega)^{-1}\, \alpha_i\, \partial_s u \circ \sigma_i. \tag{134}$$

Choosing $v_i \in V_{\mathfrak{d},i} = \{v \in V_{\mathfrak{d}} \;/\; \text{supp}\, v \subset \mathcal{T}_{1,i}\}$ in the weak formulation of ($\mathcal{P}_{\mathfrak{d},\omega}$), we get (where s_i is the abscissa on $\mathcal{T}_{1,i}$)

$$\int_{\mathcal{T}_{1,i}} \mu(s_i)\, \partial_{s_i} u\, \partial_{s_i} v_i - \omega^2 \int_{\mathcal{T}_{1,i}} \mu(s_i)\, u(s_i)\, v_i(s_i) = 0, \quad \forall v_i \in V_{\mathfrak{d},i}\,. \tag{135}$$

Performing in the above integrals the change of variables $s_i = \sigma_i(s)$, where s is an abscissa on $\mathcal{T}$, we obtain

$$\int_{\mathcal{T}} \mu(\sigma_i(s))\, \partial_{s_i} u(\sigma_i(s))\, \partial_{s_i} v_i(\sigma_i(s)) - \omega^2 \int_{\mathcal{T}} \mu(\sigma_i(s))\, u(\sigma_i(s))\, v_i(\sigma_i(s)) = 0, \tag{136}$$

for all $v_i \in V_{\mathfrak{d},i}$. Notice that the above holds with $v_i(\sigma_i(s)) \in V_{\mathfrak{d},i}$ replaced by $v(s) \in V_{\mathfrak{d}}$ (since for any $v_i \in V_{\mathfrak{d},i}$, there exists $v \in V_{\mathfrak{d}}$, s.t. $v_i \circ \sigma_i = v$). Using (55), (134), the variational formulation (136) becomes

$$\alpha_i^{-2} \int_{\mathcal{T}} \mu\, \partial_s u_i\, \partial_s v - \omega^2 \int_{\mathcal{T}} \mu\, u_i v = 0, \quad \forall v \in V_{\mathfrak{d}}. \tag{137}$$

Since $u_i(M_\star, \omega) = 1$, u_i is nothing but the solution of the Dirichlet Helmholtz problem associated to the frequency $\alpha_i\, \omega$. Thus, with (133),

$$u(\sigma_i(s), \omega) = r(\omega)\, u(s, \alpha_i\, \omega),$$

which concludes the proof. □

4.2. **Zero-frequency limit of the Helmholtz equation on compact self-similar trees.** In this section we address the question of the well-posedness of the problems ($\mathcal{P}_{\mathfrak{d},\omega}$) and ($\mathcal{P}_{\mathfrak{n},\omega}$) when $\omega = 0$ (i.e. Laplace equation), as well as provide explicit solutions to these problems. With this analysis we aim at two goals. First, we would like to show that in the region of the parameters $\mathbb{P}_{ND}$, cf. (122), the solutions of the problems ($\mathcal{P}_{\mathfrak{d},\omega}$) and ($\mathcal{P}_{\mathfrak{n},\omega}$), in general, differ. And second, we will use the knowledge of the explicit solution to the Laplace equation to distinguish between these problems when constructing transparent boundary conditions.

Let us now find explicitly the solutions to the Dirichlet/Neumann problem for the Laplace equation. This problem is well-posed, according to Lemma 1.22, in particular, because the compactness assumptions (38)-$\mathfrak{n}$ and (38)-$\mathfrak{d}$ hold true. First of all, let us formulate the following corollary of theorem 4.2 about the structure fo the solutions to the Laplace equation on a self-similar tree.

Theorem 4.3. *The function $u = u_{\mathfrak{d}}(.,0)$, ($u = u_{\mathfrak{n}}(.,0)$), which solves ($\mathcal{P}_{\mathfrak{d},\omega}$) (corresp. ($\mathcal{P}_{\mathfrak{n},\omega}$)) with $\omega = 0$, is self-similar, i.e. it satisfies for some $r_0 \in \mathbb{C}$ and all $0 \leqslant i \leqslant p-1$,*

$$u(\sigma_i(s)) = r_0\, u(s), \qquad s \in \mathcal{T}. \tag{138}$$

Proof. The statement follows by extending the proof of theorem 4.2 to $\omega = 0$ (notice that the theorem is formulated for $\omega \in \mathbb{C} \setminus \mathbb{R}$) and the definition of the quasi-self-similarity, cf. also (130) with $r_0 := r(0)$. □

In the following theorem we calculate explicitly the solutions to ($\mathcal{P}_{\mathfrak{d},\omega}$) and ($\mathcal{P}_{\mathfrak{n},\omega}$) for $\omega = 0$. In particular, we show that in the region $\mathbb{P}_{ND}$, the functions that solve ($\mathcal{P}_{\mathfrak{d},\omega}$) and ($\mathcal{P}_{\mathfrak{n},\omega}$) for $\omega = 0$ are distinct.

Theorem 4.4. *The solutions to ($\mathcal{P}_{\mathfrak{d},\omega}$) and ($\mathcal{P}_{\mathfrak{n},\omega}$) with $\omega = 0$ satisfy:*

- *if $(\boldsymbol{\mu}, \boldsymbol{\alpha}) \in \mathbb{P}_N$, then $u_{\mathfrak{n}}(.,0) = u_{\mathfrak{d}}(.,0) = \mathbb{1}_{\mathcal{T}}$.*
- *if $(\boldsymbol{\mu}, \boldsymbol{\alpha}) \in \mathbb{P}_{ND}$, then $u_{\mathfrak{n}}(.,0) = \mathbb{1}_{\mathcal{T}}$, and $u_{\mathfrak{d}}(.,0)$ is a piecewise-linear function, which satisfies (138) with*

$$r_0 = \left\langle \frac{\boldsymbol{\mu}}{\boldsymbol{\alpha}} \right\rangle^{-1}. \tag{139}$$

- *if $(\boldsymbol{\mu}, \boldsymbol{\alpha}) \in \mathbb{P}_D$, then $u_{\mathfrak{n}}(.,0) = u_{\mathfrak{d}}(.,0)$ is a piecewise-linear function, which satisfies (138) with r_0 defined in (139).*

Proof. Let us find a general form of the solution to ($\mathcal{P}_{\mathfrak{d},\omega}$), ($\mathcal{P}_{\mathfrak{n},\omega}$). First, the use of (132) results in the following identity:

$$\partial_s u \circ \sigma_i = r_0\, \alpha_i^{-1} \partial_s u.$$

Then the Kirchhoff condition (9) at the node $M_{0,0} = \sigma_i(M_\star)$ reads:

$$\partial_s u_{0,0}(M_{0,0}) = \sum_{i=0}^{p-1} r_0 \, \frac{\mu_i}{\alpha_i} \, \partial_s u_{0,0}(M_\star). \tag{140}$$

Since $\partial_s^2 u = 0$ along $\Sigma_{0,0}$, $\partial_s u(M_\star) = \partial_s u(M_{0,0})$. There are two possible solutions:

- either $\partial_s u(M_\star) = 0$, which, with $u(M_\star) = 1$, implies that $u = \mathbb{1}_{\mathcal{T}}$.
- or $\partial_s u(M_\star) \neq 0$, then (140) implies that r_0 is as in (139). As $\partial_s^2 u = 0$, u is linear on $\Sigma_{0,0}$. Due to self-similarity, $u(M_{0,0}) = r_0$, and therefore
$$u_{0,0}(s) = 1 + (r_0 - 1)s. \tag{141}$$
To summarize, u is a piecewise-linear and satisfies (132) with r_0 from (138). We will denote such a function by $\mathbb{L}_{r_0}$.

Case 1: $(\boldsymbol{\mu}, \boldsymbol{\alpha}) \in \mathbb{P}_N$. The function $\mathbb{1}_{\mathcal{T}} \in \mathrm{H}^1_\mu(\mathcal{T}) = \mathrm{H}^1_{\mu,0}(\mathcal{T})$, see (108) and theorem 3.15. Also, $\mathbb{1}_{\mathcal{T}}$ satisfies ($\mathcal{P}_{\mathfrak{d},\omega}$) and ($\mathcal{P}_{\mathfrak{n},\omega}$). Thus, by the uniqueness of the solution, cf. lemma 1.22, $u_{\mathfrak{d}}(.,0) = u_{\mathfrak{n}}(.,0) = \mathbb{1}_{\mathcal{T}}$.

Case 2: $(\boldsymbol{\mu}, \boldsymbol{\alpha}) \in \mathbb{P}_{ND}$. Notice that the function $\mathbb{1}_{\mathcal{T}} \in \mathrm{H}^1_\mu(\mathcal{T})$, see (108), and it solves ($\mathcal{P}_{\mathfrak{n},\omega}$) with $\omega = 0$. By uniqueness, $u_{\mathfrak{n}}(.,0) = \mathbb{1}_{\mathcal{T}}$.

The function $\mathbb{1}_{\mathcal{T}} \notin \mathrm{H}^1_{\mu,0}(\mathcal{T})$, because $\tau_\infty \mathbb{1}_{\mathcal{T}} = 1$, while $\mathrm{H}^1_{\mu,0}(\mathcal{T}) = \mathrm{Ker}\, \tau_\infty$, see theorem 3.5. Hence, $\mathbb{1}_{\mathcal{T}}$ does not satisfy ($\mathcal{P}_{\mathfrak{d},\omega}$), and thus $u_{\mathfrak{d}} = \mathbb{L}_{r_0}$.

Case 3: $(\boldsymbol{\mu}, \boldsymbol{\alpha}) \in \mathbb{P}_D$. In this case, $\mathrm{H}^1_{\mu,0}(\mathcal{T}) = \mathrm{H}^1_\mu(\mathcal{T})$ (theorem 3.18), hence $u_{\mathfrak{d}} = u_{\mathfrak{n}}$.

Since $\mathbb{1}_{\mathcal{T}} \notin \mathrm{H}^1_{\mu,0}(\mathcal{T})$ (the same reason as in Case 2), we deduce that $u_{\mathfrak{n}} = u_{\mathfrak{d}} = \mathbb{L}_{r_0}$. □

Thus, we see that in the region $\mathbb{P}_{ND}$, zero-frequency solutions to the Dirichlet and Neumann problems do not coincide. This result can be extended to $\omega \in \mathbb{C} \setminus \mathbb{R}$, except, possibly, some isolated points. To see this, first notice that there exists $R > 0$, such that for any sequence $(\omega_k)_{k\in\mathbb{N}} \subset B(0,R)$, s.t. $\omega_k \to 0$ as $k \to \infty$,

$$u_{\mathfrak{d}}(.,\omega_k) \to u_{\mathfrak{d}}(.,0), \qquad u_{\mathfrak{n}}(.,\omega_k) \to u_{\mathfrak{n}}(.,0), \qquad \text{strongly in } \mathrm{H}^1_\mu(\mathcal{T}). \tag{142}$$

This is an immediate corollary of proposition 1.23 (notice that (38)-$\mathfrak{d}$ and (38)-$\mathfrak{n}$ hold) combined with remark 1.20. This implies the following result.

Corollary 4.5. *The following holds true for the solutions of ($\mathcal{P}_{\mathfrak{d},\omega}$) and ($\mathcal{P}_{\mathfrak{n},\omega}$):*

- *if $(\boldsymbol{\mu}, \boldsymbol{\alpha}) \in \mathbb{P}_N \cup \mathbb{P}_D$, then $u_{\mathfrak{d}}(.,\omega) = u_{\mathfrak{n}}(.,\omega)$ for all $\omega \in \mathbb{C} \setminus \mathbb{R}$;*
- *if $(\boldsymbol{\mu}, \boldsymbol{\alpha}) \in \mathbb{P}_{ND}$, $u_{\mathfrak{d}}(.,\omega) \neq u_{\mathfrak{n}}(.,\omega)$ except, possibly, in isolated points ω of $\mathbb{C} \setminus \mathbb{R}$.*

Proof. The result in $\mathbb{P}_N \cup \mathbb{P}_D$ follows from $\mathrm{H}^1_{\mu,0}(\mathcal{T}) = \mathrm{H}^1_\mu(\mathcal{T})$, cf. theorems 3.15, 3.18.

When $(\boldsymbol{\mu}, \boldsymbol{\alpha}) \in \mathbb{P}_{ND}$, we proceed by contradiction. First of all, remark that (38), holds, cf. theorem 3.24, and thus $u_{\mathfrak{d}}(.,\omega)$ and $u_{\mathfrak{n}}(.,\omega)$ are analytic $\mathrm{H}^1_\mu(\mathcal{T})$-valued functions of $\omega \in \mathbb{C} \setminus \mathbb{R}$, see proposition 1.23. Let us now assume that there exists $\omega_\ell \in \mathbb{C} \setminus \mathbb{R}$, s.t.

$$u_{\mathfrak{d}}(.,\omega_\ell) = u_{\mathfrak{n}}(.,\omega_\ell), \qquad \lim_{\ell\to\infty} \omega_\ell = \omega \in \mathbb{C} \setminus \mathbb{R}.$$

Then, by the uniqueness continuation theorem for holomorphic vector-valued functions, see [9, Proposition A.2, p.462], $u_{\mathfrak{d}}(.,\omega) = u_{\mathfrak{n}}(.,\omega)$ in $\mathbb{C}\setminus\mathbb{R}$. However, by (142), for $\omega \to 0$, the functions $u_{\mathfrak{d}}(.,\omega)$, $u_{\mathfrak{n}}(.,\omega)$ converge correspondingly to $u_{\mathfrak{d}}(.,0)$ and $u_{\mathfrak{n}}(.,0)$, and as $u_{\mathfrak{d}}(.,0) \neq u_{\mathfrak{n}}(.,0)$, see theorem 4.4, we arrive at the contradiction. □

The above property shows that the transparent boundary conditions, which we aim to construct, should take into account the fact that the solutions of the Dirichlet and of the Neumann problem differ when $(\boldsymbol{\mu},\, \boldsymbol{\alpha}) \in \mathbb{P}_{ND}$.

5. Construction of transparent boundary conditions for the Helmholtz equation.

In this section, we investigate some properties of the DtN operator, as it was introduced in section 1.6, and more precisely the computation of its symbol as a function of the frequency $\omega \in \mathbb{C}\setminus\mathbb{R}$. We consider the case of the reference p-adic self-similar compact weighted tree with the weight $\mu(s) = 1$ on $\Sigma_{0,0}$, cf. assumption 3.1.

5.1. DtN operator for the Dirichlet and Neumann Helmholtz problems.

Before entering into the details, let us remind that depending on the value $(\boldsymbol{\mu},\, \boldsymbol{\alpha})$,

- if $(\boldsymbol{\mu},\, \boldsymbol{\alpha}) \in \mathbb{P}_N \cup \mathbb{P}_D$, the solutions of the Neumann and the Dirichlet problem for the Helmholtz equation coincide.
- otherwise, if $(\boldsymbol{\mu},\, \boldsymbol{\alpha}) \in \mathbb{P}_{ND}$, the solutions of the Neumann and the Dirichlet problem do not coincide, except, possibly, for isolated frequencies, cf. corollary 4.5.

Let us define the two Dirichlet and Neumann symbols as

$$\boldsymbol{\Lambda}_{\mathfrak{d}}(\omega) := -\,\partial_s u_{\mathfrak{d}}(M_\star,\omega), \quad \boldsymbol{\Lambda}_{\mathfrak{n}}(\omega) := -\,\partial_s u_{\mathfrak{n}}(M_\star,\omega). \tag{143}$$

According to proposition 1.23, the functions $\omega \mapsto \boldsymbol{\Lambda}_{\mathfrak{d}}(\omega)$ and $\omega \mapsto \boldsymbol{\Lambda}_{\mathfrak{n}}(\omega)$ are meromorphic in $\mathbb{C}$ and analytic in the neighborhood of the origin, since $\omega = 0$ is not an eigenvalue of the operators $\mathcal{A}_{\mathfrak{n}}$, $\mathcal{A}_{\mathfrak{d}}$, cf. lemma 1.22. Moreover, using (42) and (43),

$$\begin{cases} \boldsymbol{\Lambda}_{\mathfrak{d}}(\omega) = \boldsymbol{\Lambda}_{\mathfrak{d}}(0) - \displaystyle\sum_{n=0}^{+\infty} \frac{\alpha_{\mathfrak{d}}^n \omega^2}{(\omega_{\mathfrak{d}}^n)^2 - \omega^2}, \quad \alpha_{\mathfrak{d}}^n = \left(\frac{\partial_s \varphi_{\mathfrak{d}}^n(M_\star)}{\omega_{\mathfrak{d}}^n}\right)^2, \\ \boldsymbol{\Lambda}_{\mathfrak{n}}(\omega) = \boldsymbol{\Lambda}_{\mathfrak{n}}(0) - \displaystyle\sum_{n=0}^{+\infty} \frac{\alpha_{\mathfrak{n}}^n \omega^2}{(\omega_{\mathfrak{n}}^n)^2 - \omega^2}, \quad \alpha_{\mathfrak{n}}^n = \left(\frac{\partial_s \varphi_{\mathfrak{n}}^n(M_\star)}{\omega_{\mathfrak{n}}^n}\right)^2. \end{cases} \tag{144}$$

The convergence of the above series is uniform on the compact subsets of $\mathbb{C}$ that do not contain $\left\{\pm\,\omega_{\mathfrak{d}}^n\right\}$ (resp. $\left\{\pm\,\omega_{\mathfrak{n}}^n\right\}$); this follows from Remark 1.24 and continuity of the trace $u \to \partial_s u(M_\star)$ for functions from $D(\mathcal{A}_{\mathfrak{d}})$ (resp. $D(\mathcal{A}_{\mathfrak{n}})$).

Remark 5.1. *The formulas (144) show that the set of poles of $\boldsymbol{\Lambda}_{\mathfrak{d}}(\omega)$ (resp. $\boldsymbol{\Lambda}_{\mathfrak{n}}(\omega)$) is a subset of $\left\{\pm\,\omega_{\mathfrak{d}}^n\right\}$ (resp. $\left\{\pm\,\omega_{\mathfrak{n}}^n\right\}$). We conjecture that these sets coincide.*

Another property of the symbol of the DtN operator follows naturally from the explicit form of the zero-frequency solutions for the Helmholtz equation. It is formulated below.

Lemma 5.2. *The symbols $\boldsymbol{\Lambda}_{\mathfrak{d}}(\omega)$, $\boldsymbol{\Lambda}_{\mathfrak{n}}(\omega)$ satisfy the following:*

- *in $\mathbb{P}_N$,*
$$\boldsymbol{\Lambda}_{\mathfrak{d}}(\omega) \equiv \boldsymbol{\Lambda}_{\mathfrak{n}}(\omega), \text{ and } \boldsymbol{\Lambda}_{\mathfrak{d}}(0) = \boldsymbol{\Lambda}_{\mathfrak{n}}(0) = 0.$$
- *in $\mathbb{P}_{ND}$,*
$$\boldsymbol{\Lambda}_{\mathfrak{d}}(\omega) \neq \boldsymbol{\Lambda}_{\mathfrak{n}}(\omega), \quad \boldsymbol{\Lambda}_{\mathfrak{d}}(0) = 1 - \left\langle \frac{\boldsymbol{\mu}}{\boldsymbol{\alpha}} \right\rangle^{-1} \text{ and } \boldsymbol{\Lambda}_{\mathfrak{n}}(0) = 0.$$

- *in* $\mathbb{P}_D$,

$$\mathbf{\Lambda}_{\mathfrak{d}}(\omega) \equiv \mathbf{\Lambda}_{\mathfrak{n}}(\omega) \text{ and } \mathbf{\Lambda}_{\mathfrak{d}}(0) = \mathbf{\Lambda}_{\mathfrak{n}}(0) = 1 - \left\langle \frac{\boldsymbol{\mu}}{\boldsymbol{\alpha}} \right\rangle^{-1}.$$

Proof. Let us consider $\langle \boldsymbol{\mu}\boldsymbol{\alpha} \rangle \geqslant 1$, the proof for the rest of the cases being almost identical. If $\langle \boldsymbol{\mu}\boldsymbol{\alpha} \rangle \geqslant 1$, $\mathrm{H}^1_{\mu,0}(\mathcal{T}) = \mathrm{H}^1_{\mu}(\mathcal{T})$, hence $\mathbf{\Lambda}_{\mathfrak{d}}(\omega) = \mathbf{\Lambda}_{\mathfrak{n}}(\omega)$.

By theorem 4.4, and more precisely (141), $u = u_{\mathfrak{d}}(.,0)$ satisfies

$$u_{0,0}(s) = 1 + (r_0 - 1)s, \quad r_0 = \left\langle \frac{\boldsymbol{\mu}}{\boldsymbol{\alpha}} \right\rangle^{-1}.$$

Thus, $\mathbf{\Lambda}_{\mathfrak{d}}(0) \equiv \mathbf{\Lambda}_{\mathfrak{n}}(0) = -\,\partial_s u_{0,0}(0) = 1 - \left\langle \frac{\boldsymbol{\mu}}{\boldsymbol{\alpha}} \right\rangle^{-1}$. □

5.2. **A functional equation for $\mathbf{\Lambda}_{\mathfrak{d}}(\omega)$ and $\mathbf{\Lambda}_{\mathfrak{n}}(\omega)$.** In this section we will demonstrate how one can compute the symbols $\mathbf{\Lambda}_{\mathfrak{d}}(\omega)$ and $\mathbf{\Lambda}_{\mathfrak{n}}(\omega)$.

Lemma 5.3. *Each function $\mathbf{\Lambda}(\omega) = \mathbf{\Lambda}_{\mathfrak{d}}(\omega)$ or $\mathbf{\Lambda}_{\mathfrak{n}}(\omega)$ satisfies the following quadratic functional equation*

$$\left\{ \begin{array}{l} \text{Find } \mathbf{\Lambda}(\omega) : \mathbb{C} \setminus \mathbb{R} \mapsto \mathbb{C} \text{ such that} \\ \omega \sin\omega + \mathbf{\Lambda}(\omega)\cos\omega = \Big(\cos\omega - \mathbf{\Lambda}(\omega)\dfrac{\sin\omega}{\omega}\Big) \displaystyle\sum_{i=0}^{p-1} \frac{\mu_i}{\alpha_i} \mathbf{\Lambda}(\alpha_i\omega). \end{array} \right. \tag{145}$$

Proof. Let $u(\cdot,\omega) = u_{\mathfrak{d}}(\cdot,\omega)$ or $u_{\mathfrak{n}}(\cdot,\omega)$ and $\mathbf{\Lambda}(\omega) = -\partial_s u(M_\star,\omega)$. Along $\Sigma_{0,0}$ parametrized by $s \in [0,1]$, $u(.,\omega)|_{\Sigma_{0,0}} \equiv u_{0,0}(.,\omega)$ is the solution to the following Cauchy problem:

$$\partial_s^2 u_{0,0} + \omega^2 u_{0,0} = 0, \quad u_{0,0}(0,\omega) = 1, \quad \partial_s u_{0,0}(0,\omega) = -\mathbf{\Lambda}(\omega),$$

which leads to $u_{0,0}(s,\omega) = \cos\omega s - \mathbf{\Lambda}(\omega)\,\dfrac{\sin\omega s}{\omega}$. In particular,

$$\partial_s u_{0,0}(M_{0,0},\omega) = -\,\omega\sin\omega - \mathbf{\Lambda}(\omega)\cos\omega \tag{146}$$

Along $\Sigma_{1,i} \equiv \sigma_i(\Sigma_{0,0})$, $u(.,\omega)|_{\Sigma_{1,i}} \equiv u_{1,i}(.,\omega)$. Thus, by quasi-self-similarity (129), and the definition of $\mathbf{\Lambda}(\omega)$, we get

$$\partial_s u_{1,i}(M_{0,0},\omega) = \alpha_i^{-1}\, r(\omega)\, \partial_s u_{0,0}(M_\star,\alpha_i\omega) \equiv -\,\alpha_i^{-1}\, r(\omega)\, \mathbf{\Lambda}(\alpha_i\omega), \tag{147}$$

where the self-similarity ratio $r(\omega)$ is given by, cf. (132),

$$r(\omega) = u_{0,0}(M_{0,0},\omega) \equiv \cos\omega - \frac{\mathbf{\Lambda}(\omega)}{\omega}\,\sin\omega. \tag{148}$$

One gets (145) by substituting (146), (147), (148) into the Kirchhoff equation (9) at $M_{0,0}$:

$$\partial_s u_{0,0}(M_{0,0},\omega) = \sum_{i=0}^{p-1} \mu_i\, \partial_s u_{1,i}(M_{0,0},\omega).$$ □

Remark 5.4. *Depending on the values of $\boldsymbol{\mu}$ and $\boldsymbol{\alpha}$, the equation (145) encodes all the symbols of the DtN operators for all the self-similar trees (even non-compact). In particular, e.g., one can verify that the DtN symbol for the Helmholtz equation on the half-line ($p = 1$, $\mu = \alpha = 1$), namely, $\pm i\omega$, solves (145).*

Since this equation (145) is quadratic, one expects that it admits several (naively at least two) solutions. However, as we know, when $(\boldsymbol{\mu},\boldsymbol{\alpha}) \in \mathbb{P}_N \cup \mathbb{P}_D$, the symbols $\boldsymbol{\Lambda}_{\mathfrak{d}}(\omega)$ and $\boldsymbol{\Lambda}_{\mathfrak{n}}(\omega)$ coincide, and hence only one of these solutions corresponds to the symbol of the DtN operator. We will show the following properties:

- when $(\boldsymbol{\mu},\boldsymbol{\alpha}) \in \mathbb{P}_N \cup \mathbb{P}_D$, (145) admits a single even meromorphic solution that takes the value at the origin prescribed by lemma 5.2. This will allow us to select a physical solution (145) in the cases the symbols $\boldsymbol{\Lambda}_{\mathfrak{d}}(\omega)$ and $\boldsymbol{\Lambda}_{\mathfrak{n}}(\omega)$ coincide;
- when $(\boldsymbol{\mu},\boldsymbol{\alpha}) \in \mathbb{P}_{ND}$, (145) admits two even meromorphic solutions, which take the values at the origin prescribed by lemma 5.2. They correspond to $\boldsymbol{\Lambda}_{\mathfrak{d}}(\omega)$ and $\boldsymbol{\Lambda}_{\mathfrak{n}}(\omega)$.

First of all, notice that because the symbol of the DtN operator satisfies (145) and is an even function, analytic in the origin, a priori one of the solutions of the equation (145) is even and analytic in the origin. Moreover, in the origin this solution satisfies lemma 5.2. A priori it is not obvious that such a solution is unique. However, the uniqueness can be shown, and the corresponding result is formulated in the following lemma.

Let us draw the attention of the reader to the fact that in the lemma below, we use N or D as indices instead of $\mathfrak{n}$ or $\mathfrak{d}$ because we refer to solutions of the characteristic equation (145) and not to the DtN symbols. However, the connection between $\boldsymbol{\Lambda}_D(\omega), \boldsymbol{\Lambda}_N(\omega)$ and $\boldsymbol{\Lambda}_{\mathfrak{d}}(\omega), \boldsymbol{\Lambda}_{\mathfrak{n}}(\omega)$ will be immediately clarified with corollary 5.6.

Lemma 5.5. *Any solution of (145), continuous in the origin, satisfies*

$$\boldsymbol{\Lambda}(0) = 0 \qquad \text{or} \qquad \boldsymbol{\Lambda}(0) = 1 - \left\langle \frac{\boldsymbol{\mu}}{\boldsymbol{\alpha}} \right\rangle^{-1}.$$

If $(\boldsymbol{\mu},\boldsymbol{\alpha}) \in \mathbb{P}_N \cup \mathbb{P}_{ND}$, the equation (145) admits a unique even solution $\boldsymbol{\Lambda}(\omega) = \boldsymbol{\Lambda}_N(\omega)$ analytic in the origin that satisfies $\boldsymbol{\Lambda}_N(0) = 0$. Moreover, as $\omega \to 0$,

$$\boldsymbol{\Lambda}_N(\omega) = -\left(1 - \langle \boldsymbol{\mu}\boldsymbol{\alpha} \rangle\right)^{-1} \omega^2 + O(\omega^4).$$

If $(\boldsymbol{\mu},\boldsymbol{\alpha}) \in \mathbb{P}_D \cup \mathbb{P}_{ND}$, the equation (145) admits a unique even solution $\boldsymbol{\Lambda}(\omega) = \boldsymbol{\Lambda}_D(\omega)$ analytic in the origin that satisfies

$$\boldsymbol{\Lambda}_D(0) = 1 - \left\langle \frac{\boldsymbol{\mu}}{\boldsymbol{\alpha}} \right\rangle^{-1}.$$

Moreover, its Taylor expansion at the origin is given, as $\omega \to 0$, by

$$\boldsymbol{\Lambda}_D(\omega) = \boldsymbol{\Lambda}_D(0) - \frac{1}{3}\left(\left\langle \frac{\boldsymbol{\mu}}{\boldsymbol{\alpha}} \right\rangle^2 + \left\langle \frac{\boldsymbol{\mu}}{\boldsymbol{\alpha}} \right\rangle + 1\right)\left(\left\langle \frac{\boldsymbol{\mu}}{\boldsymbol{\alpha}} \right\rangle^2 - \langle \boldsymbol{\mu}\boldsymbol{\alpha} \rangle\right)^{-1} \omega^2 + O(\omega^4)$$

Proof. Please see the appendix C. Let us remark that it is possible to obtain a higher-order expansion of $\boldsymbol{\Lambda}_D(\omega)$ and $\boldsymbol{\Lambda}_N(\omega)$, and the corresponding formulas, since they are somewhat cumbersome, are omitted here; however, they can be found in appendix C, see, in particular, (188, 189). □

Combining the above with lemma 5.2, we arrive at the following conclusion.

Corollary 5.6. *Let $\boldsymbol{\Lambda}_N(\omega)$ and $\boldsymbol{\Lambda}_D(\omega)$ be defined in lemma 5.5. Then the following holds:*

- *if $(\boldsymbol{\mu},\boldsymbol{\alpha}) \in \mathbb{P}_N$, then $\boldsymbol{\Lambda}_{\mathfrak{n}}(\omega) = \boldsymbol{\Lambda}_{\mathfrak{d}}(\omega) = \boldsymbol{\Lambda}_N(\omega)$.*
- *if $(\boldsymbol{\mu},\boldsymbol{\alpha}) \in \mathbb{P}_{ND}$, then $\boldsymbol{\Lambda}_{\mathfrak{n}}(\omega) = \boldsymbol{\Lambda}_N(\omega)$ and $\boldsymbol{\Lambda}_{\mathfrak{d}}(\omega) = \boldsymbol{\Lambda}_D(\omega)$.*
- *if $(\boldsymbol{\mu},\boldsymbol{\alpha}) \in \mathbb{P}_D$, then $\boldsymbol{\Lambda}_{\mathfrak{n}}(\omega) = \boldsymbol{\Lambda}_{\mathfrak{d}}(\omega) = \boldsymbol{\Lambda}_D(\omega)$.*

Remark 5.7. *The corollary clarifies the notation by explaining why, when* $(\boldsymbol{\mu}, \boldsymbol{\alpha}) \in \mathbb{P}_D \cup \mathbb{P}_N$*, even though Dirichlet and Neumann problems coincide, we have chosen to consider that we solve the Dirichlet problem when* $(\boldsymbol{\mu}, \boldsymbol{\alpha}) \in \mathbb{P}_D$ *and that we solve the Neumann problem when* $(\boldsymbol{\mu}, \boldsymbol{\alpha}) \in \mathbb{P}_N$.

Remark 5.8. *The uniqueness results of lemma 5.5 fail to be true if one looks for not necessarily smooth solutions* $\mathbf{\Lambda}(\omega)$*. Let us give a counter-example in the case where all the* α_i*'s are* **rational numbers***. Then the function* $\mathbf{\Lambda}(\omega)$ *defined in* $\mathbb{C} \setminus \mathbb{R}$ *by*

$$\mathbf{\Lambda}(\omega) = \mathbf{\Lambda}_D(\omega), \quad \text{if } |\omega| \in \mathbb{Q},$$

$$\mathbf{\Lambda}(\omega) = \mathbf{\Lambda}_N(\omega), \quad \text{if } |\omega| \notin \mathbb{Q},$$

is a solution of (145), different from $\mathbf{\Lambda}_D(\omega)$ *and satisfying* $\mathbf{\Lambda}(0) = \mathbf{\Lambda}_D(0)$*. In the same way, the function* $\mathbf{\Lambda}(\omega)$ *defined in* $\mathbb{C} \setminus \mathbb{R}$ *by*

$$\mathbf{\Lambda}(\omega) = \mathbf{\Lambda}_N(\omega), \quad \text{if } |\omega| \in \mathbb{Q},$$

$$\mathbf{\Lambda}(\omega) = \mathbf{\Lambda}_D(\omega), \quad \text{if } |\omega| \notin \mathbb{Q},$$

is a solution of (145), different from $\mathbf{\Lambda}_D(\omega)$ *and satisfying* $\mathbf{\Lambda}(0) = \mathbf{\Lambda}_N(0)$.

5.3. **Positivity properties of the DtN Operator.** An important property of the DtN operator is its positivity, which is related to the energy conservation. This property will be important for obtaining an approximation of symbols $\mathbf{\Lambda}_\mathfrak{d}$, $\mathbf{\Lambda}_\mathfrak{n}$ that would lead to stable transparent boundary conditions. Let us introduce

$$\mathbb{C}^+ = \{z \in \mathbb{C} : \operatorname{Im} z > 0\}.$$

Theorem 5.9. *The symbol* $\mathbf{\Lambda}(\omega) = \mathbf{\Lambda}_\mathfrak{d}(\omega)$ *(*$\mathbf{\Lambda}(\omega) = \mathbf{\Lambda}_\mathfrak{n}(\omega)$*) satisfies the following:*

$$\operatorname{Im}\left(\omega^{-1}\mathbf{\Lambda}(\omega)\right) < 0, \qquad \text{for all } \omega \in \mathbb{C}^+. \tag{149}$$

In other words, $\mathbf{f}(\omega) = -\omega^{-1}\mathbf{\Lambda}(\omega)$ is a Herglotz function [17].

Proof. This property can be shown directly, by examining the expressions (144); however, we provide a more general proof, which relies only on the properties of the underlying sesquilinear form. We show the result for $\mathbf{\Lambda}(\omega) = \mathbf{\Lambda}_\mathfrak{d}(\omega)$, with the proof for $\mathbf{\Lambda}_\mathfrak{n}(\omega)$ being verbatim the same. For this we test the Helmholtz equation with $u_\mathfrak{d}(.,\omega)$ and use the Green's formula (cf. also (9) for the Kirchoff conditions), which gives

$$-\int_{\mathcal{T}} \mu\omega^2 \left|u_\mathfrak{d}(.,\omega)\right|^2 + \int_{\mathcal{T}} \mu \left|\partial_s u_\mathfrak{d}(.,\omega)\right|^2 + \partial_s u_\mathfrak{d}(M_\star,\omega) = 0.$$

Dividing the above by $\omega \neq 0$, and using (143), we obtain the following identity:

$$\omega^{-1}\mathbf{\Lambda}_\mathfrak{d}(\omega) = \omega^{-1}\int_{\mathcal{T}} \mu \left|\partial_s u_\mathfrak{d}\right|^2 - |\omega|^2\,\omega \int_{\mathcal{T}} \mu \left|u_\mathfrak{d}\right|^2.$$

It remains to notice that $u_\mathfrak{d} \neq 0$ and thus the imaginary part of the above is strictly negative whenever $\omega \in \mathbb{C}^+$. □

Remark 5.10. *The above property will be employed to prove that the algorithm for the evaluation of the symbol of the DtN operator, which we present in the next section, is well-defined (i.e. no division by zero occurs in the course of this algorithm). But the meaning of this positivity property is much more important than this: it is fundamental for the stability of the boundary-value problems. This is implicitly used, in particular, in theorem 6.2.*

Let us state the following two trivial properties of the Herglotz functions, useful further.

Lemma 5.11. *Let $f(\omega) : \mathbb{C} \to \mathbb{C}$ be an even function analytic in the vicinity of the origin, which admits the expansion $f(\omega) = f_0 + f_2\omega^2 + O(\omega^4)$ as $\omega \to 0$, with $f_0,\ f_2 \in \mathbb{R}$, and $f_0 \neq 0$ or $f_2 \neq 0$. Assume additionally that, for any $\omega \in \mathbb{C}^+$*

$$\mathrm{Im}(\omega^{-1} f(\omega)) < 0. \tag{150}$$

Then if $f_0 \neq 0$, then $f_0 > 0$, while, if $f_0 = 0$, then $f_2 < 0$.

Proof. For $\omega \in \mathbb{C}^+$ sufficiently small,

$$\mathrm{sign}\,\mathrm{Im}\left(\omega^{-1} f(\omega)\right) = \mathrm{sign}\,\mathrm{Im}\left(f_0\,\omega^{-1} + f_2\,\omega\right).$$

It is easy to conclude with (150). □

Remark 5.12. *The solutions $\mathbf{\Lambda}_{\mathfrak{n}}(\omega)$ and $\mathbf{\Lambda}_{\mathfrak{d}}(\omega)$ defined in corollary 5.6 via solutions $\mathbf{\Lambda}_N(\omega)$ and $\mathbf{\Lambda}_D(\omega)$ of (145) , cf. lemma 5.5, satisfy (150). From the proof of lemma 5.5, it follows that under additional conditions on the parameters $\boldsymbol{\mu}$ and $\boldsymbol{\alpha}$, it is possible to extend the definitions of*

$$\mathbf{\Lambda}_N(\omega) \text{ for } \langle \boldsymbol{\mu}\boldsymbol{\alpha} \rangle \geqslant 1 \quad \text{and} \quad \mathbf{\Lambda}_D(\omega) \text{ for } \left\langle \frac{\boldsymbol{\mu}}{\boldsymbol{\alpha}} \right\rangle \leqslant 1$$

as solutions of the equation (145). However, as already seen by verifying the conditions of lemma 5.11 for their expansions in the origin (cf. lemma 5.5), these functions no longer satisfy (150) in these regions (with an exception of a special case $\left\langle \frac{\boldsymbol{\mu}}{\boldsymbol{\alpha}} \right\rangle \equiv 1$, when $\mathbf{\Lambda}_D(\omega) \equiv \mathbf{\Lambda}_N(\omega)$). Thus, they cannot be the symbols of a DtN operator. This is consistent with corollary 5.6.

5.4. **Numerical approximation of the symbols $\mathbf{\Lambda}_{\mathfrak{n}}(\omega)$, $\mathbf{\Lambda}_{\mathfrak{d}}(\omega)$.** Let us now provide an algorithm for the numerical approximation of $\mathbf{\Lambda}_{\mathfrak{a}}(\omega)$ by $\mathbf{\Lambda}^a_{\mathfrak{a}}(\omega)$, $\mathfrak{a} = \mathfrak{d}$ or $\mathfrak{n}$. The function $\mathbf{\Lambda}^a_{\mathfrak{a}}(\omega)$ will be constructed progressively inside an increasing sequence of balls $\mathcal{B}_n$ that fill the whole complex plane as $n \to \infty$. For this, we rewrite (145) in the form

$$\mathbf{\Lambda}(\omega) = -\,\omega\,\frac{\omega\sin\omega - \cos\omega f_{\alpha,\mu}(\omega)}{\omega\cos\omega + \sin\omega f_{\alpha,\mu}(\omega)}, \qquad f_{\alpha,\mu}(\omega) = \sum_{i=0}^{p-1} \frac{\mu_i}{\alpha_i}\mathbf{\Lambda}(\alpha_i\omega). \tag{151}$$

This expression defines the values of the function $\mathbf{\Lambda}(\omega)$ via the values of the same function in $\omega_i = \alpha_i\omega$, $|\omega_i| < |\omega|$, $i = 0, \dots, p-1$. This property serves as the basis for an algorithm for evaluating the function $\mathbf{\Lambda}_{\mathfrak{a}}(\omega)$.
First of all, let us consider

$$\mathcal{B}_n = \{\omega \in \mathbb{C} \setminus \mathbb{R} \ \text{ s.t. } \ |\omega| < r_n := |\boldsymbol{\alpha}|_\infty^{-n}\, r_0\} \tag{152}$$

where $r_0 > 0$, the radius of $\mathcal{B}_0$, is such that $\mathcal{B}_0$ does not contain any pole of $\mathbf{\Lambda}_{\mathfrak{a}}(\omega)$, i.e.

$$0 < r_0 < \omega^0_{\mathfrak{a}}.$$

Then, at the continuous level, the iterative algorithm proceeds as follows.

- **Initialization**: given a truncation parameter $N \in \mathbb{N}^*$, one approximates $\mathbf{\Lambda}_{\mathfrak{a}}(\omega)$ inside $\mathcal{B}_0$ by its truncated Taylor expansion (recall that $\mathbf{\Lambda}_{\mathfrak{a}}(\omega)$ is even), i. e.

$$\mathbf{\Lambda}^a_{\mathfrak{a}}(\omega) := \sum_{n=0}^{N} \lambda^{2n}_{\mathfrak{a}}\ \omega^{2n}, \qquad \omega \in \mathcal{B}_0, \tag{153}$$

  where the (real) coefficients $\lambda^n_{\mathfrak{a}}$ are computed based on the formulas of appendix C. This is the step for which the cases $\mathfrak{a} = \mathfrak{d}$ and $\mathfrak{a} = \mathfrak{n}$ may differ.

- **Induction**: Supposing that $\mathbf{\Lambda}^a_{\mathfrak{d}}(\omega)$ has been computed inside $\mathcal{B}_n$, one computes $\mathbf{\Lambda}^a_{\mathfrak{d}}(\omega)$ inside $\mathcal{B}_{n+1} \setminus \mathcal{B}_n$ based on (151), i.e.

$$\mathbf{\Lambda}^a_{\mathfrak{a}}(\omega) = -\omega\, \frac{\omega \sin\omega - \cos\omega f^a_{\alpha,\mu}(\omega)}{\omega\cos\omega + \sin\omega f^a_{\alpha,\mu}(\omega)}, \qquad f^a_{\alpha,\mu}(\omega) = \sum_{i=0}^{p-1} \frac{\mu_i}{\alpha_i} \mathbf{\Lambda}^a_{\mathfrak{a}}(\alpha_i\omega). \tag{154}$$

  Note that the above expression completely defines $\mathbf{\Lambda}^a_{\mathfrak{a}}(\omega)$ inside $\mathcal{B}_{n+1} \setminus \mathcal{B}_n$ since, by construction of $\mathcal{B}_n$,

$$\text{for } \omega \in \mathcal{B}_{n+1} \setminus \mathcal{B}_n, \quad \alpha_i\, \omega \in \mathcal{B}_n, \quad \forall\, 0 \leqslant i \leqslant p-1.$$

One could ask whether the above algorithm is well-defined, in the sense that a division by zero never occurs in (154). This is the case, provided a certain condition on (153); this fact is a corollary of the following two lemmas.

Lemma 5.13. *Let $f(\omega) : \Omega \subset \mathbb{C}^+ \to \mathbb{C}$ satisfy (150). Then*

1. $\omega\cos\omega + \sin\omega f(\omega) \neq 0$ *in* Ω*;*
2. *the function* $F(\omega) = -\omega\, \dfrac{\omega\sin\omega - f(\omega)\cos\omega}{\omega\cos\omega + f(\omega)\sin\omega}$ *satisfies*

$$\operatorname{Im}\left(\omega^{-1}F(\omega)\right) < 0, \qquad \omega \in \Omega.$$

Proof. Let us prove the first assertion. Notice that $h(\omega)$ defined by

$$h(\omega) = \omega\cos\omega + \sin\omega f(\omega) = \omega\sin\omega\, g(\omega), \qquad g(\omega) = \cot\omega + \omega^{-1} f(\omega),$$

vanishes for some $\omega \in \mathbb{C}^+$ if and only if $g(\omega) = 0$. However, $\operatorname{Im}\cot\omega < 0$ in $\mathbb{C}^+$, cf. [17, p.64], and thus, due to (150),

$$\operatorname{Im} g(\omega) < 0 \text{ in } \mathbb{C}^+. \tag{155}$$

To prove 2. , we compute $\operatorname{Im}(\omega^{-1}F(\omega)) = -\operatorname{Im}\dfrac{1-\omega^{-1}f(\omega)\cot\omega}{\cot\omega + \omega^{-1}f(\omega)}$, which yields

$$\begin{aligned}\operatorname{sign}\operatorname{Im}(\omega^{-1}F(\omega)) &= -\operatorname{sign}\operatorname{Im}\left((1-\omega^{-1}f(\omega)\cot\omega)\overline{(\cot\omega + \omega^{-1}f(\omega))}\right)\\ &= -\operatorname{sign}\operatorname{Im}\left(\,\overline{g(\omega)} - \omega^{-1}f(\omega)|\cot\omega|^2 - |\omega^{-1}f(\omega)|^2\cot\omega\,\right).\end{aligned}$$

The above is negative, for the same reasons as (155), and because $\operatorname{Im}\overline{z} = -\operatorname{Im} z$. □

The above result shows that if $f^a_{\alpha,\mu}(\omega)$ defined in (154) satisfies (150), then no division by zero occurs in the expression (154). On the other hand, since for small $|\omega|$ the value $f^a_{\alpha,\mu}(\omega)$ is computed via the truncated Taylor expansion (153), it is natural to ask under which conditions this Taylor expansion will produce a function satisfying (150).

Lemma 5.14. *Let $f(\omega) : \mathbb{C} \to \mathbb{C}$ be an even polynomial $f(\omega) = \sum_{\ell=0}^{n} f_{2\ell}\,\omega^{2\ell}$.*

If f satisfies (150), then, necessarily,

$$f_0 \geqslant 0, \qquad f_2 \leqslant 0, \qquad f_{2\ell} = 0, \qquad \textit{for all } \ell > 1.$$

Otherwise, if either $f_0 > 0$ or $f_0 = 0$ and $f_2 < 0$, then (150) holds for $|\omega|$ small enough.

Proof. The first part of the statement follows by contradiction, by taking $\omega \in \mathbb{C}^+$ large enough. The second part of the statement mimics the proof of lemma 5.11. □

To formulate the principal result about the feasibility of the algorithm (153, 154), let us introduce an auxiliary quantity $r_*(N)$, which satisfies

$$\begin{aligned} &\text{if } N > 2, \qquad \mathrm{Im}\left(\omega^{-1}\mathbf{\Lambda}_{\mathfrak{a}}^a(\omega)\right) < 0 \text{ for all } \omega \in \mathcal{B}(0, r_*(N)) \cap \mathbb{C}^+, \\ &\text{if } N \leqslant 2, \qquad r_*(N) = +\infty. \end{aligned} \tag{156}$$

Then we can formulate the following lemma about the properties of the algorithm.

Lemma 5.15. *Let $N \in \mathbb{N}$ and $r_0 < r_*(N)$. Then the algorithm based on (153, 154) is well-defined. Moreover, the function computed by this algorithm satisfies*

$$\mathrm{Im}\left(\omega^{-1}\mathbf{\Lambda}_{\mathfrak{a}}^a(\omega)\right) < 0, \qquad \textit{for all } \omega \in \mathbb{C}^+. \tag{157}$$

Proof. It is easy to see that it is sufficient to check that the stated result holds for the first step of the algorithm (i.e. the construction of $\mathbf{\Lambda}_{\mathfrak{a}}^a(\omega)$ in $\mathcal{B}_1$). Then one proceeds by induction, by employing lemma 5.13.

First of all, thanks to lemma 5.14 (in the case $N \leqslant 2$) or (156) (for $N > 2$), the function computed by (153) satisfies

$$\mathrm{Im}\left(\omega^{-1}\mathbf{\Lambda}_{\mathfrak{a}}^a(\omega)\right) < 0, \qquad \forall\, \omega \in B\big(0, r_*(N)\big).$$

Next, using the definition of the function $f_{\alpha,\mu}$, see (151), and the one of $\mathcal{B}_1$, see (152),

$$\forall\, \omega \in \mathcal{B}_1 \cap \mathbb{C}^+, \quad \mathrm{Im}\,\left(\omega^{-1}\, f_{\alpha,\mu}(\omega)\right) < 0.$$

Then applying lemma 5.13, item 1, with

$$\Omega := \mathcal{B}_1 \cap \mathbb{C}^+ \quad \text{and} \quad f(\omega) = f_{\alpha,\mu}(\omega),$$

we deduce that

$$\forall\, \omega \in \mathcal{B}_1 \cap \mathbb{C}^+, \quad \omega\, \cos\omega + \sin\omega\, f_{\alpha,\mu}(\omega) \neq 0.$$

Thus, there is no problem to extend the function $\mathbf{\Lambda}_{\mathfrak{a}}^a(\omega)$ to $\mathcal{B}_1 \setminus \mathcal{B}_0 \cap \mathbb{C}^+$ using the formula (154). Moreover, by the item 2 of lemma 5.13, the function $\mathbf{\Lambda}_{\mathfrak{d}}^a(\omega)$ satisfies

$$\mathrm{Im}\,\left(\omega^{-1}\,\mathbf{\Lambda}_{\mathfrak{a}}^a(\omega)\right) < 0 \quad \text{in } \mathcal{B}_1 \cap \mathbb{C}^+.$$

□

Remark 5.16. *We did not investigate the (expected) convergence of our algorithm when $N \to +\infty$ and / or $r_0 \to 0$ but verified it numerically. Note that by construction, $\mathbf{\Lambda}_{\mathfrak{a}}^a(\omega)$ is polynomial in $\mathcal{B}_0$, rational in each $\mathcal{B}_{n+1} \setminus \mathcal{B}_n$ and discontinuous across each $\partial\mathcal{B}_n$.*

In practice, we compute a discrete approximation of $\mathbf{\Lambda}_{\mathfrak{a}}^a(\omega)$ along the rays on the complex plane $\mathcal{A}rg\,\omega = \mathrm{const}$. First notice that if suffices to compute $\mathbf{\Lambda}_{\mathfrak{d}}^a(\omega)$ in the quarter plane $\mathcal{A}rg\,\omega \in]0, \pi/2]$ since, once this is done, one completes the construction of $\mathbf{\Lambda}_{\mathfrak{d}}^a(\omega)$ using $\mathbf{\Lambda}_{\mathfrak{a}}^a(\omega) = \mathbf{\Lambda}_{\mathfrak{a}}^a(-\omega) = \mathbf{\Lambda}_{\mathfrak{d}}^a(\overline{\omega})$, which follows from (30).

Next, we consider the following polar mesh of the quarter plane $\mathcal{A}rg\,\omega \in]0, \pi/2]$: let $N_\theta \in \mathbb{N}$ be the number of the discretization points in the polar angle and $N_0 \in \mathbb{N}$ that defines the number of the discretization points in the ball $\mathcal{B}_0$. Let us define

$$\omega_j^n = n\, \Delta r\, e^{ij\Delta\theta}, \quad n \geqslant 1, \quad 1 \leqslant j \leqslant N_\theta,$$

where $\Delta r = \frac{r_0}{N_0}$ and $\Delta\theta = \frac{\pi}{2N_\theta}$, cf. figure 7. The value N_0 is chosen so that

$$N_0 > (|\boldsymbol{\alpha}|_\infty^{-1} - 1)^{-1}. \tag{158}$$

Then, for each fixed j one computes the $\{\omega_j^n, n \geqslant 1\}$ in the following way:

- As long as $n \leqslant N_0$, $\mathbf{\Lambda}_{\mathfrak{d}}^a(\omega_j^n)$ is computed via the **initialization step**.

- As soon as $n > N_0$, $\mathbf{\Lambda}^a_{\mathfrak{d}}(\omega_j^n)$ is computed using the **induction step**, with an additional approximation induced by a linear interpolation procedure. More precisely, thanks to (158), which appears as a necessary condition for the explicit nature of our algorithm, we deduce (the verification is left to the reader) that, for each $0 \leqslant i \leqslant p-1$, there exists $\ell < n$ and $\eta \in [0,1]$ such that

$$\alpha_i\, \omega_j^n = \eta\, \omega_j^\ell + (1-\eta)\, \omega_j^{\ell-1} \quad \text{with } \ell < n.$$

Remark that the condition (158) ensures that $\alpha_i \omega_j^n < \omega_j^{n-1}$ for all $n > N_0$. Then, in formula (154) applied to $\omega = \omega_j^n$, one makes the substitution

$$\mathbf{\Lambda}^a_{\mathfrak{d}}(\alpha_i \omega_j^n) \longrightarrow \eta\, \mathbf{\Lambda}^a_{\mathfrak{d}}(\omega_j^\ell) + (1-\eta)\, \mathbf{\Lambda}^a_{\mathfrak{d}}(\omega_j^{\ell-1}).$$

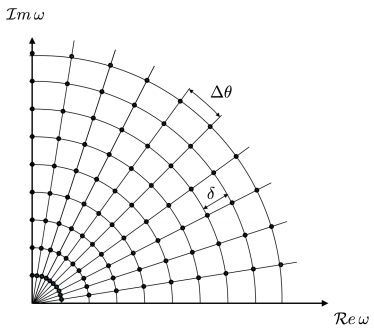

FIGURE 7. Polar mesh of the quarter plane

5.5. **Numerical results for $\mathbf{\Lambda}_{\mathfrak{d}}(\omega)$ and $\mathbf{\Lambda}_{\mathfrak{n}}(\omega)$.** We consider a dyadic symmetric tree (cf. figure 4) characterized by $p = 2$, $\alpha_1 = \alpha_2 = \alpha$ and $\mu_1 = \mu_2 = \mu$, and compute the symbols of the DtN operators $\mathbf{\Lambda}_{\mathfrak{d}}$ and $\mathbf{\Lambda}_{\mathfrak{n}}$ for different values of $(\boldsymbol{\mu}, \boldsymbol{\alpha})$.

The approximation of $\mathbf{\Lambda}_{\mathfrak{d}}(\omega)$ and $\mathbf{\Lambda}_{\mathfrak{n}}(\omega)$. First of all, let us take $\alpha = \mu = 0.6$. In this case $(\boldsymbol{\mu}, \boldsymbol{\alpha}) \in \mathbb{P}_{ND}$, and thus $\mathbf{\Lambda}_{\mathfrak{d}}(\omega) \neq \mathbf{\Lambda}_{\mathfrak{n}}(\omega)$, see corollary 5.6. The plots of $|\mathbf{\Lambda}_{\mathfrak{d}}(\omega)|$ and $|\mathbf{\Lambda}_{\mathfrak{n}}(\omega)|$ are shown in figure 8 (for $\omega \in \mathbb{C}$). These results indicate that the algorithm based on (153, 154) detects the location of the poles of the meromorphic functions $\mathbf{\Lambda}_{\mathfrak{d}}(\omega)$ and $\mathbf{\Lambda}_{\mathfrak{n}}(\omega)$, and allows to define the values of these functions for $\omega \notin \mathbb{R}$.

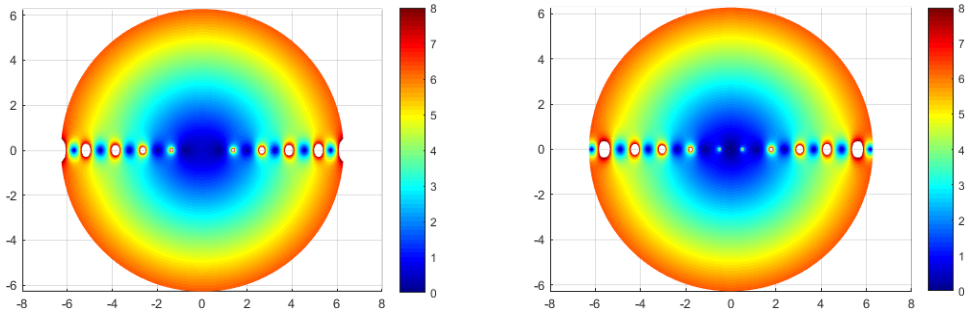

FIGURE 8. Plots of $|\mathbf{\Lambda}_{\mathfrak{d}}(\omega)|$ (left) and $|\mathbf{\Lambda}_{\mathfrak{n}}(\omega)|$ (right), for $|\omega| < 2\pi$, $\alpha = \mu = 0.6$

The property (149) of $\mathbf{\Lambda}_{\mathfrak{d}}(\omega)$ and $\mathbf{\Lambda}_{\mathfrak{n}}(\omega)$. As shown in lemma 5.15, the property (149) is preserved by the algorithm (153, 154) (provided certain conditions on N and r_0 in (153)). In figure 9 we illustrate this fact.

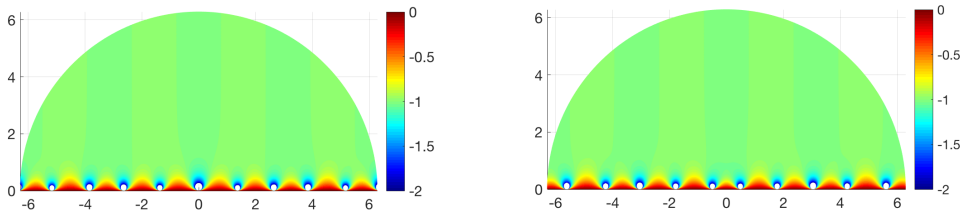

FIGURE 9. Plots of $\mathrm{Im}\left(\omega^{-1}\mathbf{\Lambda}_{\mathfrak{d}}(\omega)\right)$ (left) and $\mathrm{Im}\left(\omega^{-1}\mathbf{\Lambda}_{\mathfrak{n}}(\omega)\right)$ (right), for $|\omega| < 2\pi$, $\alpha = \mu = 0.6$. Remark that $\omega^{-1}\mathbf{\Lambda}_{\mathfrak{d}}(\omega)$ has a pole in $\omega = 0$, unlike $\omega^{-1}\mathbf{\Lambda}_{\mathfrak{n}}(\omega)$.

Meromorphic solutions of (145) $\mathbf{\Lambda}_D(\omega)$ and $\mathbf{\Lambda}_N(\omega)$, which are not symbols of the DtN operator. Finally, let us demonstrate what happens to the functions $\mathbf{\Lambda}_D(\omega)$ and $\mathbf{\Lambda}_N(\omega)$ in the regions where they fail to be the symbols of the DtN operators, see corollary 5.6 and remark 5.12. For this we set $\alpha = 0.6$ and $\mu = 0.2$ (so that $(\boldsymbol{\mu}, \boldsymbol{\alpha}) \in \mathbb{P}_N$), and compute $\mathbf{\Lambda}_D(\omega)$, and next set $\alpha = 0.6$ and $\mu = 2$ (so that $(\boldsymbol{\mu}, \boldsymbol{\alpha}) \in \mathbb{P}_D$) and evaluate $\mathbf{\Lambda}_N(\omega)$. The absolute values of these functions are shown in figure 10. As one can see, the function

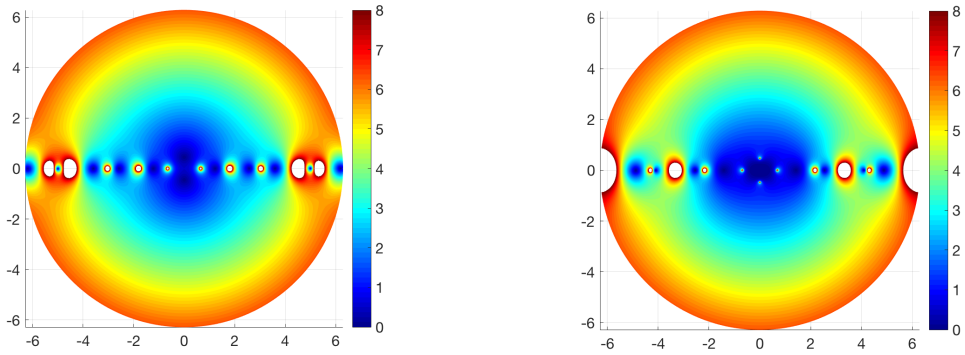

FIGURE 10. Plots of $|\mathbf{\Lambda}_D(\omega)|$ (left) for $\alpha = 0.6$, $\mu = 0.2$ and of $|\mathbf{\Lambda}_N(\omega)|$ (right) for $\alpha = 0.6$, $\mu = 2$.

$\mathbf{\Lambda}_D(\omega)$ has a zero on the imaginary axis (two dark blue spots on the imaginary axis in the left plot in figure 10), and the function $\mathbf{\Lambda}_N(\omega)$ has a pole in $i\mathbb{R}$. These two behaviors are incompatible with (149).

6. Local approximate transparent boundary conditions for a fractal tree.

In this section, we present a stable low-order local approximation of the DtN operator, based on the expansions provided in lemma 5.5, see corollary 5.6.

6.1. **Construction of conditions of order 1 and 2.** First of all, in practice we are interested in arbitrary p-adic self-similar trees rather than just reference ones; the corresponding DtN operators, however, can be easily expressed via the DtN operators of the reference trees by a simple scaling argument. Given a **reference** p-adic self-similar tree $\mathcal{T}$ and a corresponding p-adic self-similar tree whose root edge has length ℓ, i.e. $\mathcal{T}_\ell := \ell\,\mathcal{T}$ (with $(\boldsymbol{\mu}, \boldsymbol{\alpha})$ remaining the same for both trees), the symbol of the (Neumann or Dirichet) DtN operator $\mathbf{\Lambda}_{\mathfrak{a},\ell}$ for $\mathcal{T}_\ell$ is related to the corresponding DtN operator for the reference tree $\mathbf{\Lambda}_{\mathfrak{a}}(\omega)$ via

$$\mathbf{\Lambda}_{\mathfrak{a},\ell}(\omega) = \ell^{-1}\,\mathbf{\Lambda}_{\mathfrak{a}}(\omega\,\ell). \tag{159}$$

Let us come back to the transparent conditions (23) of section 1.6. For simplicity, but without any loss of generality, let us consider the case where the tree is the self-similar tree $\mathcal{T}(\ell)$ associated to $(\boldsymbol{\mu}, \boldsymbol{\alpha})$ and that we want to solve the wave equation with a non-homogeneous Dirichlet condition at the entrance of the tree. Suppose that we wish to truncate the computational domain after the n^{th} generation, by prescribing the DtN condition at each of the end points $M_{n,j}, 0 \leqslant j \leqslant p^n - 1$, which is thus nothing but (23) and (24), rewritten as

$$\mu_{n,j}\,\partial_s u = -\sum_{k\in\mathcal{C}_{n,j}} \mu_{n+1,k}\,\Lambda_{n+1,k} u \qquad \text{at the point } M_{n,j}, \tag{160}$$

where we recall that $\mathcal{C}_{n,j}$ is given in (8) and that $\Lambda_{n+1,k}$ is the DtN operator associated to the subtree $\mathcal{T}_{n+1,k}$, see (22). Because of the self-similarity properties and lemma 2.4

$$\mathcal{C}_{n,j} = \{pj+i,\ 0 \leqslant i \leqslant p-1\}, \quad \mu_{n+1,pj+i} = \mu_i\,\mu_{n,j}.$$

Moreover, as the length of the root edge of the tree of $\mathcal{T}_{n+1,pj+i}$ is $\alpha_i\,\ell_{n,j}$ with $\ell_{n,j} = \alpha_{n,j}\,\ell$, we have

$$\Lambda_{n+1,pj+i} = \Lambda_{\mathfrak{a},\alpha_i\ell_{n,j}},$$

where we have used (159) for notation, with $\mathfrak{a} = \mathfrak{d}$ or $\mathfrak{n}$. Thus the transparent boundary condition at the point $M_{n,j}$ rewrites

$$\partial_s u = -\sum_{i=0}^{p-1} \mu_i\,\Lambda_{\mathfrak{a},\alpha_i\ell_{n,j}}\,u \quad \text{at the point } M_{n,j}. \tag{161}$$

From the compactness property of the tree, one expects that, since $\ell_{n,j}$ decays exponentially fast to 0 with n, to get a good approximation of $\Lambda_{\mathfrak{a},\alpha_i\ell_{n,j}}$, it suffices, according to the formula (159), to have a good approximation of $\mathbf{\Lambda}_{\mathfrak{a}}(\omega)$ for small values of $|\omega|$. In this perspective, truncated Taylor expansions around the origin offer an attractive solution since they lead to local boundary conditions. Then, the only theoretical question is to know if the truncation process preserves the stability of the new boundary value problem. In what follows, we shall investigate this question by looking at second order Taylor expansions. More precisely, we propose the approximations

$$\mathbf{\Lambda}_{\mathfrak{a}}(\omega) \simeq \mathbf{\Lambda}^{(2)}_{\mathfrak{a}}(\omega) := \lambda_{\mathfrak{a},0} + \lambda_{\mathfrak{a},0}\,\omega^2, \tag{162}$$

where according to lemma 5.5, we have for the Dirichlet problem (and $\left\langle \dfrac{\boldsymbol{\mu}}{\boldsymbol{\alpha}} \right\rangle > 1$)

$$\lambda_{\mathfrak{d},0} = 1 - \left\langle \frac{\boldsymbol{\mu}}{\boldsymbol{\alpha}} \right\rangle^{-1}, \quad \lambda_{\mathfrak{d},2} = -\frac{1}{3}\left(1 + \left\langle \frac{\boldsymbol{\mu}}{\boldsymbol{\alpha}} \right\rangle + \left\langle \frac{\boldsymbol{\mu}}{\boldsymbol{\alpha}} \right\rangle^2\right)\left(\left\langle \frac{\boldsymbol{\mu}}{\boldsymbol{\alpha}} \right\rangle^2 - \langle \boldsymbol{\mu}\boldsymbol{\alpha} \rangle\right)^{-1}, \tag{163}$$

while for the Neumann case (which means that $\langle \boldsymbol{\mu}\boldsymbol{\alpha} \rangle < 1$)

$$\lambda_{\mathfrak{n},0} = 0, \qquad \lambda_{\mathfrak{n},2} = -\left(1 - \langle \boldsymbol{\mu}\boldsymbol{\alpha} \rangle\right)^{-1}. \tag{164}$$

Remark 6.1. *We will refer to these approximations as to the second-order conditions, because they are constructed using the first three terms of the expansion of the symbol of the DtN in ω (as $\lambda_{\mathfrak{a},1} \equiv 0$). We could have taken only the first two terms in the expansion, and in this case these conditions will be referred to as having the order one.*

Note that one has the following sign properties:

$$\lambda_{\mathfrak{a},0} \geqslant 0, \quad \lambda_{\mathfrak{a},2} \leqslant 0, \quad \mathfrak{a} = \mathfrak{d}, \mathfrak{n}. \tag{165}$$

Then, (162) combined with (159), suggests the following approximation of the operators $\Lambda_{\mathfrak{a},\alpha_i \ell_{n,j}}$ appearing in (161) by second order differential operators:

$$\Lambda_{\mathfrak{a},\alpha_i \ell_{n,j}} \sim \Lambda^{(2)}_{\mathfrak{a},\alpha_i \ell_{n,j}} := \lambda_{\mathfrak{a},0}\, \alpha_i^{-1}\, \ell_{n,j}^{-1} - \lambda_{\mathfrak{a},2}\, \alpha_i\, \ell_{n,j}\, \partial_t^2. \tag{166}$$

This leads to the following boundary value problem on the truncated tree $\mathcal{T}^n$: find $u^n_{\mathfrak{a},2} : \mathcal{T} \times \mathbb{R}^+ \to \mathbb{R}$ (the approximate solution) such that

$$\begin{cases} \mu\, \partial_t^2 u^n_{\mathfrak{a},2} - \partial_s(\mu\, \partial_s u^n_{\mathfrak{a},2}) = 0, \quad \text{on } \mathcal{T}^n \times \mathbb{R}^+, \\ \partial_s u^n_{\mathfrak{a},2} + \displaystyle\sum_{i=0}^{p-1} \mu_i \left(\lambda_{\mathfrak{a},0}\, \alpha_i^{-1}\, \ell_{n,j}^{-1}\, u^n_{\mathfrak{a},2} - \lambda_{\mathfrak{a},2}\, \alpha_i\, \ell_{n,j}\, \partial_t^2 u^n_{\mathfrak{a},2} \right) = 0, \\ \text{at } M_{n,j},\ 0 \leqslant j \leqslant J(n), \\ u^n_{\mathfrak{a},2}(.,0) = \partial_t u^n_{\mathfrak{a},2}(.,0) = 0, \end{cases} \tag{167}$$

completed by initial conditions and the Dirichlet condition at the entrance of the tree. The weak formulation of the above problem reads

$$\begin{cases} \text{Find } u^n_{\mathfrak{a},2}(\cdot,t) : [0,T] \to \mathrm{H}^1_\mu(\mathcal{T}^n) \ / \ u^n_{\mathfrak{a},2}(M_\star,t) = f(t) \text{ and} \\ \dfrac{d^2}{dt^2} \displaystyle\int_{\mathcal{T}^n} \mu\, u^n_{\mathfrak{a},2}(\cdot,t)\, v + \int_{\mathcal{T}^n} \mu\, \partial_s\, u_{\mathfrak{a},2}(\cdot,t)\, \partial_s v \\ - \left\langle \boldsymbol{\mu}\boldsymbol{\alpha} \right\rangle \lambda_{\mathfrak{a},2} \dfrac{d^2}{dt^2} \displaystyle\sum_{j=0}^{J(n)} \mu_{n,j}\, \ell_{n,j}\, u^n_{\mathfrak{a},2}(M_{n,j},t)\, v(M_{n,j}), \\ + \left\langle \dfrac{\boldsymbol{\mu}}{\boldsymbol{\alpha}} \right\rangle \lambda_{\mathfrak{a},0} \displaystyle\sum_{j=0}^{J(n)} \mu_{n,j}\, \ell_{n,j}^{-1}\, u^n_{\mathfrak{a},2}(M_{n,j},t)\, v(M_{n,j}) = 0, \\ \forall\ v \in V(\mathcal{T}^n) = \{ v \in \mathrm{H}^1_\mu(\mathcal{T}^n) \,/\, v(M_\star) = 0 \}, \\ u^n_{\mathfrak{a},2}(.,0) = \partial_t u^n_{\mathfrak{a},2}(.,0) = 0. \end{cases} \tag{$\mathcal{P}_{\mathfrak{a},n}$}$$

Remark that, contrary to the case of the exact problems, where the distinction between Neumann and Dirichlet problems occurred in the variational spaces, for the approximate problems, the difference appears in the bilinear forms, via the coefficients $(\lambda_{\mathfrak{a},0}, \lambda_{\mathfrak{a},2})$.

Our main theoretical result is the following stability result.

Theorem 6.2. *Let $\mathfrak{a} = \mathfrak{n}$ (resp. $\mathfrak{a} = \mathfrak{d}$) and let $u_\mathfrak{a}$ be the solution of problem ($\mathcal{P}_{\mathfrak{a},n}$) for $\mathfrak{a} = \mathfrak{n}$ (resp. $\mathfrak{a} = \mathfrak{d}$) with the source term f. Moreover, let f be compactly supported in*

$(0,T_0)$, with $T_0<T$. Then, the energy $\mathcal{E}^n_{\mathfrak{a},2}(t)$ defined by

$$\begin{aligned}\mathcal{E}^n_{\mathfrak{a},2}(t) &:= \frac{1}{2}\int_{\mathcal{T}^n}\mu\Big\{|\partial_t u^n_{\mathfrak{a},2}(\cdot,t)|^2+|\partial_t u_{\mathfrak{a}}(\cdot,t)|^2\Big\}\\ &- \frac{1}{2}\langle\boldsymbol{\mu\alpha}\rangle\lambda_{\mathfrak{a},2}\sum_{j=0}^{J(n)}\ell_{n,j}\,\mu_{n,j}\,|\partial_t u^n_{\mathfrak{a},2}(M_{n,j},t)|^2\\ &+ \frac{1}{2}\Big\langle\frac{\boldsymbol{\mu}}{\boldsymbol{\alpha}}\Big\rangle\lambda_{\mathfrak{a},0}\sum_{j=0}^{J(n)}\ell_{n,j}^{-1}\,\mu_{n,j}\,|u^n_{\mathfrak{a},2}(M_{n,j},t)|^2\end{aligned}$$

is constant for $t>T_0$. As a consequence, the approximate boundary conditions are uniformly stable in the sense that the approximate solution is bounded in energy norm by a constant which is independent of the truncation order n.

Proof. Again the existence and uniqueness result is a classical exercise on the theory of second order linear hyperbolic problems. The result about the energy is obtained in the usual way after multiplying the first equation of (167) by ∂_t and integrating the result over $\mathcal{T}^n$. Finally, the stability result, i.e. that $\mathcal{E}^n_{\mathfrak{a},2}(t)$ defines an energy (is non-negative), follows from (165). □

6.2. **Numerical validation of conditions of order 1 and 2.** In this section we validate the performance of our approximate conditions numerically on the example of the dyadic symmetric tree (cf. figure 4). Our goal is to check the influence of the order (1 or 2) of the absorbing boundary condition together with the influence of the truncation order n of the tree. For each experiment, this evaluation will be made by by comparing the corresponding approximate solution to a reference solution computed with a large tree $\mathcal{T}^N$ made of the N first generations with N large (and the second order absorbing boundary condition).

6.2.1. *Discretization.* We shall not discuss in detail the method that we used for the discretization of the truncated problem since it is quite classical.

The spatial discretization is done on a uniform spatial mesh with step size h whose nodes include, in particular, the vertices of the tree. To eliminate the effect of the spatial discretization on the accuracy of experiments, we use very small values of h, so that it is compatible with the large reference tree $\mathcal{T}^N$: each edge of the last generation is divided into K segments. All computations are done on the same mesh: more precisely, for the computations made on $\mathcal{T}^n$ with $n\ll N$, we use the restriction to $\mathcal{T}^n$ of the mesh of $\mathcal{T}^N$. We use standard mass-lumped 1D-Lagrange finite elements (with a trivial adaptation for the basis functions to ensure their continuity at the vertices of the tree). For brevity we will use the same notation for the semidiscretized in space and the continuous solution.
For the time discretization, we use an explicit scheme coupled with an implicit discretization of the boundary terms. In particular, given a time step Δt, and $t^k=k\Delta t$, we denote by $u^{n,k}_{\mathfrak{a},2}\approx u^n_{\mathfrak{a},2}(\cdot,t^k)$. Then in ($\mathcal{P}_{\mathfrak{a},n}$), all the second-derivatives (related to volumic and boundary terms) are discretized by

$$\partial_t^2 u_{\mathfrak{a},2}(\cdot,t^k)\sim\frac{u^{n,k}_{\mathfrak{a},2}-2\,u^{n,k}_{\mathfrak{a},2}+u^{n,k}_{\mathfrak{a},2}}{\Delta t^2},$$

the volumic term in the stiffness bilinear form of ($\mathcal{P}_{\mathfrak{a},n}$) is discretized explicitly, i.e.

$$\int_{\mathcal{T}^n}\mu\,\partial_s\,u_{\mathfrak{a},2}(\cdot,t^k)\,\partial_s v\;\sim\;\int_{\mathcal{T}^n}\mu\,\partial_s\,u^{n,k}_{\mathfrak{a},2}\,\partial_s v,$$

and, finally, the boundary 0-order term is discretized implicitly:

$$\left\langle \frac{\boldsymbol{\mu}}{\boldsymbol{\alpha}} \right\rangle \lambda_{\mathfrak{a},0} \sum_{j=0}^{J(n)} \mu_{n,j}\, \ell_{n,j}^{-1}\, u_{\mathfrak{a},2}^{n}(M_{n,j}, t^k)\, v(M_{n,j})$$
$$\sim \left\langle \frac{\boldsymbol{\mu}}{\boldsymbol{\alpha}} \right\rangle \lambda_{\mathfrak{a},0} \sum_{j=0}^{J(n)} \left\langle \frac{\boldsymbol{\mu}}{\boldsymbol{\alpha}} \right\rangle \mu_{n,j} \ell_{n,j}^{-1} \Big(\frac{u_{\mathfrak{a},2}^{n,k} + 2\, u_{\mathfrak{a},2}^{n,k} + u_{\mathfrak{a},2}^{n,k}}{4} \Big)(M_{n,j})\, v(M_{n,j}).$$

As a consequence, the resulting numerical scheme is stable under the classical CFL condition $\mathrm{CFL} = \frac{\Delta t}{\Delta x} \leqslant 1$. Moreover, the resolution of the problem remains fully explicit.

6.2.2. *Numerical Experiments.* We present the numerical simulations for the scattering problem with the Dirichlet condition at infinity

$$\begin{cases} \mu \partial_t^2 u(s,t) - \partial_s\big(\mu \partial_s u\big)(s,t) = 0, & (s,t) \in \mathcal{T} \times \mathbb{R}^+, \\ u(s,0) = f(s), & s \in \mathcal{T}, \\ \partial_t u(s,0) = g(s), & s \in \mathcal{T}, \\ \partial_t u(M_\star, t) + \partial_s u(M_\star, t) = 0, & t \in \mathbb{R}^+, \end{cases} \tag{168}$$

on the dyadic tree with the parameters

$$\alpha_0 = \alpha_1 = \mu_0 = \mu_1 = 0.6,$$

with the length of the first branch $\ell = 2$. The source terms $f(s), g(s)$ are supported and centered on the first branch and are given by

$$f(s) = \exp\big(-30(s-1)^2\big), \quad g(s) = -\partial_s f(s).$$

According to figure 8, the smallest positive pole of $\Lambda_{\mathfrak{d}}(\omega)$ is

$$\omega_{\mathfrak{d}}^0 \approx 1.37,$$

Thus we cannot expect a good approximation of $\Lambda_{\mathfrak{d}}(\omega)$ by the truncated Taylor expansion for $|\omega| \geqslant \omega_{\mathfrak{d}}^0$.

Due to the choice of the source term, for time t small enough $u(s,t)$ is given on the first branch by $f(s-t)$. Let us then consider the Fourier transform of f, given by

$$\widehat{f}(\omega) = \exp\left(-\frac{\omega^2}{120}\right).$$

We observe in particular that for

$$|\omega| \geqslant \omega_{\text{cut}} = 30, \quad |\widehat{f}(\omega)| \leqslant e^{-7.5} \lesssim 6.10^{-4}.$$

We perform the simulations with this source. To truncate the tree (find n), we need to examine how well $\Lambda_{\mathfrak{d}}(\ell\alpha^{n+1}\omega)$ is approximated for $|\omega| < |\omega_{\text{cut}}|$, cf. (161). In particular, n should satisfy $\big|\ell\alpha^{n+1}\omega_{\text{cut}}\big| < \omega_{\mathfrak{d}}^0$. This estimate provides a lower bound for the truncation order n to expect a reasonable accuracy of the absorbing boundary condition (162):

$$\ell\alpha^{n+1}\omega_{\text{cut}} < \omega_{\mathfrak{d}}^0 \quad \Longrightarrow \quad n > \frac{\ln \omega_{\mathfrak{d}}^0 - \ln(\omega_{\text{cut}}\ell)}{\ln \alpha} - 1, \quad \text{which gives } n \geqslant 7. \tag{169}$$

In what follows, we compare the reference solution, computed on the tree $\mathcal{T}^N$, $N = 22$ (the solution of ($\mathcal{P}_{\mathfrak{a},n}$) with $\mathfrak{a} = \mathfrak{d}$), to

- the solution $u^n_{\mathfrak{d},0}$ defined as the solution of (167) where the the absorbing condition is replaced by the Dirichlet condition, hereafter referred to as the 0 order condition,
- the solution $u^n_{\mathfrak{d},1}$ defined as the solution of (167) with $\lambda_{\mathfrak{a},0} = \lambda_{\mathfrak{d},0}$ and $\lambda_{\mathfrak{a},2} = 0$, hereafter referred to as the first order condition,
- the solution $u^n_{\mathfrak{d},2}$ defined as the solution of (167) with $\lambda_{\mathfrak{a},0} = \lambda_{\mathfrak{d},0}$ and $\lambda_{\mathfrak{a},2} = \lambda_{\mathfrak{d},2}$, hereafter referred to as the second order condition.

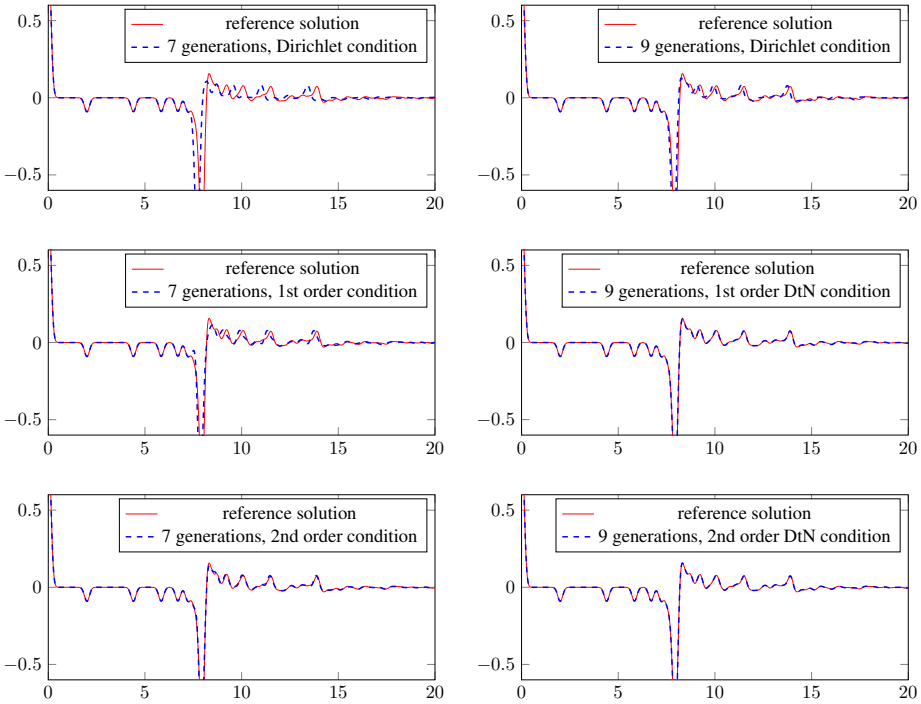

FIGURE 11. Left row: the dependence of $u(M,t)$ on time for the exact (red solid line) and the truncated tree on 7 generations (blue dashed line). Top: Dirichlet condition. Middle: the first order DtN condition. Bottom: the second order DtN condition.
Right row: the dependence of $u(M,t)$ on time for the exact (red solid line) and the truncated tree on 9 generations (blue dashed line). Top: Dirichlet condition. Middle: the first order DtN condition. Bottom: the second order DtN condition.

In figure 11 we plot these computed solutions at the middle of the root branch of the tree M as functions of time $t \in [0,T]$, $T = 20$, for $n = 7$ and $n = 9$ (which is compatible with (169)). The reference solution is in red, the approximate solution is in blue. As we can observe, the solution obtained on the truncated tree becomes closer and closer to the reference solution as the number of generations or the order of the truncating operator increases.

These qualitative results are quantified by table 1 and figure 12 where we computed the L^2

in time error between the reference and the approximate solutions (both computed at the point M). In table 1, we demonstrate in particular the improved accuracy of the absorbing boundary conditions (162) compared to taking $n = 7$ and the Dirichlet (0-order) condition.

Number of generations $n+1$	Dirichlet condition	First order condition	Second order condition	Gain with first order	Gain with second order
5	0.429	0.320	1.23×10^{-1}	1.34	3.05
6	0.370	0.205	5.01×10^{-2}	1.80	7.35
7	0.217	0.075	1.37×10^{-2}	2.89	15.83
8	0.083	0.018	2.72×10^{-3}	4.53	30.5
9	0.023	0.0031	3.84×10^{-4}	7.47	59.9

TABLE 1. L^2-error between the exact and approximate solutions, with respect to the number of generations and the order of the approximate boundary condition.

In figure 12 we demonstrate that the convergence of the absorbing boundary conditions with respect to n is close to exponential, and, as expected, the error decreases with the order of the absorbing boundary condition. Let us remark that in this work we do not address the error analysis of these conditions, postponing this question to future works.

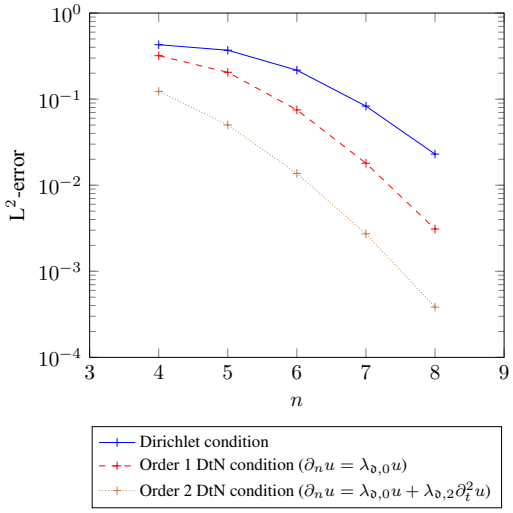

FIGURE 12. L^2-error between exact and approximate solutions, with respect to the number of generations and the order of the approximate boundary condition.

7. **Conclusions and Prospectives.** The contributions of this work are of both theoretical and numerical nature. First of all, from the theoretical point of view, we have presented an extensive analysis of the properties of a weighted wave equation in an infinite compact tree with self-similar endings. One particularly tricky question is the treatment of the boundary conditions (Neumann or Dirichlet) at 'infinity', the understanding of which requires a deep analysis of particular weighted Sobolev spaces on compact fractal p-adic trees. From the computational point of view, based on this analysis, we have constructed transparent boundary conditions for truncating the computational domain for solving the weighted wave equation on such fractal trees. The key ingredient is the construction of a reference DtN operator associated to a p-adic self-similar tree, which is a time convolution operator whose symbol (the Fourier transform of the convolution kernel) is characterized as a particular solution of a non-linear functional equation. This solution is a meromorphic function, analytic in the vicinity of the origin. The analysis of the equation allows us in particular to compute the second-order Taylor expansion of this symbol around the origin, which we use for constructing approximate local boundary conditions. We have proven that these conditions are stable and their use results in a satisfactorily accurate approximation of the solutions. However, because the range of frequencies for which this Taylor expansion provides a good approximation is limited (to the pole-free region around the origin), in practice the use of such low-order conditions is likely to become prohibitively expensive for high-frequency problems. That is why we intend in a future work to improve the approximations of the boundary conditions, by considering two different approaches. The first idea is to replace the polynomial approximation by a rational approximation, in the spirit of [15], which would take into account the most significant poles of the exact symbol. The second idea is to consider the exact boundary conditions. In this case the main difficulty lies in the time discretization, for which we intend to adapt the convolution quadrature method [10].

Acknowledgements. The authors are grateful to Konstantin Pankrashkin (University of Paris-Sud) for fruitful discussions.

Appendix A. **Proof of lemma 3.16.** The first case of the lemma is obvious. First of all, it is not difficult to verify by induction that:

$$x_n \leqslant \gamma^n \, x_0 + \sum_{\ell=0}^{n-1} \varepsilon_\ell \, \gamma^{n-1-\ell}. \tag{170}$$

The first term in the rhs of (170) converges to zero because $\gamma < 1$. For the second term, we split the sum into two parts that we estimate separately:

$$\left| \begin{array}{lll} \displaystyle\sum_{\ell=0}^{\lceil \frac{n}{2} \rceil} \varepsilon_\ell \, \gamma^{n-1-\ell} \leqslant \left(\lceil \tfrac{n}{2} \rceil + 1 \right) \, |\varepsilon|_\infty \, \gamma^{n-\lceil \frac{n}{2} \rceil - 1} & \longrightarrow 0 & (\text{since } \gamma < 1) \\ \displaystyle\sum_{\ell=\lceil \frac{n}{2} \rceil + 1}^{n-1} \varepsilon_\ell \, \gamma^{n-1-\ell} \leqslant \frac{1}{1-\gamma} \sup_{\ell \geqslant \lceil n/2 \rceil} \varepsilon_\ell & \longrightarrow 0 & (\text{since } \varepsilon_n \to 0) \end{array} \right.$$

The second case is slightly trickier. First of all, we obtain by induction the equivalent of the inequality (170), that is:

$$x_n \leqslant x_0 \prod_{\ell=0}^{n-1} \gamma_\ell + \sum_{k=0}^{n-1} \varepsilon_k \left(\prod_{\ell=k+1}^{n-1} \gamma_\ell \right). \tag{171}$$

or equivalently, setting $\Gamma_n = \prod_{\ell=0}^{n} \gamma_\ell$,

$$x_n \leqslant \Gamma_{n-1}\, x_0 + \sum_{k=0}^{n-1} \left(\Gamma_{n-1}/\Gamma_k\right) \varepsilon_k. \tag{172}$$

The first term in the rhs of (171) converges to 0 because, since $1 - ax \leqslant \mathrm{e}^{-ax}$ for $x \geqslant 0$,

$$\gamma_\ell = 1 - \frac{a}{\ell+1} \quad \Longrightarrow \quad \Gamma_n := \prod_{\ell=0}^{n} \gamma_\ell \;\leqslant\; \mathrm{e}^{-\sum_{\ell=0}^{n} \frac{a}{\ell+1}} \to 0, \qquad n \to \infty.$$

On the other hand, for $n \geqslant N+1$ (N to be fixed later), the second term in the rhs of (171) satisfies, since $\Gamma_{n-1}/\Gamma_k < 1$,

$$\sum_{k=0}^{n-1} \left(\Gamma_{n-1}/\Gamma_k\right) \varepsilon_k \leqslant \sum_{k=0}^{N} \left(\Gamma_{n-1}/\Gamma_k\right) \varepsilon_k + \sum_{k=N+1}^{+\infty} \varepsilon_k.$$

Since $\sum_{n=0}^{\infty} \varepsilon_n < \infty$, for any $\varepsilon > 0$, we can choose $N = N_\varepsilon$ so that $\sum_{k=N+1}^{+\infty} \varepsilon_k < \frac{\varepsilon}{2}$:

$$n \geqslant N_\varepsilon + 1 \quad \Longrightarrow \quad \sum_{k=0}^{n-1} \left(\Gamma_{n-1}/\Gamma_k\right) \varepsilon_k \;\leqslant\; \Gamma_{n-1}\, S_\varepsilon + \frac{\varepsilon}{2}, \quad S_\varepsilon := \sum_{k=0}^{N_\varepsilon} \frac{\varepsilon_k}{\Gamma_k}\,.$$

Since $\Gamma_n \to 0$, for n large enough $\Gamma_{n-1}\, S_\varepsilon < \frac{\varepsilon}{2}$ and the conclusion follows.

Appendix B. **Proof of lemma 3.22. Step 1:** proof that (124) implies the compactness. Let $\gamma_n \to 0$, $n \to \infty$, be s.t. (124) holds. Let u_n be a bounded sequence in V. Our goal is to show that it has a convergent in $\mathrm{L}^2_\mu(\mathcal{T})$ subsequence. First, up to the extraction of a first subsequence, we can assume that u_n converges weakly in V to some limit u.

Let us consider the sequence $u_n|_{\mathcal{T}^0}$, which is bounded in $\mathrm{H}^1_\mu(\mathcal{T}^0)$. Since $\mathrm{H}^1_\mu(\mathcal{T}^0)$ is compactly embedded into $\mathrm{L}^2_\mu(\mathcal{T}^0)$, there exists a subsequence u^0_n of u_n, s.t.

$$u^0_n\big|_{\mathcal{T}^0} \to u^0 \equiv u_{|\mathcal{T}^0} \quad \text{in } \mathrm{L}^2_\mu(\mathcal{T}^0).$$

Similarly, $u^0_n\big|_{\mathcal{T}^1}$ is bounded in $\mathrm{H}^1_\mu(\mathcal{T}^1)$ and we extract from u^0_n a subsequence u^1_n, s.t.

$$u^1_n\big|_{\mathcal{T}^1} \to u^1 \equiv u_{|\mathcal{T}^1} \quad \text{in } \mathrm{L}^2_\mu(\mathcal{T}^1).$$

By induction, we can thus build a double-indexed sequence $\{u^k_n, (n,k) \in \mathbb{N}^2\}$ satisfying

$$n \to u^{k+1}_n \text{ is a subsequence of } n \to u^k_n \quad \text{and} \quad u^k_n \to u^k \equiv u_{|\mathcal{T}^k} \quad \text{in } \mathrm{L}^2_\mu(\mathcal{T}^k). \tag{173}$$

Let us now define the diagonal subsequence of u^n

$$\widetilde{u}_n = u^n_n \in V, \tag{174}$$

for which

$$\widetilde{u}_n \to u \quad \text{in } \mathrm{L}^2_\mu(\mathcal{T}^k), \quad \forall k \geqslant 1. \tag{175}$$

Indeed, for all k, $\{u^n_n, n \geqslant k\}$ is a subsequence of $n \to u^k_n$ which converges to u in $\mathrm{L}^2_\mu(\mathcal{T}^k)$ thanks to (173).

Next, let us demonstrate that $\tilde{u}_n \to u$ in $\mathrm{L}^2_\mu(\mathcal{T})$. Notice that

$$\|\widetilde{u}_n - u\|^2_{\mathrm{L}^2_\mu(\mathcal{T})} = \|\widetilde{u}_n - u\|^2_{\mathrm{L}^2_\mu(\mathcal{T}^k)} + \|\widetilde{u}_n - u\|^2_{\mathrm{L}^2_\mu(\mathcal{T}\setminus\mathcal{T}^k)}\,, \qquad k \in \mathbb{N}. \tag{176}$$

It remains to apply (124) to $v = \widetilde{u}_n - u$. Since $\widetilde{u}_n - u$ is bounded in $\mathrm{H}^1_\mu(\mathcal{T})$, there exists $C > 0$, s.t.

$$\|\widetilde{u}_n - u\|^2_{\mathrm{L}^2_\mu(\mathcal{T})} \leqslant \|\widetilde{u}_n - u\|^2_{\mathrm{L}^2_\mu(\mathcal{T}^k)} + C\,\gamma_k^2, \qquad k \in \mathbb{N}. \tag{177}$$

Let $\varepsilon > 0$. We first fix k large enough such that $C\,\gamma_k^2 < \varepsilon/2$. Next, exploiting (175), we choose n large enough ($n \geqslant N_k(\varepsilon)$) so that $\|\widetilde{u}_n - u\|^2_{\mathrm{L}^2_\mu(\mathcal{T}^k)} < \varepsilon/2$ and we conclude that

$$n \geqslant N_k(\varepsilon) \quad \Longrightarrow \quad \|\widetilde{u}_n - u\|^2_{\mathrm{L}^2_\mu(\mathcal{T})} < \varepsilon.$$

Thus, $\widetilde{u}_n$ converges to u in $\mathrm{L}^2_\mu(\mathcal{T})$.

Step 2: proof that the compactness implies (124). Assume that the embedding of V in $\mathrm{L}^2_\mu(\mathcal{T})$ is compact. Let us introduce

$$\gamma_n = \sup_{u\in\mathcal{B}} \|u\|_{\mathrm{L}^2_\mu(\mathcal{T}\setminus\mathcal{T}^n)}, \quad \mathcal{B} = \{u \in V \;/\; \|u\|_{\mathrm{H}^1_\mu(\mathcal{T})} = 1\}. \tag{178}$$

Note that $\mathcal{T}^n \subset \mathcal{T}^{n+1}$ implies that γ_n is a decreasing sequence. Let us find a subsequence of γ_n that converges to 0, which would prove that $\gamma_n \to 0$ as $n \to \infty$, i.e. (124). By compactness of $\mathcal{B}$, there exists $u_n \in \mathcal{B}$ that realizes the supremum in (178), *i.e.*

$$\gamma_n = \|u_n\|_{\mathrm{L}^2_\mu(\mathcal{T}\setminus\mathcal{T}^n)} \ . \tag{179}$$

Again, by compactness of $\mathcal{B}$, u_n has a subsequence $(u_{\varphi(n)})_{n\in\mathbb{N}}$, such that

$$u_{\varphi(n)} \longrightarrow u \in V, \quad \text{strongly in } \mathrm{L}^2_\mu(\mathcal{T}), \quad \text{weakly in } \mathrm{H}^1_\mu(\mathcal{T}). \tag{180}$$

Writing $u_{\varphi(n)} = (u_{\varphi(n)} - u) + u$ and using the triangular inequality, we get

$$\gamma_{\varphi(n)} \leqslant \|u\|_{\mathrm{L}^2_\mu(\mathcal{T}\setminus\mathcal{T}^{\varphi(n)})} + \left\|u_{\varphi(n)} - u\right\|_{\mathrm{L}^2_\mu(\mathcal{T})}. \tag{181}$$

This shows that $\gamma_{\varphi(n)}$ tends to 0. Thus, $\gamma_n \to 0$ as $n \to \infty$.

Appendix C. Proof of lemma 5.5. Let $\mathbf{\Lambda}$ be continuous in the origin. Taking the limit $\omega \to 0$ in (145), we obtain the following equation :

$$\mathbf{\Lambda}(0) = \left\langle \frac{\boldsymbol{\mu}}{\boldsymbol{\alpha}} \right\rangle (1 - \mathbf{\Lambda}(0))\mathbf{\Lambda}(0), \quad \text{or, alternatively,} \quad \mathbf{\Lambda}(0)\left(1 - \left\langle \frac{\boldsymbol{\mu}}{\boldsymbol{\alpha}} \right\rangle + \left\langle \frac{\boldsymbol{\mu}}{\boldsymbol{\alpha}} \right\rangle \mathbf{\Lambda}(0)\right) = 0.$$

The above equation has the following solutions:

- when $\left\langle \dfrac{\boldsymbol{\mu}}{\boldsymbol{\alpha}} \right\rangle \neq 1$, there are two solutions:

$$\mathbf{\Lambda}(0) = 0 \ \text{ or } \ \mathbf{\Lambda}(0) = 1 - \left\langle \frac{\boldsymbol{\mu}}{\boldsymbol{\alpha}} \right\rangle^{-1}. \tag{182}$$

- when $\left\langle \dfrac{\boldsymbol{\mu}}{\boldsymbol{\alpha}} \right\rangle = 1$, there is a single solution $\mathbf{\Lambda}(0) = 0$.

Hence the first part of the lemma. To prove the rest of the lemma we will show that under the appropriate assumptions on $\boldsymbol{\mu}$ and $\boldsymbol{\alpha}$, the value in 0 defines in a unique way any even function, analytic in a neighborhood of the origin, satisfying (145) in this neighborhood. Thus, let $\mathbf{\Lambda}(\omega)$ be an even function, analytic around the origin. Then for $|\omega|$ small enough, we have

$$\mathbf{\Lambda}(\omega) = \sum_{\ell=0}^{\infty} \lambda_{2\ell}\, \omega^{2\ell}. \tag{183}$$

Inserting this expansion into (145), we obtain the following equation:

$$\begin{aligned}
&\omega \sum_{n=0}^{\infty} \frac{(-1)^n \omega^{2n+1}}{(2n+1)!} + \Big(\sum_{n=0}^{\infty} \lambda_{2n}\, \omega^{2n}\Big)\Big(\sum_{n=0}^{\infty} \frac{(-1)^n \omega^{2n}}{(2n)!}\Big) \\
&\quad = \sum_{i=0}^{p-1} \frac{\mu_i}{\alpha_i}\Big(\sum_{n=0}^{\infty} \frac{(-1)^n \omega^{2n}}{(2n)!}\Big)\Big(\sum_{n=0}^{\infty} \lambda_{2n}\, \alpha_i^{2n}\, \omega^{2n}\Big) \\
&\quad - \sum_{i=0}^{p-1} \frac{\mu_i}{\alpha_i}\Big(\sum_{n=0}^{\infty} \lambda_{2n}\, \omega^{2n}\Big)\Big(\sum_{n=0}^{\infty} \frac{(-1)^n \omega^{2n}}{(2n+1)!}\Big)\Big(\sum_{n=0}^{\infty} \lambda_{2n}\, \alpha_i^{2n}\, \omega^{2n}\Big).
\end{aligned} \tag{184}$$

Next, we wish to identify the terms in ω^{2m} of the left and right hand sides of (184). First of all, for $m = 0$, $\lambda_0 = \mathbf{\Lambda}(0)$, defined in (182).

For $m \geqslant 1$, one notices that the coefficient in ω^{2m} in the left hand side of (184) is

$$\begin{aligned}
L_{2m} &:= \frac{(-1)^{m-1}}{(2m-1)!} + \sum_{k=0}^{m} \frac{(-1)^{m-k}\, \lambda_{2k}}{(2(m-k))!} \\
&= \frac{(-1)^{m-1}}{(2m-1)!} + \lambda_{2m} + \sum_{k=0}^{m-1} \frac{(-1)^{m-k}\, \lambda_{2k}}{(2(m-k))!}.
\end{aligned} \tag{185}$$

As for the right hand side, we next observe that

$$\sum_{n=0}^{\infty} \frac{(-1)^n \omega^{2n}}{(2n)!} - \Big(\sum_{n=0}^{\infty} \lambda_{2n}\omega^{2n}\Big)\Big(\sum_{n=0}^{\infty} \frac{(-1)^n \omega^{2n}}{(2n+1)!}\Big) = \sum_{n=0}^{\infty} c_{2n}\, \omega^{2n},$$

where we have set

$$c_{2n} := \frac{(-1)^n}{(2n)!} - \sum_{q=0}^{n} \frac{(-1)^{n-q} \lambda_{2q}}{(2n-2q+1)!}. \tag{186}$$

The coefficient in ω^{2m} in the right hand side of (184) is

$$R_{2m} := \sum_{k=0}^{m} \Big(\sum_{i=0}^{p-1} \mu_i\, \alpha_i^{2k-1}\Big)\, \lambda_{2k}\, c_{2m-2k} \equiv \sum_{k=0}^{m} \eta_{2k}\, \lambda_{2k}\, c_{2m-2k},$$

where we defined

$$\eta_n := \sum_{i=0}^{p-1} \mu_i \alpha_i^{n-1}, \qquad n \geqslant 0.$$

In other words, with (186),

$$R_{2m} = \sum_{k=0}^{m} \eta_{2k}\, \lambda_{2k}\, \frac{(-1)^{m-k}}{(2m-2k)!} - \sum_{k=0}^{m} \sum_{q=0}^{m-k} \eta_{2k}\, \lambda_{2k}\, \frac{(-1)^{m-k-q} \lambda_{2q}}{(2m-2k-2q+1)!}.$$

Isolating the terms involving λ_m, that correspond to $k = m$ in the first sum, $(k = 0, q = m)$ and $(k = m, q = 0)$ in the second sum, we get

$$\begin{aligned}
R_{2m} &= \big(\eta_{2m} - (\eta_0 + \eta_{2m})\lambda_0\big)\, \lambda_{2m} + \sum_{k=0}^{m-1} \frac{(-1)^{m-k}}{(2m-2k)!}\, \eta_{2k}\, \lambda_{2k} \\
&\quad - \eta_0\, \lambda_0 \sum_{q=0}^{m-1} \frac{(-1)^{m-q}\, \lambda_{2q}}{(2m-2q+1)!} - \sum_{k=1}^{m-1} \sum_{q=0}^{m-k} \eta_{2k}\, \lambda_{2k} \frac{(-1)^{m-k-q}\, \lambda_{2q}}{(2m-2k-2q+1)!}.
\end{aligned} \tag{187}$$

With $L_{2m} = R_{2m}$ (see (185) and (187)), we obtain a linear equation for λ_{2m}:

$$\begin{aligned} A_m\lambda_{2m} = \frac{(-1)^m}{(2m-1)!} - \sum_{k=0}^{m-1} \frac{(-1)^{m-k}\,\lambda_{2k}}{(2(m-k))!} \\ + \sum_{k=0}^{m-1} \frac{(-1)^{m-k}}{(2m-2k)!}\,\eta_{2k}\,\lambda_{2k} - \ \eta_0\,\lambda_0 \sum_{q=0}^{m-1} \frac{(-1)^{m-q}\lambda_{2q}}{(2m-2q+1)!} \\ - \sum_{k=1}^{m-1}\sum_{q=0}^{m-k} \eta_{2k}\,\lambda_{2k} \frac{(-1)^{m-k-q}\lambda_{2q}}{(2m-2k-2q+1)!}, \end{aligned} \tag{188}$$

$$\text{where} \quad A_m = 1\ - \eta_{2m}\ + (\eta_0 + \eta_{2m})\lambda_0. \tag{189}$$

Thus, to prove the uniqueness of an even solution analytic in the origin, it is sufficient to fix λ_0 to either of the values (182), and show that $A_m \neq 0$ for all $m \geqslant 1$. As we will see later, this is the only place where Dirichlet and Neumann problems can de distinguished.

Now it remains to consider the two cases of the statement of the lemma, see also (123):

- If $(\boldsymbol{\mu}, \boldsymbol{\alpha}) \in \mathbb{P}_N \cup \mathbb{P}_{ND} \Leftrightarrow \langle \boldsymbol{\mu}\boldsymbol{\alpha} \rangle < 1$. We are interested in the solution that satisfies

  $$\lambda_0 \equiv \boldsymbol{\Lambda}(0) = 0.$$

  In this case, we get the following expression for (189):

  $$A_m = 1\ - \eta_{2m}, \qquad m \geqslant 1. \tag{190}$$

  Notice that $\eta_{m+1} < \eta_m$ for all $m \geqslant 0$, and hence $A_{m+1} > A_m$, for all $m \geqslant 1$. Thus

  $$A_1 = 1 - \langle \boldsymbol{\mu}\boldsymbol{\alpha} \rangle > 0 \quad \Longrightarrow \quad A_m > 0 \text{ for all } m \geqslant 1, \tag{191}$$

  hence the uniqueness of the solution with $\boldsymbol{\Lambda}(0) = 0$. With (188), it is easy to compute the first two terms of the expansion in ω^2 of the solution $\boldsymbol{\Lambda}$ in the origin. In particular, $\lambda_2 = -(1 - \langle \boldsymbol{\mu}\boldsymbol{\alpha} \rangle)^{-1}$, hence the announced Taylor expansion.

- If $(\boldsymbol{\mu}, \boldsymbol{\alpha}) \in \mathbb{P}_D \cup \mathbb{P}_{ND} \Leftrightarrow \left\langle \dfrac{\boldsymbol{\mu}}{\boldsymbol{\alpha}} \right\rangle > 1$. We are interested in the solutions satisfying

  $$\lambda_0 \equiv \boldsymbol{\Lambda}(0) = 1 - \left\langle \frac{\boldsymbol{\mu}}{\boldsymbol{\alpha}} \right\rangle^{-1}.$$

  In this case (189) becomes

  $$A_m = 1\ - \eta_{2m}\ + (\eta_0 + \eta_{2m})\,(1 - \eta_0^{-1}) = \eta_0 - \eta_{2m}\,\eta_0^{-1}. \tag{192}$$

  Like before, it is easy to see that $A_{m+1} > A_m$, for all $m \geqslant 1$. Moreover,

  $$A_1 = \left\langle \frac{\boldsymbol{\mu}}{\boldsymbol{\alpha}} \right\rangle - \langle \boldsymbol{\mu}\boldsymbol{\alpha} \rangle \left\langle \frac{\boldsymbol{\mu}}{\boldsymbol{\alpha}} \right\rangle^{-1} = \left\langle \frac{\boldsymbol{\mu}}{\boldsymbol{\alpha}} \right\rangle^{-1} \left(\left\langle \frac{\boldsymbol{\mu}}{\boldsymbol{\alpha}} \right\rangle^2 - \langle \boldsymbol{\mu}\boldsymbol{\alpha} \rangle \right) > 0, \tag{193}$$

  because $\left\langle \dfrac{\boldsymbol{\mu}}{\boldsymbol{\alpha}} \right\rangle^2 > \left\langle \dfrac{\boldsymbol{\mu}}{\boldsymbol{\alpha}} \right\rangle > \langle \boldsymbol{\mu}\boldsymbol{\alpha} \rangle$.

  Hence $A_m > 0$ for all $m \geqslant 1$, thus the uniqueness of the solution. With (188), it is then immediate to obtain the announced Taylor expansion.

REFERENCES

[1] Yves Achdou, Fabio Camilli, Alessandra Cutrì, and Nicoletta Tchou. Hamilton–Jacobi equations constrained on networks. *Nonlinear Differential Equations and Applications NoDEA*, 20(3):413–445, 2013.

[2] Yves Achdou, Christophe Sabot, and Nicoletta Tchou. Diffusion and propagation problems in some ramified domains with a fractal boundary. *ESAIM: Mathematical Modelling and Numerical Analysis*, 40(4):623–652, 2006.

[3] Yves Achdou, Christophe Sabot, and Nicoletta Tchou. Transparent boundary conditions for a class of boundary value problems in some ramified domains with a fractal boundary. *C. R. Math. Acad. Sci. Paris*, 342(8):605–610, 2006.

[4] Yves Achdou, Christophe Sabot, and Nicoletta Tchou. Transparent boundary conditions for the Helmholtz equation in some ramified domains with a fractal boundary. *J. Comput. Phys.*, 220(2):712–739, 2007.

[5] Yves Achdou and Nicoletta Tchou. Boundary value problems with nonhomogeneous Neumann conditions on a fractal boundary. *C. R. Math. Acad. Sci. Paris*, 342(8):611–616, 2006.

[6] Yves Achdou and Nicoletta Tchou. Neumann conditions on fractal boundaries. *Asymptot. Anal.*, 53(1-2):61–82, 2007.

[7] Yves Achdou and Nicoletta Tchou. Boundary value problems in ramified domains with fractal boundaries. In *Domain decomposition methods in science and engineering XVII*, volume 60 of *Lect. Notes Comput. Sci. Eng.*, pages 419–426. Springer, Berlin, 2008.

[8] Felix Ali Mehmeti and Serge Nicaise. Nonlinear interaction problems. *Nonlinear Anal.*, 20(1):27–61, 1993.

[9] Wolfgang Arendt, Charles J. K. Batty, Matthias Hieber, and Frank Neubrander. *Vector-valued Laplace transforms and Cauchy problems*, volume 96 of *Monographs in Mathematics*. Birkhäuser/Springer Basel AG, Basel, second edition, 2011.

[10] Lehel Banjai, Christian Lubich, and Francisco-Javier Sayas. Stable numerical coupling of exterior and interior problems for the wave equation. *Numer. Math.*, 129(4):611–646, 2015.

[11] Gregory Berkolaiko and Peter Kuchment. *Introduction to quantum graphs*, volume 186 of *Mathematical Surveys and Monographs*. American Mathematical Society, Providence, RI, 2013.

[12] J. A. Bondy and U. S. R. Murty. *Graph theory with applications*. American Elsevier Publishing Co., Inc., New York, 1976.

[13] Paul Cazeaux, Céline Grandmont, and Yvon Maday. Homogenization of a model for the propagation of sound in the lungs. *Multiscale Model. Simul.*, 13(1):43–71, 2015.

[14] Sebastian M. Cioabă and M. Ram Murty. *A first course in graph theory and combinatorics*, volume 55 of *Texts and Readings in Mathematics*. Hindustan Book Agency, New Delhi, 2009.

[15] Bjorn Engquist and Andrew Majda. Absorbing boundary conditions for the numerical simulation of waves. *Math. Comp.*, 31(139):629–651, 1977.

[16] Agelos Georgakopoulos, Sebastian Haeseler, Matthias Keller, Daniel Lenz, and Radosław K. Wojciechowski. Graphs of finite measure. *J. Math. Pures Appl. (9)*, 103(5):1093–1131, 2015.

[17] Fritz Gesztesy and Eduard Tsekanovskii. On matrix-valued Herglotz functions. *Math. Nachr.*, 218:61–138, 2000.

[18] Patrick Joly and Adrien Semin. Construction and analysis of improved Kirchoff conditions for acoustic wave propagation in a junction of thin slots. In *ESAIM: Proceedings*, volume 25, pages 44–67. EDP Sciences, 2008.

[19] Tosio Kato. *Perturbation Theory for Linear Operators*. Springer, 1980.

[20] John L. Kelley. *General topology*. Springer-Verlag, New York-Berlin, 1975. Reprint of the 1955 edition [Van Nostrand, Toronto, Ont.], Graduate Texts in Mathematics, No. 27.

[21] Peter Kuchment. Graph models for waves in thin structures. *Waves in Random Media*, 12(4):R1–R24, 2002.

[22] Benoit B Mandelbrot. *The fractal geometry of nature*, volume 173. Macmillan, 1983.

[23] Bertrand Maury, Delphine Salort, and Christine Vannier. Trace theorems for trees, application to the human lungs. *Network and Heteregeneous Media*, 4(3):469 – 500, September 2009.

[24] K. Naimark and M. Solomyak. Eigenvalue estimates for the weighted Laplacian on metric trees. *Proc. London Math. Soc. (3)*, 80(3):690–724, 2000.

[25] K. Naimark and M. Solomyak. Geometry of Sobolev spaces on regular trees and the Hardy inequalities. *Russ. J. Math. Phys.*, 8(3):322–335, 2001.

[26] S. Nicaise. Elliptic operators on elementary ramified spaces. *Integral Equations Operator Theory*, 11(2):230–257, 1988.

[27] Hans Pasterkamp, Steve S Kraman, and George R Wodicka. Respiratory sounds: advances beyond the stethoscope. *American journal of respiratory and critical care medicine*, 156(3):974–987, 1997.

[28] Nicolas Pozin, Spyridon Montesantos, Ira Katz, Marine Pichelin, Irene Vignon-Clementel, and Céline Grandmont. A tree-parenchyma coupled model for lung ventilation simulation. *Int. J. Numer. Methods Biomed. Eng.*, 33(11):e2873, 30, 2017.

[29] Michael Redd and Barry Simon. *Methods of Modern Mathematical Physics*. Academic Press, 1980.

[30] Jacob Rubinstein and Michelle Schatzman. Variational problems on multiply connected thin strips. I. Basic estimates and convergence of the Laplacian spectrum. *Arch. Ration. Mech. Anal.*, 160(4):271–308, 2001.

[31] Jacob Rubinstein and Michelle Schatzman. Variational problems on multiply connected thin strips. II. Convergence of the Ginzburg-Landau functional. *Arch. Ration. Mech. Anal.*, 160(4):309–324, 2001.

[32] D Rueter, H-P Hauber, D Droeman, P Zabel, and S Uhlig. Low-frequency ultrasound permeates the human thorax and lung: a novel approach to non-invasive monitoring. *Ultraschall in der Medizin-European Journal of Ultrasound*, 31(01):53–62, 2010.

[33] Adrien Semin. *Propagation d'ondes dans des jonctions de fentes minces*. PhD thesis, Université de Paris-Sud 11, 11 2010.

[34] Michael Solomyak. Laplace and Schrödinger operators on regular metric trees: the discrete spectrum case. In *Function spaces, differential operators and nonlinear analysis (Teistungen, 2001)*, pages 161–181. Birkhäuser, Basel, 2003.

[35] Michael Solomyak. On approximation of functions from Sobolev spaces on metric graphs. *J. Approx. Theory*, 121(2):199–219, 2003.

[36] Michael Solomyak. On the spectrum of the laplacian on regular metric trees. *Waves in Random Media*, 14(1):S155–172, 2004.

[37] Olaf Steinbach. *Numerical approximation methods for elliptic boundary value problems*. Springer, New York, 2008. Finite and boundary elements, Translated from the 2003 German original.

E-mail address: patrick.joly@inria.fr
E-mail address: maryna.kachanovska@ensta-paristech.fr
E-mail address: semin@mathematik-tu-darmstadt.de